

ESTIMATION OF THE DISTRIBUTION OF CONDUCTION
VELOCITIES IN INTACT PERIPHERAL NERVES

by

Zsolt Laszlo Kovacs

Electrical Engineer, Escola Politecnica da
Universidade de Sao Paulo
(1972)

S.M., Escola Politecnica da Universidade de
Sao Paulo
(1973)

SUBMITTED IN PARTIAL FULFILLMENT OF THE
REQUIREMENTS FOR THE DEGREE OF
DOCTOR OF PHILOSOPHY

at the

MASSACHUSETTS INSTITUTE OF TECHNOLOGY

May, 1977

Signature of Author *Zsolt Kovacs*
Department of Electrical Engineering, May 5, 1977
Certified by .. *Timothy A. Johnson*
Thesis Supervisor
Accepted by
Chairman, Departmental Committee on Graduate Students

Estimation of the Distribution of Conduction Velocities in

Intact Peripheral Nerves

by

Zsolt Laszlo Kovacs

Submitted to the Department of Electrical Engineering and Computer Science on May 5, 1977 in partial fulfillment of the requirements for the degree of Doctor of Philosophy.

The compound action potential recorded from a peripheral nerve is related to the distribution of conduction velocities, which in normal and healthy nerves depends on the fiber diameter spectrum, as observed experimentally by Erlanger and Gasser. We examine the problem of obtaining a statistical estimate of the distribution of conduction velocities, from the compound action potential recorded by surface electrodes. A measurement strategy is proposed in which the compound action potential evoked by a supramaximal electrical stimulation and the potential evoked by a threshold stimulation of the nerve are measured. A least squares estimator of the distribution of conduction velocities which uses these measurements is then proposed. The performance of this estimator is evaluated by comparing the estimated distribution of conduction velocities with that revealed by standard histological techniques.

A detailed probabilistic model of the pathological changes in diabetic neuropathy, which is consistent with the electrophysiological and histological data obtained in the past by others, is developed. Estimates of the conduction velocity distributions in a population of neurologically normal subjects and in a population of subjects suffering from diabetic sensory neuropathy have been determined. The data are analyzed according to this probabilistic model, and the following interpretations are suggested: that either all fiber groups undergo uniform segmental demyelination and remyelination; or that in such a neuropathy, the large fast conducting fibers are affected by segmental demyelination, remyelination and axonal degeneration.

THESIS SUPERVISOR: Timothy L. Johnson

TITLE: Associate Professor of Electrical Engineering and Computer Science.

Acknowledgements

I would like to thank my thesis advisor and great friend Prof. Timothy Johnson for his assistance, encouragement and advice during this thesis work. I would also like to thank Dr. Daniel Sax, who was on the thesis committee and provided a constant orientation in the medical related problems which appeared in the course of this work. I am also grateful for all the interesting, stimulating and creative discussions I had with Professors Jerome Lettvin and Emilio Bizzi, who were also the readers of this thesis.

I am deeply indebted to all those individuals who helped with their special skills at the several stages of this research. Mr. Norman Leafer was of invaluable help in testing the human subjects; Ms. Carol Soeldner made possible with her skillful help an important experiment with a monkey; Dr. J. Incze supervised the histological studies; Mr. J. Hutchinson helped in fixing bugs with the electronic equipment and Mr Arthur Giordani did an outstanding drafting job.

I am also grateful for the interesting conversations and stimulating discussions with Prof. W.Nauta from the Department of Psychology at M.I.T. and Prof. Thomas Weiss, from the Research Laboratory of Electronics. Dr. Michael Trachtenberg lent one of his monkeys, for which I am deeply indebted.

I wish to thank fellow graduate students, Mr. Pal Toldalagi and Paulo Villela for the creative discussions in some of the topics of the thesis.

Finally, I wish to express my most sincere gratitude to my wife Elizabeth for her understanding and sacrifices over the past three years.

Financial support was provided by the Fundacao de Amparo a Pesquisa do Estado de Sao Paulo, Brazil, and facilities provided by the Electronic Systems Laboratory at M.I.T., the Boston Veterans Administration Hospital Clinical Neurophysiology Laboratory, the Neurology Service at the Veterans Administration Outpatient Clinic in Boston and the Department of Neurology, Boston University Medical School.

Dedicated to
Elizabeth,
Eliane and
Robert

"The collecting of scientific data is a discriminating activity, like the picking of flowers ... and the selection of flowers considered worth of picking as well as their arrangement into a bouquet, are ultimately matters of personal taste".

Arthur Koestler, in

"The Act of Creation"

TABLE OF CONTENTS

CHAPTER		
1 - PREVIEW AND MOTIVATION		9
2 - PERIPHERAL NERVES		13
2.1 - Introduction		13
2.2 - Properties of Myelinated Nerve Fibers		18
2.2.1 - Relations Between Some of the Measurable Parameters of Myelinated Nerve Fibers		18
2.2.1.1 - Relation Between Conduction Velocity and Fiber Diameter		20
2.2.1.2 - Relation Between External Diameter and Internodal Length		21
2.2.1.3 - Relation Between the Myelin Thickness and Conduction Velocity.		21
2.2.1.4 - Relations Between Spike Duration, Rise Time and Conduction Velocity		21
2.2.1.5 - Relation Between the Amplitude of the Recorded Action Potential and the Diameter of the Nerve Fiber		23
2.3 - Electrophysiological Studies in Intact Periphe- pheral Nerves		25
2.3.1 - The Reconstruction of the Compound Action Potential by Erlanger and Gasser.		27

CHAPTER

2.3.2 - The Separation of Populations of Nerve Fibers by Crosscorrelation	32
2.4 - Summary and Conclusions	35
3 - ESTIMATION OF THE DISTRIBUTION OF CONDUCTION VELOCITIES	37
3.1 - Introduction	37
3.2 - The Model	39
3.2.1 - Experimental Verification of Linearity	45
3.2.2 - The Measurement Strategy	51
3.2.3 - Electrode Artifact Removal	56a
3.3 - The Estimation Problem	57
3.3.1 - Explicit Solution of the Minimization Problem	62
4 - EXPERIMENTAL VERIFICATION OF THE TECHNIQUE	65
4.1 - Introduction	65
4.2 - The Experiment	67
4.2.1 - Methods	68
4.2.1.1 - The Subject	68
4.2.1.2 - Electrophysiological Procedures	68
4.2.1.3 - Histological Procedures	73
4.2.2 - Results	78
5 - APPLICATIONS TO CLINICAL NEUROLOGY	80
5.1 - Introduction	80

CHAPTER	
5.2 - The Distribution of Conduction Velocities in Diabetic Neuropathy	82
5.2.1 - Peripheral Neuropathies	82
5.2.2 - Experimental Procedures	86
5.2.2.1 - Subjects and Methods	86
5.2.2.2 - Data Processing and Results	89
5.3 - Modeling the Diabetic Neuropathy	106
6 - CONCLUDING REMARKS AND SUGGESTIONS FOR FURTHER RESEARCH	130
APPENDIX	
1 - THE ESTIMATOR EQUATIONS	134
2 - THE STIMULUS ARTEFACT	137
3 - INSTRUMENTATION AND TESTING PROCEDURES	147
4 - EVALUATION OF THE ESTIMATOR USING SYNTHETIC COMPOUND ACTION POTENTIAL	152
5 - COMPUTER PROGRAM LISTINGS	156
REFERENCES	171

CHAPTER 1

PREVIEW AND MOTIVATION

The problem of identifying the populations of nerve fibers of different sizes in a nerve trunk on the basis of their different conduction velocities was first investigated by Gasser and Erlanger [G2], [E2] in 1924. As result of their pioneering work, a system for classifying nerve fibers into A,B and C groups and alpha, beta and gamma subgroups emerged, which with some small changes is still the most widely used system for classifying nerve fibers. They also developed at that time an empirical technique for interpreting the compound action potential in nerves, known as the "reconstruction of the compound action potential"

method. The basis of this reconstruction procedure is that the compound action potential is the linear superposition of the action potentials from the component nerve fibers. Despite the relatively simple setting and modeling of the problem, their technique hasn't been refined in these past 50 years. For instance, Buchthal and Rosenfalck [B1] in an important survey study on nerve conduction published in 1966, analyze the compound action potential recorded from human peripheral nerve repeating the Gasser and Erlanger reconstruction method without any improvements.

As a starting point for this thesis the basic ideas of Gasser and Erlanger are reviewed and refined on the basis of some information now available about the intrinsic properties of nerve fibers and peripheral nerves. It is recognized then that the compound action potential is a linear transformation of the distribution of conduction velocities, which is defined in an appropriate sense in terms of the fiber diameter spectrum. The problem of statistically estimating this distribution from the compound action potential recorded with surface electrodes is then approached and a solution is proposed.

The ability to estimate in a non-invasive way the fiber size composition of a peripheral nerve is very desirable for the study and understanding of the peripheral neuropathies (diseases of

peripheral nerves) in humans. Currently, the only reliable quantitative way of obtaining such information is through the direct biopsy of the peripheral nerve. Because of the relatively large damage caused by biopsy, it is of very restricted use in routine clinical care and research. The basic motivation for the development of the technique described in this dissertation was to produce a non-invasive electrophysiological method which could - at least as a screening technique - replace nerve biopsy

The estimated distribution of conduction velocities from the electrophysiological data was compared to the one revealed by standard histological techniques in the ulnar nerve of a rhesus monkey. The details of this experiment are treated in Chapter 4 of this thesis.

A population of neurologically normal subjects and another population of individuals suffering from diabetic sensory neuropathy were studied. An approximate probabilistic model to describe the pathological changes in peripheral nerves which undergo segmental demyelination and remyelination as well as axonal degeneration was constructed. The model is consistent with most of the available histological and experimental data on these pathological processes as reported by various researchers. Based on this model, the observed changes in the distribution of conduction velocities of the diabetic population are interpreted. This interpretation suggests

that the major changes are either segmental demyelination and remyelination affecting all fibers groups uniformly, or segmental demyelination and remyelination and axonal degeneration affecting primarily the large fibers.

The use of surface recording electrodes in all experimental studies reported in this thesis generated the need to solve some specific problems such as low signal-to-noise ratios, large stimulus artefacts and the corruption of the signals by biological noise such as muscle EMG. These specific problems are treated in Appendices 2 and 3.

The primary contribution of this thesis is that a quantitative measure of the fiber size composition of a peripheral nerve is obtained by a purely electrophysiological and non-invasive technique.

CHAPTER 2

PERIPHERAL NERVES

2.1 - INTRODUCTION

Peripheral nerves are communication channels which convey information between the central nervous system - the brain and the spinal cord - and the rest of the body. They are in general composed of afferent and efferent fibers, the former transmitting information from the periphery to the brain and spinal cord and the latter in the opposite direction. The composition of peripheral nerves was first investigated by Sherrington in 1894 [S4] using the histological techniques available at that time, and he recognized that efferent fibers innervating muscles were larger than those innervating the skin. Eccles and Sherrington [E3] demonstrated in 1930 the existence

of two distinct size groups of motor fibers which were later labeled alpha and gamma. While at that time the direct histological techniques were the most important tools for studying peripheral nerves, some researchers started to look at the electrical properties of nerves, demonstrating that electrical impulses are transmitted at finite velocities.

The study of the electrical activity of peripheral nerves, was greatly facilitated by the invention in 1890 of the cathode ray oscillograph by Braun and by its later improvement. Gasser and Erlanger [G1] succeeded in recording action potentials from the frog's sciatic nerve using the Braun tube in 1922. The work of Gasser and Erlanger and their associates in the following 15 years produced important discoveries about the electrical properties of peripheral nerves and nerve fibers and stimulated many fundamental questions about them. Among other things, they were able to separate different groups of fibers on the basis of their different conduction velocities. Three main groups were recognized and labeled A, B and C with velocity ranges 5-90 m/sec, 2-5 m/sec and .3-2 m/sec. respectively. Group A fibers were further revealed to be clustered in α , β and γ subgroups. A and B fibers are myelinated while the C fibers are unmyelinated. Usually, fiber size is related to function, although in a non-unique way. This relation has been studied more recently by Boyd [B6] and others. This classification of nerve fibers is still widely used today with some modi-

fications. Gasser and Erlanger were also the first to conjecture about the relation of the conduction velocity of a nerve fiber to its diameter in 1927 when they proposed a linear relationship [G2]; this was later substantiated by Hursh in 1939 [H1]. In 1937, Erlanger and Gasser [E1] demonstrated experimentally that the compound action potential recorded from an excised peripheral nerve is the linear superposition of the individual action potentials in each of its component fibers. In the following years, the electrical properties of nerve fibers were more thoroughly understood when a theoretical explanation of the generation and propagation of the action potentials in non-myelinated fibers was advanced by Hodgkin and Huxley in 1952 [H3]. Lillie was the first to suggest in 1925 that excitation and the active processes which maintain propagation of the action potential in myelinated fibers, take place only at the nodes of Ranvier [L7]. The saltatory nature of the conduction of the action potentials in these fibers was experimentally substantiated by the works of Tasaki [T4] and Huxley and Stampfli [H2]. The picture seemed more or less complete for normal and healthy peripheral nerves.

The study and the understanding of diseased nerves was much less spectacular. Histological studies in abnormal, crushed and degenerated peripheral nerves had been carried out concomitantly with normal nerves. In 1948, Hodes [H4] used the electrophysiological measurements of motor nerve conduction velocity as a tool in diagnosing peripheral neuropathies in man and ten years

later Gilliatt and Sears started to study pure sensory fiber populations with electrophysiological techniques in human neuropathies [G6]. The reason for this lag in the electrophysiological study of neuropathies is more or less obvious: in man, the recordings of the electrical activities in nerves had to be made with the nerve fibers in situ ; the first successful percutaneous recording from human nerves was obtained by Eichler in 1938[E4] but understandably he had no means of enhancing the very poor signal to noise ratio which goes with this technique, and his work was forgotten until 1949, when Dawson and Scott [D2] were able to improve the signal to noise ratio by photographic superposition of several nerve responses. The introduction of electronic averaging later allowed the systematic study of the neuropathies.

In all the peripheral neuropathies so far studied by electrophysiological techniques, the pattern is more or less the same: there is a global or local reduction in the maximum conduction velocity and amplitude, and the time dispersion of the compound action potential is increased. These observations have been correlated to various physiological changes: axonal and Wallerian degeneration of the nerve fibers, segmental demyelination, remyelination, selective loss of fibers etc. Since the initial work of Gilliatt and Sears 18 years ago, the picture of diseased peripheral nerves has become much clearer with the publication of many studies on the electrophysiological and histological corre-

lates of neuropathies. But there is still much to be understood and explained.

2.2 - PROPERTIES OF MYELINATED NERVE FIBERS

It is now a well established fact that mammalian peripheral nerves are in general composed of myelinated A fibers and unmyelinated C fibers. The B group is usually lumped with the A group. Afferent myelinated fibers innervate sensory corpuscles or complexes in the skin, specialized sensory receptors, muscle spindles and tendon organs or joint receptors. Efferent myelinated fibers innervate extrafusal or intrafusal muscle fibers and control some specialized sensory receptors. The unmyelinated fibers serve mainly autonomic functions and some sensory functions. Fibers in the C group conduct action potentials at very slow speeds and the intensities of the generated action potentials are so small that they are almost impossible to be measured at the surface of the skin. Because of these reasons we will not be concerned with C fibers in this thesis, and by peripheral nerve we will always mean the myelinated portion of the peripheral nerve.

The most common terms defining some of the morphological features of an afferent myelinated nerve fiber are shown in Figure

2.2.1

2.2.1 - Relations Between some of the Measurable Parameters of Myelinated Nerve Fibers

Some morphological and physical parameters of nerve fibers

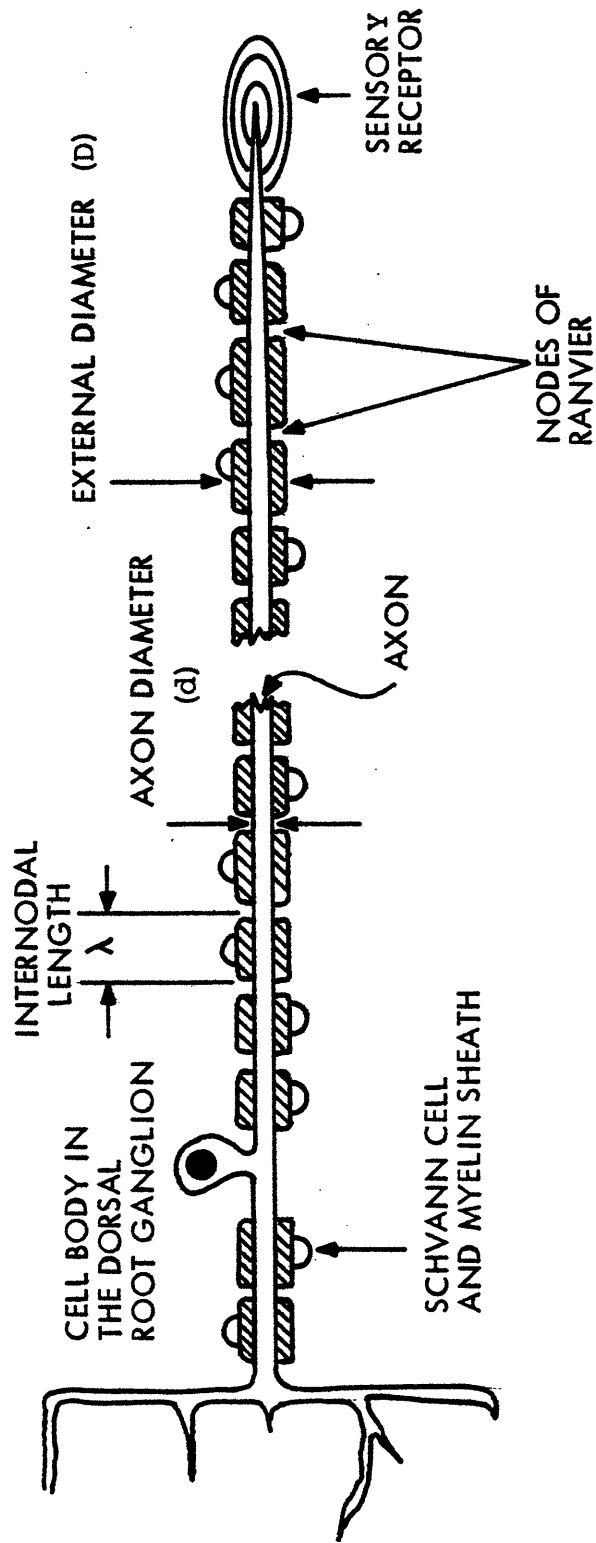


FIGURE 2.2.1

which can be readily measured by histological techniques such as the external diameter, internodal length, myelin thickness, or by electrophysiological techniques such as the conduction velocity, the action potential duration and amplitude have been related experimentally. We will now briefly describe these findings.

2.2.1.1 - Relation between conduction velocity and diameter

As early as 1927, Gasser and Erlanger [G2] advanced the hypothesis that a linear relationship exists between the fiber conduction velocity and the fiber diameter, namely $v = K_v D$, which was experimentally verified by Hursh [H1] in 1939. Hursh found $K_v = 6.0$ m/sec. μ . This linear relationship was later substantiated by similar studies done in a variety of species. The values of K_v found by different investigators are not consistent. Boyd [B5] in 1964 found that fibers in the ventral root of the cat have K_v ranging from 4.5 to 5.7 m/sec. μ . Sanders and Whitteridge [S2] found the smallest reported value for $K_v = 3.0$ m/sec. μ , in the rabbit. Also in the rabbit, Cragg and Thomas [C5] reported $K_v = 4.4$ m/sec. μ . In man indirect measurements of K_v gave $K_v = 5.2$ m/sec. μ , by McLoed and Wray [M2] in 1967. The sources of these differences in the value of K_v are not certain but are most likely a combination of the different methods and techniques used by different workers and actual differences of K_v between species and even individuals.

2.2.1.2 - Relation between external diameter and internodal length

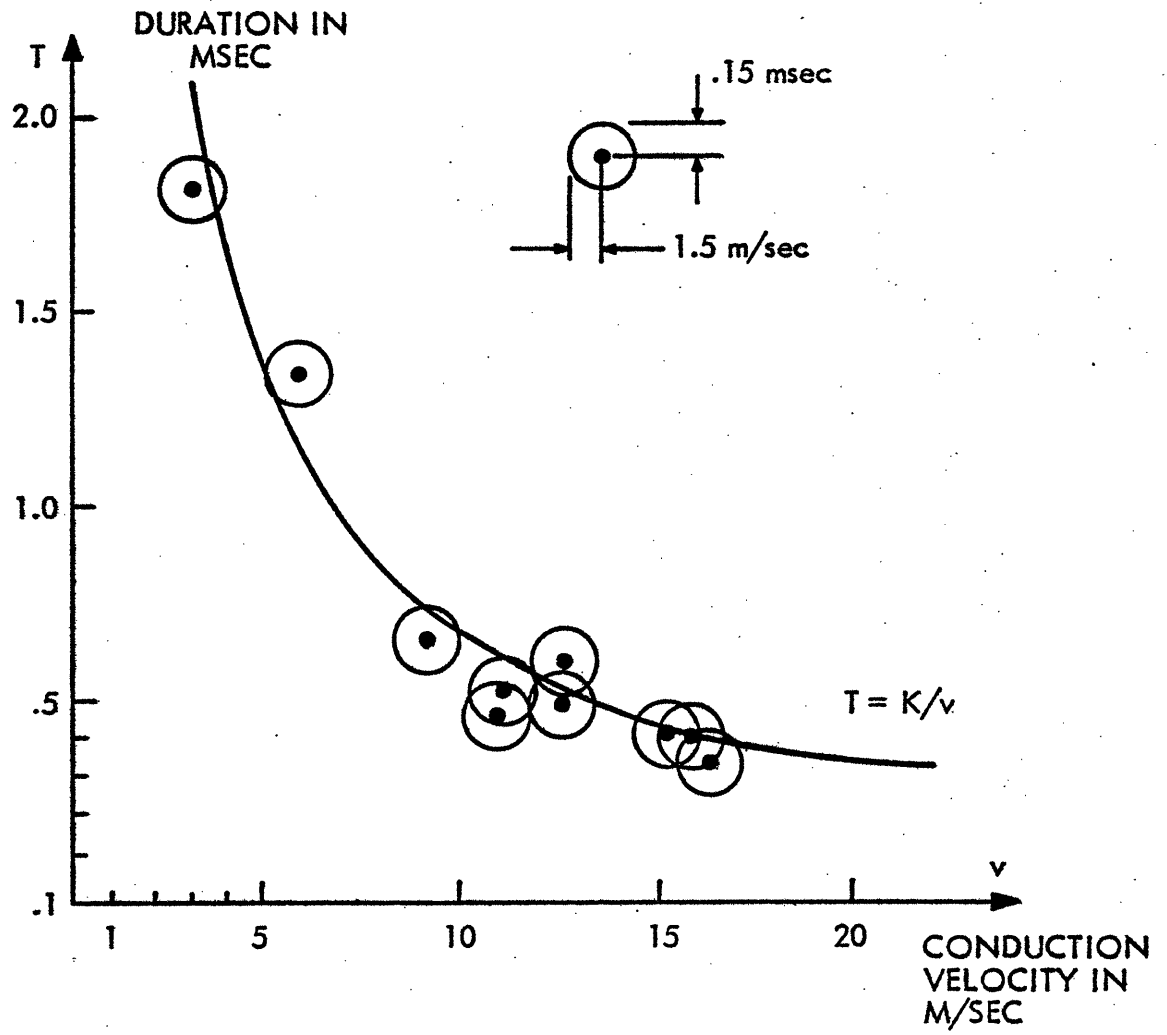
This relation has also been found linear, namely $\lambda = K_{\lambda} D$. The value of K_{λ} in the cat was determined by Hursh [H1] who found it to be about .090 mm/ μ . Later workers found that K_{λ} in different species can be as low as .050 mm/ μ in the rabbit, or as large as .146 mm/ μ in the frog. In man, the value of K_{λ} has been consistently reported as about .095 mm/ μ [T2].

2.2.1.3 - Relation between myelin thickness and conduction velocity

Sanders and Whitteridge [S2] found that myelin thickness is linearly related to conduction velocity and therefore to fiber diameter. Gasser and Grundfest in 1939 [G7] established that the ratio of the axon diameter/ total diameter is roughly constant, markedly in large fibers, and it has the value of .7. Smith and Koles [S7] obtained the same result from an analytical model for myelinated fibers.

2.2.1.4 - Relation between spike duration, rise time, and conduction velocity.

The duration of the action potential, T , and the conduction velocity of the nerve fiber seem to bear an inverse relationship, namely $T = K_T/v$. If the direct measurements of T and v done by Erlanger and Gasser [E1, pg. 26] are used to determine the least squares estimate of K_T , then the graph shown in Figure 2.2.2 is



ERLANGER AND GASSER DATA, TABLE J, PG. 26

FIGURE 2.2.2

obtained. Other workers have also recognized this inverse relation, which is extensively treated in Paintal [P3]; he also reports a similar relationship between the rise time of the action potential - defined in some appropriate sense - and the conduction velocity. These findings are consistent with the assumption that the action potentials in two different fibers with conduction velocities v_1 and v_2 are roughly related to each other as $h_1(t) = h(v_1 t) = h(v_2 (v_1/v_2) t) = h_2((v_1/v_2) t)$, which will be treated extensively in Chapter 3.

2.2.1.5 - Relation between the amplitude of the recorded action potential and the diameter of the nerve fiber

In 1951, based on core conductor theory and some simple geometrical and physical relations, Rushton [R4] concluded among other things that the transmembrane action current should be proportional to the square of the axon diameter. If we accept that the ratio of the axon diameter to the external diameter of the fiber is constant, then the action current should also be proportional to the square of the external diameter. However, Rushton was bothered by the fact that while all his other conclusions were in perfect agreement with the experimentally observed facts, this one conflicted with the empirical observation by Blair and Erlanger in 1933 that the height of the recorded action potential was proportional to the fiber conduction velocity [Bl1] ,

which is in turn proportional to the external diameter. Rushton apparently didn't realize that the transmembrane potential $v_m(t)$ which is roughly the quantity measured in excised conditions as noted by Lorente de N6 [L8], is in fact proportional to axon diameter and it is related to the transmembrane current $i_m(t)$ as

$$i_m(t) = Kd \frac{\partial^2 v_m(t)}{\partial x^2}$$

where d is the axon diameter. Therefore Rushton's results are in fact in agreement with the experimental findings. However, with the nerve fiber in situ and surrounded by a volume conductor, the bipolarly recorded signal from the nerve $s(t)$ will be proportional to the transmembrane current, in which case, Rushton's conclusions are applicable, namely that the height of $s(t)$ is proportional to d^2 and to the external diameter D^2 .

2.3 - ELECTROPHYSIOLOGICAL STUDIES IN PERIPHERAL NERVE TRUNKS

In this section we will restrict our attention only to those peripheral nerves which are primarily composed of muscle and cutaneous afferents and efferents. Such are the median, ulnar and radial nerves in the arm or the sural and peroneal nerves in the leg, for example. The basic knowledge about the composition, physiology, and electrical properties of peripheral nerves was obtained mainly from the study of these specific nerves. They also have the important clinical role of providing material for biopsies, and of being used in the basic electrophysiological measurements for the diagnosis and understanding of polyneuropathies.

In man, the basic electrophysiological measurements done clinically on a routine basis are the determination of the maximum motor and sensory conduction velocities in the above mentioned nerves. The measurement of the motor conduction velocity is much simpler than for sensory conduction velocity, and for this reason was performed more than one hundred years earlier. The basic procedure for measuring the motor conduction velocity is the following: the nerve is stimulated at two different positions and the evoked muscle twitch is recorded. The known distance between the two sites of stimulation and the difference between the latencies of the two responses are used to find the conduction velocity. This was the procedure used by Von Helmholtz in 1852 [V1], who could

get only a mechanical record of the muscle twitch. He obtained the surprisingly accurate value of 61 ± 5 m/sec. for the motor conduction velocity in the human median nerve.

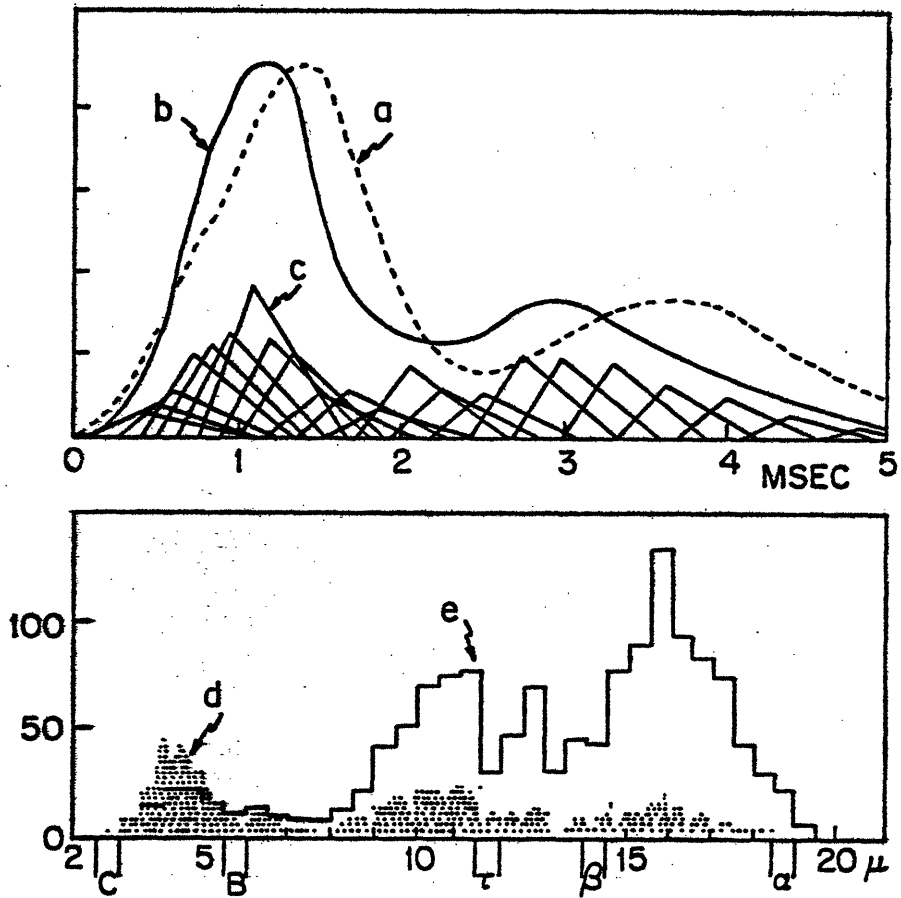
The measurement of pure sensory conduction velocity in man was first performed by Dawson and Scott [D2] in 1949. The basic procedure consists of stimulating a pure sensory branch of the peripheral nerve, one which innervates a finger for example, and recording the evoked compound action potential at some known distance from the site of stimulation. In general, a reliable measurement of the compound action potential can only be obtained through the averaging of several individual responses. The potential from the nerve can be measured either by large surface electrodes placed on the skin above the nerve, as Dawson and Scott did [D2], or by using needle electrodes which are introduced close to the nerve as reported by Gilliatt [G8]. The latency of the recorded action potential is used to calculate the sensory conduction velocity.

More complete information can be obtained about the peripheral nerve by analyzing in detail the compound action potential. Erlanger and Gasser [E1] showed in 1937 that the compound action potential from a nerve can be estimated from the fiber diameter histogram as long as the form of the single action potential is known. Their reasoning and procedures are described in the following section.

2.3.1 - The Reconstruction Of the Compound Action Potential by Erlanger and Gasser.

In the specific experiment described in this paragraph, Erlanger and Gasser [E1] used the frog's sciatic nerve. In order to obtain the compound action potential, they proceeded as follows: The nerve was excised and placed on two pairs of electrodes. One pair, closer to the proximal end of the nerve, was used for electrical stimulation. The other more distal pair, had one pole on the crushed end of the nerve, while the other could be moved along the intact portion. A typical compound action potential recorded under such conditions is shown in figure 2.3.1 a). After measuring the compound action potential, they took a cross section of the nerve and obtained the diameter histogram which is shown in figure 2.3.1 d). The individual action potential from each fiber was assumed to have the same triangular shape and have amplitude proportional to the square of its external diameter as shown in figure 2.3.1 c) and e). The latency of each fiber was assumed to be inversely proportional to the external diameter as discussed in paragraph 2.2.1.1. The reconstructed compound action potential resulted as the algebraic sum of these triangles scaled and displaced according to the diameter histogram, as shown in figure 2.3.1 b).

The most striking difference between the recorded compound action potential and the reconstructed action potential is that the



(FROM ERLANGER AND GASSER, [E1])

- a) Recorded Compound Action Potential
- b) Reconstructed Compound Action Potential
- c) Assumed basic shape of the Single Action Potentials
- d) Fiber Diameter Histogram
- e) Distribution of Conduction Velocities

FIGURE 2.3.1

later goes a bit slower before the first peak, when it starts leading the former with a constantly increasing difference. By the time of the second peak, the reconstructed action potential has a lead of almost one millisecond. If the diameter-to-velocity conversion factor K_v , as discussed in paragraph 2.2.1.1, is changed in a way to improve the match between the two curves in the slower portions of the compound action potential, then the mismatch is accentuated for the faster components. It seems to us that one of the essential facts that Erlanger and Gasser didn't consider in their reconstruction method, is that the duration of the action potential in each individual nerve fiber depends on the conduction velocity of that fiber as their own data suggested, and which was discussed in paragraph 2.2.1.4 and displayed in Figure 2.2.2. If this "stretching" of the slower action potentials is taken into account, then it will work against the mentioned systematic error, and the agreement between the two curves is significantly improved.

After showing that the compound action potential was a direct function of the diameter histogram of a nerve trunk - in fact a function which could be defined quite precisely despite the approximate nature of the basic assumptions - the reconstruction method played its role and seemed forgotten.

In 1966, in an extensive survey study on nerve conduction velocity measurements, Buchthal and Rosenflack [B1] applied

the Erlanger and Gasser reconstruction method to their own observations with one significant difference: they measured the compound action potential in the median nerve of one subject and reconstructed it using the diameter histogram taken from the median nerve of another subject, thus assuming implicitly that the diameter histogram is the same in all healthy human median nerves. They made their records with needle electrodes placed near the nerve in a bipolar configuration, so that the basic action potential had to be approximated by an arrangement of linear segments more complicated than a triangle, with at least three degrees of freedom to adjust. These three degrees of freedom were in fact adjusted until the best match between the reconstructed and the recorded action potentials was obtained. One could wonder what this reconstruction was intended to prove: a closer look will indicate that a fairly large set of possible compound action potentials can be reconstructed from any given diameter histogram by varying the three available degrees of freedom in the basic action potential.

Later, Landau, Clare and Bishop [L6] tried to correlate the compound action potential recorded from the optic nerve to the diameter histogram. They turned to the Erlanger and Gasser method as the natural way to examine that relationship. They realized that the process of adding up triangles is lengthy, inefficient, time consuming and impractical, so they decided to replace the triangles by impulses in order to see the effect of such simplification

on the reconstructed potential. The result turned out to be very unsatisfactory as would be expected. In order to compensate for the lack of overlap between the impulses of adjacent velocity groups, they multiplied each impulse by the diameter it represented. The idea behind this was that by using the triangles, the degree of overlap between adjacent groups would decrease with the diameter; by using impulses, this would be compensated for by multiplying each impulse by the diameter. These ideas can be stated more clearly: if \underline{d} is the "bin width" of the diameter histogram then adjacent bins at D and $D+d$ will contribute triangles delayed by K/D and $K/(D+d)$ respectively in the Erlanger and Gasser reconstruction method; therefore, the two adjacent triangles will be separated by a time $Kd/(D+d)D$ which is roughly proportional to the inverse of D^2 and not of D as Landau et al. have reasoned.

In the 1930's the Erlanger and Gasser method was a very ingenious way to demonstrate the validity of some of the basic properties and intrinsic relations of peripheral nerves and the electrical signals recorded from them, as well as the dependence of the characteristics of a whole peripheral nerve on the properties of its constituent fibers. From the more recent works we can conclude that the ideas proposed by Erlanger and Gasser haven't evolved for nearly half a century, nor have all the possibilities been explored and developed.

For the sake of completeness we feel committed to comment on

another approach to the study of fiber populations which conduct at different velocities in a peripheral nerve. This is presented in the next paragraph.

2.3.2 - The Separation of Populations of Nerve Fibers by Crosscorrelation.

In a work done in 1962 , Casby, Siminoff and Housenecht [c1] approached the problem of separating nerve fiber populations on the basis of their conduction velocities, by making the basic assumption that for any naturally occurring nerve stimulation, the electrical activity induced in the population of fibers is essentially an ergodic random process. The signal recorded by an electrode at some position along the nerve is the sum of possibly hundreds of independent random processes, namely

$$s(t,x) = \sum_{i=1}^N r_i(t) \quad (2.1)$$

where $r_i(t)$ is the train of action potential spikes in the i -th nerve fiber. The signal recorded by another electrode placed at $x+d$ will be

$$s(t,x+d) = \sum_{i=1}^N r_i(t-d/v_i) \quad (2.2)$$

where v_i is the conduction velocity of the i -th fiber. We can write (2.2) in terms of the delays $\tau_i = d/v_i$

$$s(t, x+d) = \sum_{i=1}^N r_i(t-\tau_i) \quad (2.3)$$

If we now sum all those $r_i(t)$ which are propagated at velocities v_i such that the associated delays τ_i are in some small range centered at τ^j , and call the sum $u^j(t)$, then

$$s(t, x) = \sum_{j=1}^M u^j(t) \quad (2.4)$$

$$s(t, x+d) = \sum_{j=1}^M u^j(t-\tau^j) \quad (2.5)$$

Now we take the following expectation,

$$E\{s(t, x)s(t+T, x+d)\} = E\left\{\sum_{j=1}^M u^j(t)u^j(t-\tau^j+T)\right\} \quad (2.6)$$

the expectations of all the cross terms $u^j(t)u^k(t')$, $j \neq k$, are zero because the processes were assumed independent. The right hand side of expression (2.6) is the sum of the autocorrelation functions of the $u^j(t)$ processes, namely,

$$E\{s(t, x)s(t+T, x+d)\} = \sum_{j=1}^M R^j(T-\tau^j) \quad (2.7)$$

If the $R^j(t)$ are such that their energies are confined essentially to intervals T^j which are smaller than the separation between adjacent τ^j then the crosscorrelogram between $s(t, x)$ and $s(t, x+d)$, as expressed by (2.7), will show separate peaks for each velocity group, and the intensity of the activity in any given group will be

approximately proportional to the square root of the corresponding peak in the cross-correlogram.

This cross-correlogram method was applied by Casby et al. to signals recorded by electrodes separated by distances varying from 3 to 10 mm. The signals were elicited by natural stimulations of the area innervated by the nerve, such as: pin prick, hair stroking, tapping, burning, etc. The published results show clearly the different groups of fibers responding to each stimulus. The technique is highly invasive since the nerve has to be exposed, and is therefore restricted to animal studies.

In 1973, during the course of a doctoral research at M.I.T. Rothchild [R2], [R3], used these same ideas - apparently unaware of the work of Casby, Siminoff and Housenecht - to isolate the activity of different fiber populations in the sciatic nerve of the frog.

2.4 - SUMMARY AND CONCLUSIONS

We have seen that there are experimentally established relationships between the physical and electrical characteristics of peripheral nerve fibers. We have also seen that the compound action potential depends in a relatively well defined way on the distribution of these physical characteristics over the whole nerve cross-section, and that information on how some of these physical characteristics are distributed can be obtained from the electrical response of a nerve to a stimulus, which may be an electrical shock or some natural stimulation. Two different methods used in the past have been described. Both of them have been designed to reveal peaks of activity at delays τ_i which depend on the conduction velocities v_i of the different populations, namely $\tau_i = d/v_i$, where d is distance along the nerve, in one case between the stimulating and recording electrodes and in the other case between two recording electrodes. In principle, the peaks can be separated as much as one wishes simply by increasing the distance d . This process is ultimately limited by the total length of the nerve. At this point, it is interesting to illustrate the actual limitations and capabilities of such methods. Suppose that the total length of the nerve is L , and that the duration of the action potentials conducted at velocity v_1 is T_1 . Suppose that another action potential is traveling along the nerve at velocity v_2 . The question is: What is

the minimum difference between v_2 and v_1 so that the two action potentials can be recorded separately? The maximum separation is obviously when $d = L$. Assuming $v_2 < v_1$, we obtain that:

$$v_2 < v_1 / (1 + \frac{T_1 v_1}{L})$$

Using some reasonable values for T_1 and L , say 1 msec. and 25 cm, for $v_1 = 75$ m/sec. we get $v_2 < 57$ m/sec. The conclusion from this analysis is that these methods allow complete separation only of fiber populations which are centered at very different conduction velocities. In other words: these methods have a very low velocity resolution power.

In the next Chapter, a model which is consistent with most of the available experimental evidence is proposed, relating the properties of whole nerve trunks to the characteristics of its constituent fibers. Based on this model a technique is proposed to evaluate in a quantitative way the distribution of conduction velocities which depends on the diameter spectrum of a peripheral nerve. The experimental validation and verification of the proposed technique will be presented in Chapter 4.

CHAPTER 3

ESTIMATION OF THE DISTRIBUTION OF CONDUCTION VELOCITIES

3.1 - INTRODUCTION

A model relating the bipolarly recorded electrical signal from a peripheral nerve in situ to some of the properties of its constituent fibers is constructed. It is shown that the signal depends on the distribution of conduction velocities of the nerve, which will be defined in a precise way as a function of the fiber diameter histogram. Up to this point, the model is conceptually identical to that of Erlanger and Gasser [E1] , discussed in the previous Chapter, with some minor modifications based on more complete experimental evidence. It is then shown that the know-

ledge of the basic action potential recorded from a single nerve fiber or from a set of nearly identical nerve fibers, and the knowledge of the compound action potential can provide enough information to estimate the distribution of conduction velocities.

It is assumed that the electrical signals from the nerve are recorded bipolarly with a pair of surface electrodes in order to assure the easy applicability of the technique to human studies, and that the involved signal-to-noise ratios are very low. The determination of the distribution of conduction velocities is then viewed as a statistical estimation problem.

3.2 - THE MODEL

A nerve immersed in a biological medium, with its axis parallel to the direction labeled x , is schematically represented in Figure 3.2.1. On the surface S of the skin, recording electrodes are placed centered at coordinates $(0, y_1)$ and (x_2, y_2) . In some of the fibers action potentials are initiated at a point $(-p, 0)$, along the nerve by an electrical pulse applied through a pair of stimulating electrodes. We will start the analysis of this situation by deriving an expression for the potentials recorded by the electrodes due to an action potential propagating in only one of the fibers of the nerve.

The biological medium has in general non-homogeneous electrical properties; that is, parameters like electrical conductivity may change from one region to another region inside the medium. Typical values of the conductivities of some biological tissues are given by Plonsey [P1], and the extreme values for the conductivity are .67 mhos/meter for the blood and .04 mhos/meter for the fatty tissue. This non-homogeneous and in some sense random distribution of the electrical conductivities in the medium makes the description of the current fields virtually an impossible task. Fortunately for our purposes we need only some asymptotic results. The following assumptions are made about the medium:

- i) the medium possesses linearity.

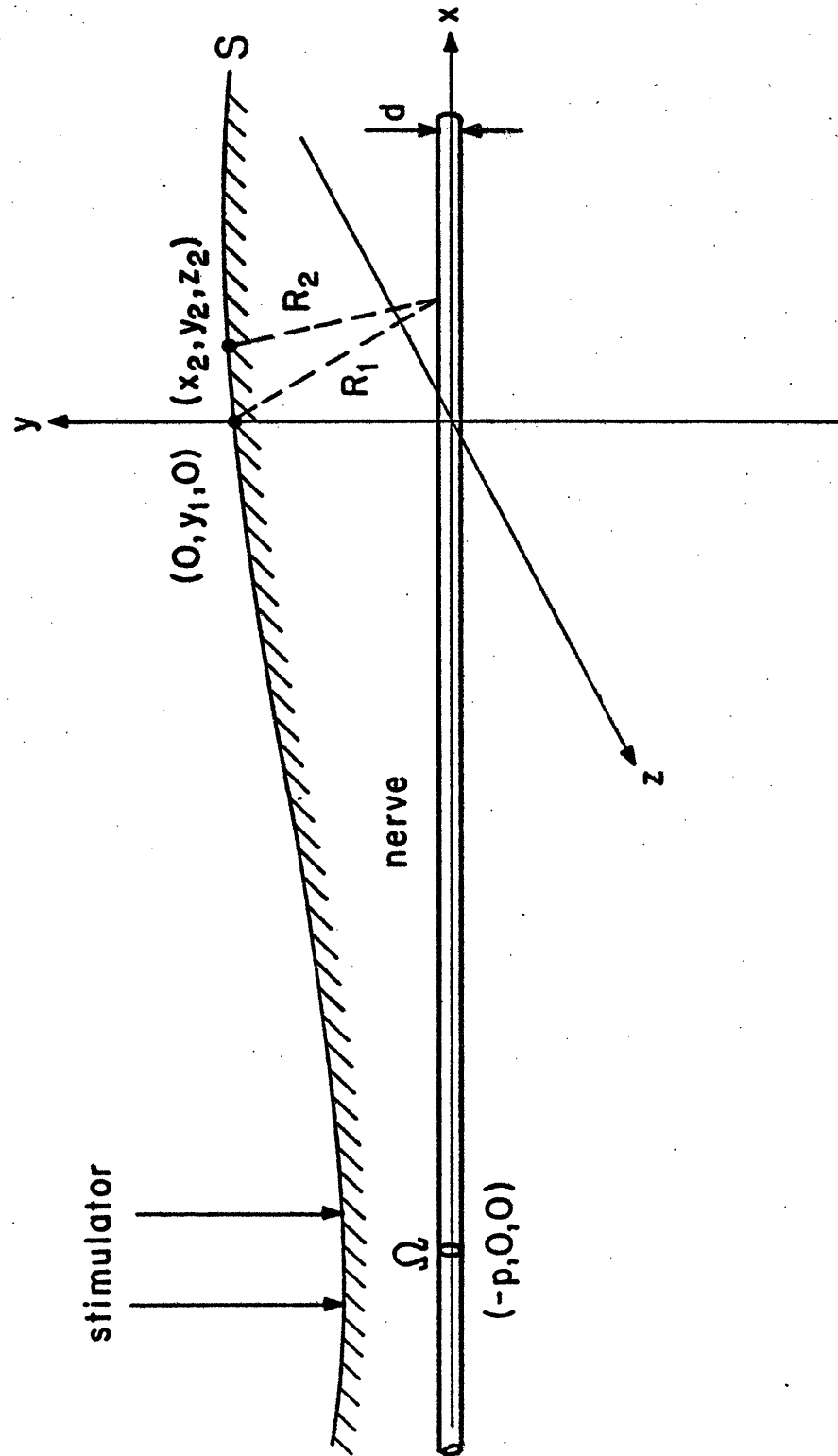


FIGURE 3.2.1

ii) all the propagation, capacitive and inductive effects are negligible.

iii) the diameter of the nerve trunk is negligible as compared to the distances of the recording electrodes from the nerve.

The assumption that the medium is linear - which means that the laws of electrodynamics are applicable - has been substantiated by the experimental work of Lorente de Nó [18], who was also one of the first to study the electrical fields generated by nerves using electromagnetic theory. The second assumption about the medium - which allows a quasi-static formulation of the problem - is only approximate and it may sometimes be a gross simplification. For instance, in muscle tissue, the ratio of the capacitive currents to resistive currents may be as high as .15 at 1 Khz. This value is about the largest for a variety of tissues analysed by Plonsey [P1], which for other tissues stays around .05. The third assumption is relatively safe since the diameters of the peripheral nerves which will be experimentally studied in this thesis - the ulnar and the median nerves - are about 2 mm, while the distance from the surface of the skin is about 10 mm. This will allow us to overlook the different effects of the inhomogeneous medium upon the current fields generated by different fibers of the nerve [G9],[B1]; that is, they can be assumed to be equally affected.

Under these simplifying assumptions, the potentials at the electrodes are expressed by:

$$\phi(0, y_1) = c \int_V (I_U(x, y, z) / R_1) dV \quad (3.1)$$

$$\phi(x_2, y_2) = c \int_V (I_U(x, y, z) / R_2) dV \quad (3.2)$$

where c is a constant which depends on the average electrical properties of the medium; $R_j^2 = (x-x_j)^2 + (y-y_j)^2 + (z-z_j)^2$, $j=1,2$; I_U is the volume current source density, and the integral is over a volume V which includes all current sources due to the propagated action potential. From the quasi-static nature of the problem (assumption ii) it follows that the potential arising from a given current source element in a fiber will have the same temporal behavior as that element, namely:

$$\phi(x_j, y_j, t) = c \int_V (I_U(x, y, z, t) / R_j) dV \quad (3.3)$$

so that the dependence of the potential on the conduction velocity v can be written as

$$\phi(x_j, y_j, t) = c \int_V (I_U(x-vt, y, z) / R_j) dV \quad (3.4)$$

The potential difference $\phi_i(t)$ between the two electrodes due to an action potential in the i -th fiber of the nerve, assuming that the electrode properties are stationary in time, is therefore given by:

$$\phi_i(t) = \phi(-v_i t, y_1) - \phi(x_2 - v_i t, y_2) \triangleq h(v_i t) \quad (3.5)$$

We will now derive an expression for the potential difference recorded by the electrodes due to action potentials propagating on N different fibers of the nerve, not necessarily all with the same propagation velocity. This potential is the compound action potential recorded by surface electrodes. The following additional assumptions are made:

iv) the action potentials propagated by different fibers have essentially the same shape, $h(x - v_i t)$, which means that the potentials recorded from fibers i and j are related as:

$$\phi_i(t) = h(v_i t) = h(v_j (v_i/v_j) t) = \phi_j(v_i t/v_j) \quad (3.6)$$

without accounting for the scaling as described in paragraph 2.2.1.5.

v) the skin/electrode junctions are linear.

Assumption iv) is supported by the experimental work of Erlanger and Gasser [E1] as described in paragraph 2.2.1.4. It must be emphasised that it depends strongly on the quasi-static formulation of the problem, and it is probably much more sensitive to departures from this simplification than to the minute variations in the shape of the action potentials from fiber to fiber.

We introduce now the following notation:

$$h(v_i t) = h_i(t) \quad (3.7)$$

Because of v) and considering that the amplitude of the recorded action potential depends on the conduction velocity as established in paragraph 2.2.1.5, we have that the potential recorded by the electrodes due to activity in N fibers of the nerve is:

$$\phi(t) = \sum_{i=1}^N K v_i^2 h_i(t) \quad (3.8)$$

Let's partition the interval $[v^m, v^M]$ where v^m and v^M are the minimum and the maximum values of the conduction velocities which fibers of the nerve may have, into $M < N$ subintervals $\Delta_j = [v_{j-1}, v_j]$ $j=1 \dots M$, and let's define the distribution of conduction velocities β_j as the number of fibers which have conduction velocities in Δ_j , scaled by $K v_j^2$. We can then approximate $\phi(t)$ by:

$$\phi(t) = \sum_{j=1}^M \beta_j h(v_j, t) \quad (3.9)$$

The vector $\beta = [\beta_1 \dots \beta_M]$ represents the distribution of conduction velocities, and it depends on the fiber diameter histogram $S(D)$ in a well defined way: $S(D)$ can be represented by the M -vector $S = \dots [S_1 \dots S_M]$, where S_j is the number of nerve fibers which have the external diameter in the range $[D_{j-1}, D_j)$. Since $D_j = v_j / K_V$ as established in paragraph 2.2.1.1. we get that

$$\beta_j = K v_j^2 S(v_j / K_V) = K v_j^2 S_j \quad (3.10)$$

Expression (3.8) establishes a linear relation between the recorded compound action potential and the distribution of conduction velocities. The validity of this relation can be substantiated by the following experiment, described in the next paragraph.

3.2.1 - Experimental Verification of Linearity

Two nonoverlapping sets of fibers can be stimulated separately by stimuli s_1 and s_2 when the nerve branches at some point into two or more distinct sections. First the set of fibers which forms one of the branches is stimulated by s_1 , and $\phi_1(t)$ is recorded. Then the other set of fibers in the other branch is stimulated by s_2 , and $\phi_2(t)$ is recorded. Finally, both sets are stimulated simultaneously with s_1 and s_2 respectively and $\phi_{1+2}(t)$ is recorded. Because of linearity, we must have that:

$$\phi_1(t) + \phi_2(t) = \phi_{1+2}(t) \quad (3.11)$$

The ulnar nerve which together with the median and the radial nerves innervates the human hand, has three main sensory branches which innervate fingers 4 and 5, as shown in Figure 3.2.2. The branches labeled 1) and 2) can be stimulated independently from the branch labeled 3) by a pair of stimulating ring electrodes placed on finger 5. Also, branch 3) can be stimulated independently by a stimulus s_2 applied to finger 4. The recording of the compound ac-

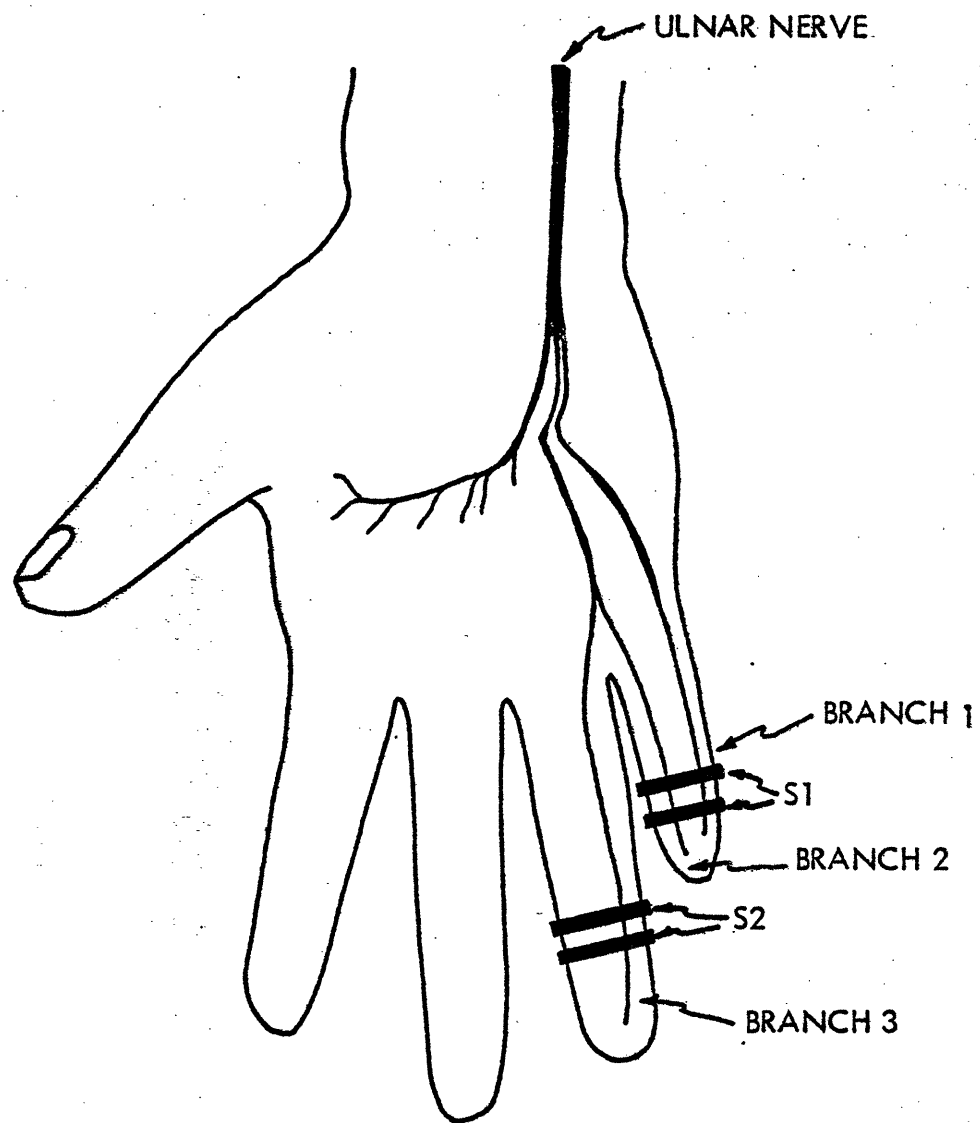


FIGURE 3.2.2

tion potential is done by two by two electrodes pasted on the skin at the elbow over the ulnar nerve. The following measurements were made:

a) branch 3) was stimulated by a brief electrical shock of 100 microsec. duration and amplitude 18V, applied to the ring electrodes placed on finger 4. Since it was just below the threshold for pain, it was supposed to stimulate nearly all fibers in that branch. The stimulus was applied at the rate of 2/second and in order to improve the signal-to-noise ratio 2048 individual responses were averaged. The averaged waveform is shown in Figure 3.2.3.

b) branches 1) and 2) were stimulated using the ring electrodes placed on finger 5. The stimulus was an electrical shock, delivered at the rate of 2/second, with 100 microsec. duration and 12V amplitude, also just below the threshold for pain; 2048 individual responses were averaged and the resulting waveform is shown in Figure 3.2.4.

c) all branches in both fingers were stimulated simultaneously by the same stimuli used in a) and b) ; the average of 2048 individual responses is shown in Figure 3.2.5, and with different time and amplitude scales, in Figure 3.2.6

If linearity holds, then it should be true that:

$$Y_{s_1} + Y_{s_2} - Y_{s_1+s_2} = 0 \quad (3.12)$$

if the measurements were perfect - that is without measurement noise.

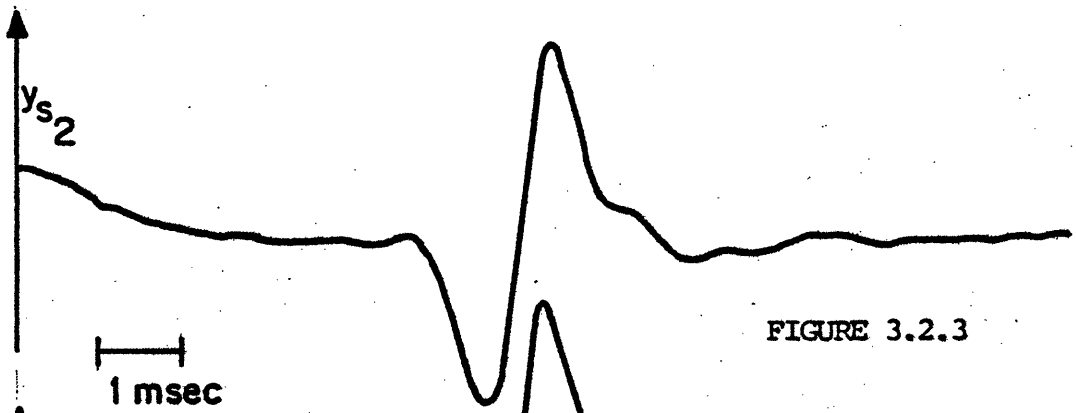


FIGURE 3.2.3



FIGURE 3.2.4

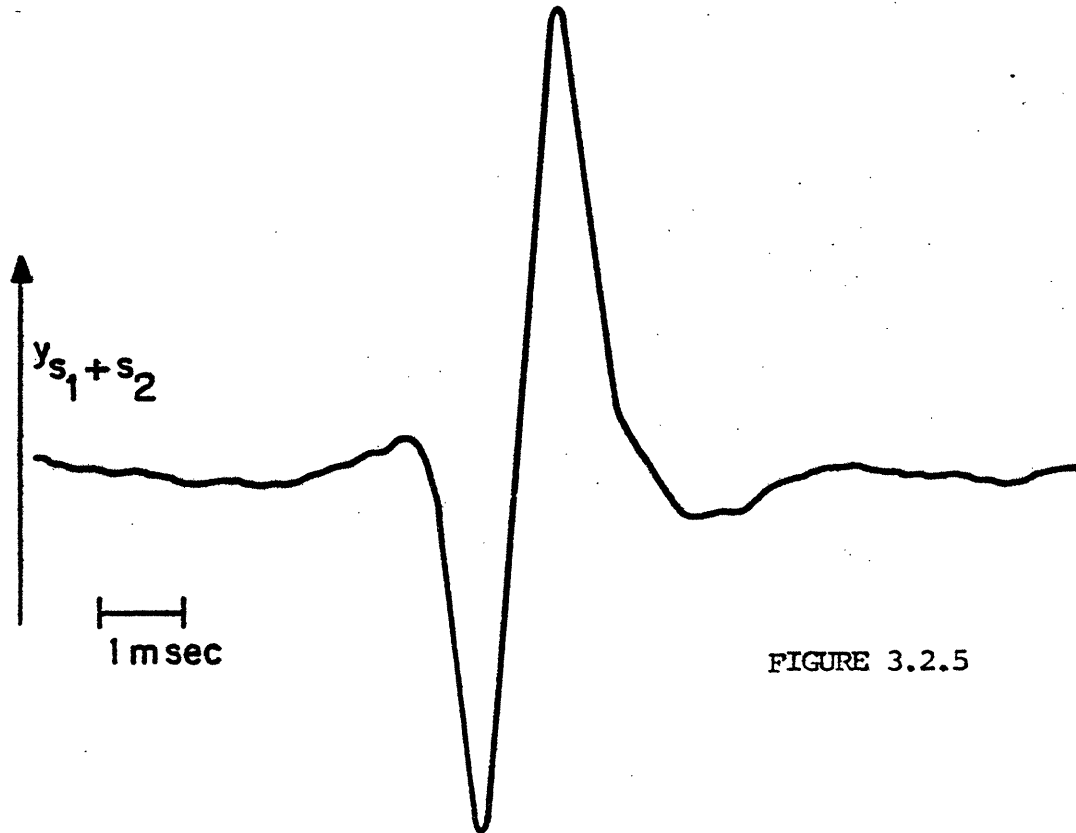
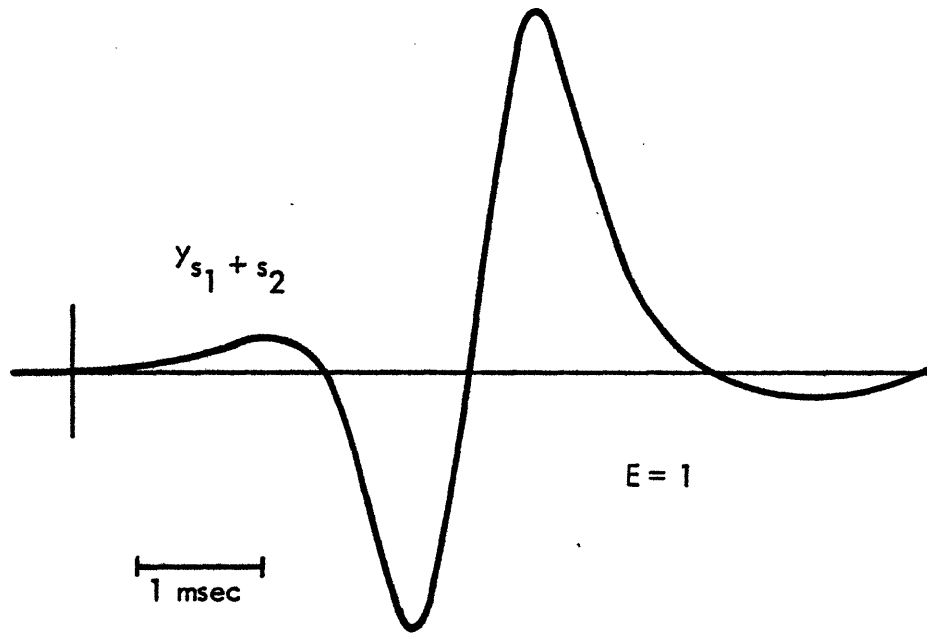
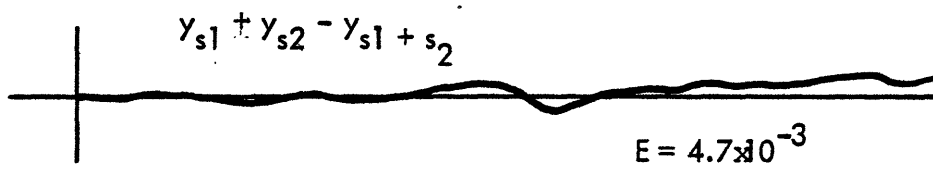


FIGURE 3.2.5



(a)



(b)

FIGURE 3.2.6

For noisy measurements, we should have:

$$y_{s_1} + y_{s_2} = y_{s_1+s_2} = w \quad (3.13)$$

where $w = w_{s_1} + w_{s_2} + w_{s_1+s_2}$ is the sum of all the measurement noises, which are assumed to be zero mean, independent gaussian processes. The residual according to (3.13) is shown in Figure 3.2.6

b). Assuming that the squared norm of $y_{s_1+s_2}$ is one, then the squared norm of the residual is 4.7×10^{-3} . This shows that at least for these branches of the ulnar nerve, the linearity assumption is justified.

3.2.2 - The Measurement Strategy

The measurement of $\phi(t)$ as defined by (3.8) is always corrupted by noise. The problem of estimating the distribution of conduction velocities $\underline{\beta}$ can therefore be posed in the following way: given,

$$y(t) = \sum_{j=1}^M \beta_j h(v_j, t) + n_y(t), \quad 0 \leq t \leq T \quad (3.14)$$

where $\underline{\beta}$ and $h(v_j, t)$ are as defined in the previous paragraph and $n_y(t)$ is measurement noise, modeled as a gaussian, zero mean, white noise process with $E\{n(t)n(\tau)\} = \sigma^2 \delta(t-\tau)$; we would like to estimate $\underline{\beta}$. Let's consider that only a finite set of discrete samples of $y(t)$ are taken at times $t_i = i\Delta$, $i = 0, \dots, T/\Delta$. Expression (3.14) can then be written as:

$$\underline{y} = H\underline{\beta} + \underline{n}_y \quad (3.15)$$

where \underline{y} and \underline{n}_y are vectors in R^N , $N = T/\Delta + 1$; $\underline{\beta}$ is in R^M ; H is a linear map $H: R^M \rightarrow R^N$, with elements defined by $H = [h_{i,j}] = [h(v_j, t_i)]$. The estimation of $\underline{\beta}$ would be a well posed linear estimation problem if $h(v_j, t)$ were known exactly, and the maximum likelihood estimate of $\underline{\beta}$ under such conditions is given in [R1] or [L5] by

$$\hat{\underline{\beta}} = (H'H)^{-1} H'y \quad (3.16)$$

Unfortunately this classical result cannot be applied because H is completely unknown a priori.

We will now approach the problem of how a priori information about H may be obtained by stimulating the nerve near the threshold. First, we will discuss the response of the nerve under such conditions. In 1933, Blair and Erlanger [B11] observed that when an electrical pulse is applied repeatedly to a nerve the following types of responses can be observed:

a) subthreshold : the nerve fiber will not respond to any of the stimulating pulses.

b) near threshold: the nerve fiber will respond to some of the pulses and it will skip others in a random way.

c) suprathreshold: the nerve fiber will respond to all of the stimulating pulses.

The range of stimulus intensities over which the nerve fiber behaves as in b) (that is, near threshold) has been found to vary from fiber to fiber, as reported by Verveen and Derksen [V2], but it is of the order of 1% of the threshold intensity. The threshold intensity is defined as the intensity which causes a 50% probability of response.

Another fact observed by Tasaki in 1953 [T3] is that the threshold of a nerve fiber is inversely proportional to fiber diameter. His results are shown in Figure 3.2.7. Based on his data, we would expect that if a weak stimulus is applied to the nerve, say at the level A indicated in the Figure, then only a few fast conducting fibers will res-

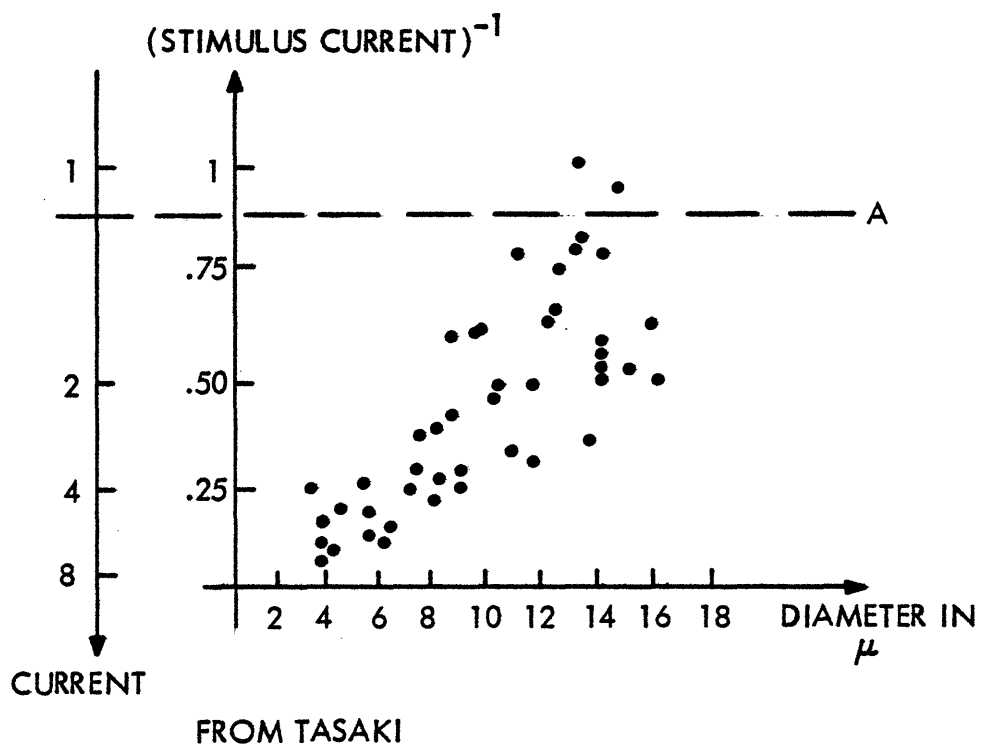


FIGURE 3.2,7

pond. In the example, only two of the largest fibers would be stimulated, with diameters of about 13.5 and 14.5 microns. Using $K_v = 6$ m/sec.micron, the respective velocities are 81 m/sec and 87 m/sec. Under these conditions, the average of a large number of recorded compound action potentials will be composed of action potentials from these fibers. Suppose that the action potential for each fiber lasts about 1.5 msec. At a distance of 15 cm from the site of stimulation, they will be separated by .17 msec., so that the averaged compound action potential will last about 1.67 msec. We could consider it, with some error, as having the shape of a single action potential travelling at 84 m/sec., the mean of the two fiber velocities, assuming that both were stimulated at threshold. The conclusion is that by using near threshold stimulus intensity, a response typical of the fastest fibers is obtained.

This result is slightly complicated by the additional fact that when a fiber is stimulated near threshold, there is a random variation in the onset time of the elicited action potentials, [B11], [P4]. For short electrical pulses, say up to 100 microsec. duration, this randomness associated to the timing of the action potentials is around $\pm .1$ msec. as reported by Erlanger and Gasser in [E1], but for stimuli of longer duration, say above 2 msec, it can be as much as $\pm .6$ msec. as reported by Poussard [P4]. Therefore, when a single nerve fiber is stimulated repeatedly at threshold intensity and a large number of individual responses are averaged (say $N > 1000$), the

resulting waveform is to a very good approximation given by:

$$y(t) = P_r(s) \int_{\tau_0}^{\tau_1} r(t - \tau) p(\tau, s) d\tau \quad (3.17)$$

where $P_r(s)$ is the probability of response for the stimulus intensity s ; $p(t, s)$ is the probability density of the fiber responding with delay t , when the stimulus has intensity s and $r(t)$ is the action potential which would be recorded using suprathreshold stimulus intensity. The probability density $p(t, s)$ was reported by Poussard [P4], Verveen and Derksen [V2] and others as a gaussian density. The standard deviation of $p(t, s)$ for s at threshold is roughly .05 msec. and its mean depends on the recording distance and the fiber velocity. Because of (3.17), we can more accurately say that in the example we have been discussing, when the nerve is stimulated repeatedly with a stimulus intensity A indicated in Figure 3.2.7, the average of the recorded action potentials is approximately the response of a population of fibers with conduction velocities distributed according to a probability density which depends on the recording distance and on $p(t, s)$ but which is nearly gaussian, with mean 84 m/sec. For a recording distance of 15 cm, the standard deviation in the apparent velocity is 2.5... m/sec., which is comparable to the deviation due to excitation of different fiber sizes (e.g. 81 vs. 87 m/sec.). There may also be an "entrainment" of the action potentials from fibers which conduct at similar velocities.* If this occurs, the dispersion in the apparent conduction velocity is reduced.

* Lettvin, J.- personal communication.

The conclusion from this analysis is that when a peripheral nerve is stimulated repeatedly by a weak electrical pulse, the averaged recorded compound potential can be considered as being approximately a scaled version of a single action potential travelling at a velocity which is the mean, v_r , of a narrow population of faster fibers.

The following experimental procedure can therefore be used to obtain some information about the matrix H in expression (3.15): a noise corrupted measurement of $h(v_r t)$ is obtained by averaging a large number of nerve responses to a weak electrical pulse, where v_r is the mean velocity in the sense defined above. This measurement can be written in sampled data form as:

$$\underline{z} = \underline{h}_r + \underline{n}_z \quad (3.18)$$

where \underline{n}_z represents measurement noise and it is modeled as a vector of zero mean, gaussian and independent random variables; $\underline{z}, \underline{h}_r$ and \underline{n}_z are vectors in R^N ; $h_{r_i} = h(v_r t_i)$.

The nerve is then stimulated with a pulse strong enough to excite nearly all myelinated fibers and the recorded compound action potential $y(t)$ is given by (3.14) or in sampled data form by (3.15). With these two measurements we would like to generate an estimate of the distribution of conduction velocities $\underline{\beta}$. This estimation problem is examined in Section 3.3.

3.2.3 - Electrode Artifact Removal

The signal recorded from the nerve is assumed to be the linear super-position of the following components: a) The compound action potential $\sum_{j=1}^M h(v_j t) \beta_j$ produced in the nerve by the stimulus; b) A "stimulus artefact" $a(t)$ introduced by the stimulating electrodes; c) A D.C. bias, b , of the recording electrodes and d) recording noise $w(t)$. The recorded signal $y(t)$ is therefore modeled as:

$$y(t) = \sum_{j=1}^M h(v_j t) \beta_j + a(t) + b + w(t)$$

In order to estimate the distribution of conduction velocities β_j , $j = 1 \dots M$, the artefact $a(t)$ and the bias terms have to be removed from the record, $y(t)$. In this section the modeling and the problem of estimating the parameters which describe $a(t)$ are examined.

The stimulus artefact was the major unwanted signal corrupting the measurements in most of the records. In order to better understand it, several experiments were done. The most appealing hypothesis which emerged from these experiments, was that the stimulus artefact has two major components: one is the propagation of the electrical pulse through the biological medium to the recording electrodes, and the other is due to the propagation of the stimulus by electromagnetic radiation, from the stimulating electrodes to the recording electrodes. The first component is usually very small if the preparation is carefully grounded

while the second component is minimized by shielding all cables.

The hypothesis about the composition of the stimulus artefact is consistent with the experimental observation that the stimulus artefact grows linearly with stimulus intensity. This is now briefly reported

The experimental set up was the same as for measuring the compound action potential from the median nerve and it is described in detail in Appendix 3. The electrical stimulus, consisting of an electrical pulse of 50 microseconds duration was increased from 0 to 84 Volts and measurements were taken at 13 different intensities. At each of these intensities, the stimulus artefact was measured by averaging 1024 individual responses, and one such average response is shown in Figure 3.2.8. The peak-to-peak values were plotted against stimulus intensity. The linear regression line of the peak-to-peak values versus stimulus intensity was computed using least-squares and it is shown in Figure 3.2.9.

The linear nature of the artefact suggested the following solution - soon discarded for obvious reasons - to eliminate it from the action potential records: First, using a very small stimulus intensity, so that no nerve fiber in the trunk is stimulated the artefact is measured:

$$y_1(t) = a(t) + n_1(t), \quad t \in [0, T] \quad (3.18a)$$

where $n_1(t)$ is measurement noise with zero mean and spectral density

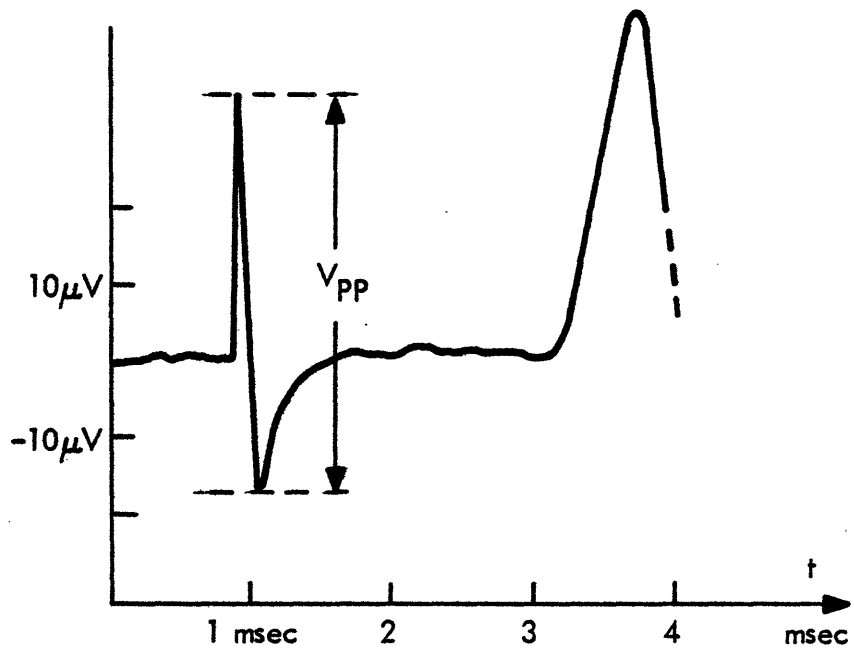


FIGURE 3.28

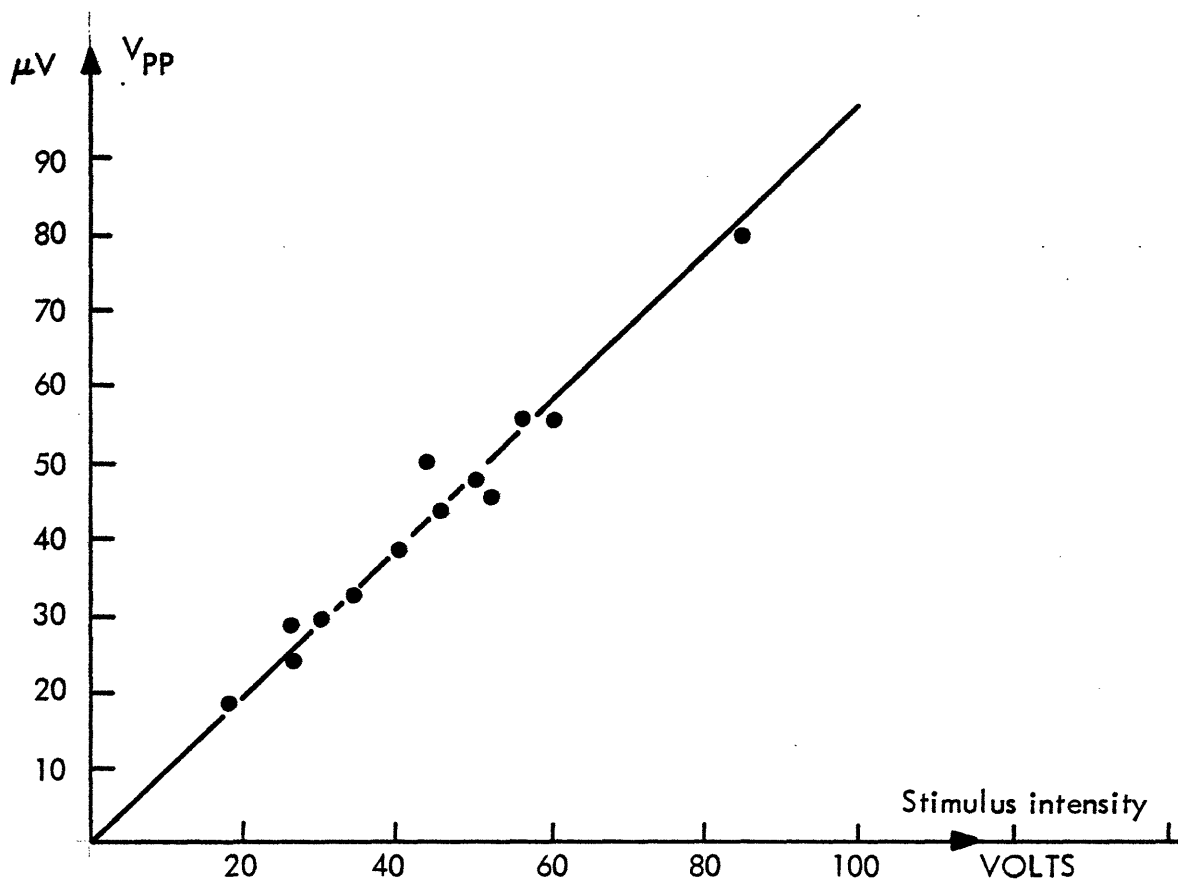


FIGURE 3.29

σ_1^2 . Then the compound action potential is measured:

$$y_2(t) = r(t) + Ka(t) + n_2(t), \quad t \in [0, T] \quad (3.18b)$$

where $r(t)$ is the signal from the nerve, and $n_2(t)$ is zero mean noise with spectral density σ_2^2 . The scaling factor K is estimated by the ratio of the stimulus intensities used to obtain $y_1(t)$ and $y_2(t)$. The artefact free signal is then obtained by:

$$\begin{aligned} Y_2(t) &= y_2(t) - Ky_1(t) = \\ &= r(t) + n_2(t) - Kn_1(t) = \\ &= r(t) + n(t) \end{aligned} \quad (3.18c)$$

where the noise $n(t)$ has spectral density $\sigma_n^2 = \sigma_2^2 + K^2\sigma_1^2$. Clearly, we need a very small σ_1^2 in order to have σ_n^2 reasonably small because K is in general large. We have calculated that under typical conditions ($K = 10$, $\sigma_n^2 = 2\sigma_2^2$, and $y_2(t)$ obtained by averaging 1024 responses at the rate of 10 stimulus/sec) $y_1(t)$ should be the average of about 10^5 individual responses which would take about 3 hours of averaging. This approach was abandoned. The following solution to eliminate the artefact was finally used:

It was realized that the artefact could usually be modeled with a very good accuracy by the following function:

$$\begin{aligned} a(t) &= A(1 - at)\exp(-at) && t > 0 \\ &= 0 && \text{otherwise} \end{aligned} \quad (3.18d)$$

In the actual artefact the discontinuity at $t = 0$ is obviously non-existent, therefore there is always a large error between the model and the actual signal in the neighborhood of $t = 0$. Otherwise the model matches the artefact quite well. The least-squares estimation of A and α is described in Appendix 2.

3.3 - THE ESTIMATION PROBLEM

The following estimation problem is considered, given:

$$Z = H + W \quad (3.19)$$

$$\underline{y} = H\underline{\beta} + \underline{v} \quad (3.20)$$

where $Z = z_{ij}$, $H = h_{ij}$ are matrices in $R^{N \times M}$, $\underline{y} \in R^N$, $\underline{\beta} \in R^M$, $N < M$; \underline{v} is a vector of N independent random variables, with $E\{v_i\} = 0$; $E\{v_i v_j\} = \sigma_2^2 \delta_{i,j}$ and $W = w_{ij}$ is a matrix of $N \times M$ independent random variables with $E\{w_{ij}\} = 0$ and $\sigma_{ij}^2 = \sigma_1^2$. We would like to get the joint least squares estimate of H and $\underline{\beta}$, namely the pair $\hat{H}, \hat{\underline{\beta}}$ for which $\ell(H, \underline{\beta})$,

$$\ell(H, \underline{\beta}) = \alpha ||Z-H||^2 + ||\underline{y}-H\underline{\beta}||^2 \quad (3.21)$$

$$\alpha = \sigma_2^2 / \sigma_1^2 \quad (3.22)$$

is minimum. We note that if the random variables \underline{v} and W are gaussian then the values of H and $\underline{\beta}$ which realize the minimum of $\ell(H, \underline{\beta})$ are also the maximum likelihood estimates of those variables.

Before attempting the minimization of $\ell(H, \underline{\beta})$ we should determine whether it has a minimum for all values of the measurements Z and \underline{y} . We note that since $\ell(H, \underline{\beta})$ is a sum of norms it implies that is bounded below and that $\inf \ell(H, \underline{\beta}) = 0$. Furthermore, since $\ell(H, \underline{\beta})$ is continuous and continuously differentiable, if a minimum exists it must

satisfy the necessary conditions:

$$\frac{\partial \ell(H, \beta)}{\partial H} = \alpha(H - Z) + (H\beta - Y)\beta' = 0 \quad (3.23)$$

$$\frac{\partial \ell(H, \beta)}{\partial \beta} = H'H\beta - H'Y = 0 \quad (3.24)$$

which - as shown in Appendix 1 - is equivalent to:

$$\beta\beta'Z'Y + (\alpha Z'Z - Y'YI)\beta - \alpha Z'Y = 0 \quad (3.25)$$

$$H = Z + (\alpha + \beta\beta')^{-1}(Y - Z\beta)\beta' \quad (3.26)$$

Considering the orthonormal transformation Φ such that $\Phi'(Z'Z)\Phi = \Delta$; where Δ is the Jordan form of $Z'Z$ and defining $\underline{\gamma} = \Phi'\beta$, $\underline{u} = \Phi'Z'Y$, conditions (3.25) and (3.26) are equivalent to solving:

$$\gamma_j = \alpha u_j / (r + \alpha \lambda_j^2 - Y'Y) \quad , j = 1 \text{ to } M \quad (3.27)$$

where r is defined by $r = \underline{\gamma}'\underline{u}$ and it is a root of:

$$r = \sum_{j=1}^M \alpha u_j^2 / (r + \alpha \lambda_j^2 - Y'Y) \quad (3.28)$$

The λ_j^2 , j from 1 to M are the eigenvalues of the matrix $Z'Z$.

Now let's define for all $\beta \in R^M$, the function $f(\beta)$ as:

$$f(\beta) = \min_{H \in R^{N \times M}} \ell(H, \beta) = \ell(H(\beta), \beta) \quad (3.29)$$

we note that since for each β , $\ell(H, \beta)$ is a quadratic function of H , it has also a minimum which satisfies necessary condition (3.23).

It is now shown that if $\lambda_{\min}^2 \neq 0$, where λ_{\min}^2 is the minimum eigenvalue of $Z'Z$ and $u_{\min}^2 \neq 0$ then for one of the roots of (3.25) we have that:

$$f(\underline{\beta}) \leq \alpha \lambda_{\min}^2 \quad (3.30)$$

then it is shown that:

$$\lim_{\|\underline{\beta}\| \rightarrow \infty} f(\underline{\beta}) \geq \alpha \lambda_{\min}^2 \quad (3.31)$$

therefore for $\lambda_{\min}^2 \neq 0$, and $u_{\min}^2 \neq 0$ the value of $\underline{\beta}$ which realizes the minimum must be such that $\|\underline{\beta}\| < \infty$, that is $\underline{\beta} \in R^M$ and it is among the roots of (3.25). To complete the proof, let's show (3.30) and (3.31). In fact:

$$f(\underline{\beta}) = \min_{H \in R^{N \times M}} \ell(H, \underline{\beta}) = \ell(H(\underline{\beta}), \underline{\beta}) \quad (3.32)$$

where $H(\underline{\beta})$ is given by (3.26). Replacing it in (3.32), we obtain:

$$f(\underline{\beta}) = \alpha \|\underline{Y} - Z\underline{\beta}\|^2 / (\alpha + \|\underline{\beta}\|^2) \quad (3.33)$$

and,

$$f(\underline{\beta}) = \frac{\alpha}{\alpha + \|\underline{\beta}\|^2} (\underline{Y}'\underline{Y} - \underline{\beta}'Z'\underline{Y} + \underline{\beta}'(Z'Z\underline{\beta} - Z'\underline{Y})) \quad (3.34)$$

Let $\underline{\beta}^*$ be a root of (3.25), then

$$\alpha Z'(Z\underline{\beta}^* - \underline{Y}) = \underline{Y}'\underline{Y}\underline{\beta}^* - \underline{\beta}^* \underline{\beta}^{*'} Z'\underline{Y} \quad (3.35)$$

which if replaced in (3.34) gives:

$$f(\underline{\beta}^*) = \underline{y}'\underline{y} - \underline{\beta}^{*'}\underline{z}'\underline{y} \quad (3.36)$$

or in terms of r as defined previously:

$$f(\underline{\beta}^*) = \underline{y}'\underline{y} - r^* \quad (3.37)$$

where $r^* = \underline{u}'\underline{y}^* = \underline{\beta}^{*'}\underline{z}'\underline{y}$ and is a root of (3.28). The right hand side of equation (3.28) is plotted in Figure 3.3.1 and the intersections with the line $g(r) \triangleq r$ are its roots. If $u_{\min} \neq 0$, then there is always a real root r^* such that:

$$r^* > -(\alpha\lambda_{\min}^2 - \underline{y}'\underline{y}) \quad (3.38)$$

that is

$$f(\underline{\beta}^*) < \alpha\lambda_{\min}^2 \quad (3.39)$$

Consider now,

$$\begin{aligned} \lim_{\|\underline{\beta}\| \rightarrow \infty} f(\underline{\beta}) &= \lim_{\|\underline{\beta}\| \rightarrow \infty} \alpha \|\underline{y} - \underline{z}\underline{\beta}\|^2 / (\alpha + \|\underline{\beta}\|^2) \\ &= \lim_{\|\underline{\beta}\| \rightarrow \infty} \alpha (\underline{y}'\underline{y} + \underline{\beta}'\underline{z}'\underline{z}\underline{\beta} - 2\underline{y}'\underline{z}\underline{\beta}) / (\alpha + \|\underline{\beta}\|^2) \\ &= \lim_{\|\underline{\beta}\| \rightarrow \infty} \alpha \left(\sum_{j=1}^M \lambda_j^2 \gamma_j^2 - 2 \sum_{j=1}^M \gamma_j u_j + \underline{y}'\underline{y} \right) / (\alpha + \|\underline{y}\|^2) \end{aligned} \quad (3.40)$$

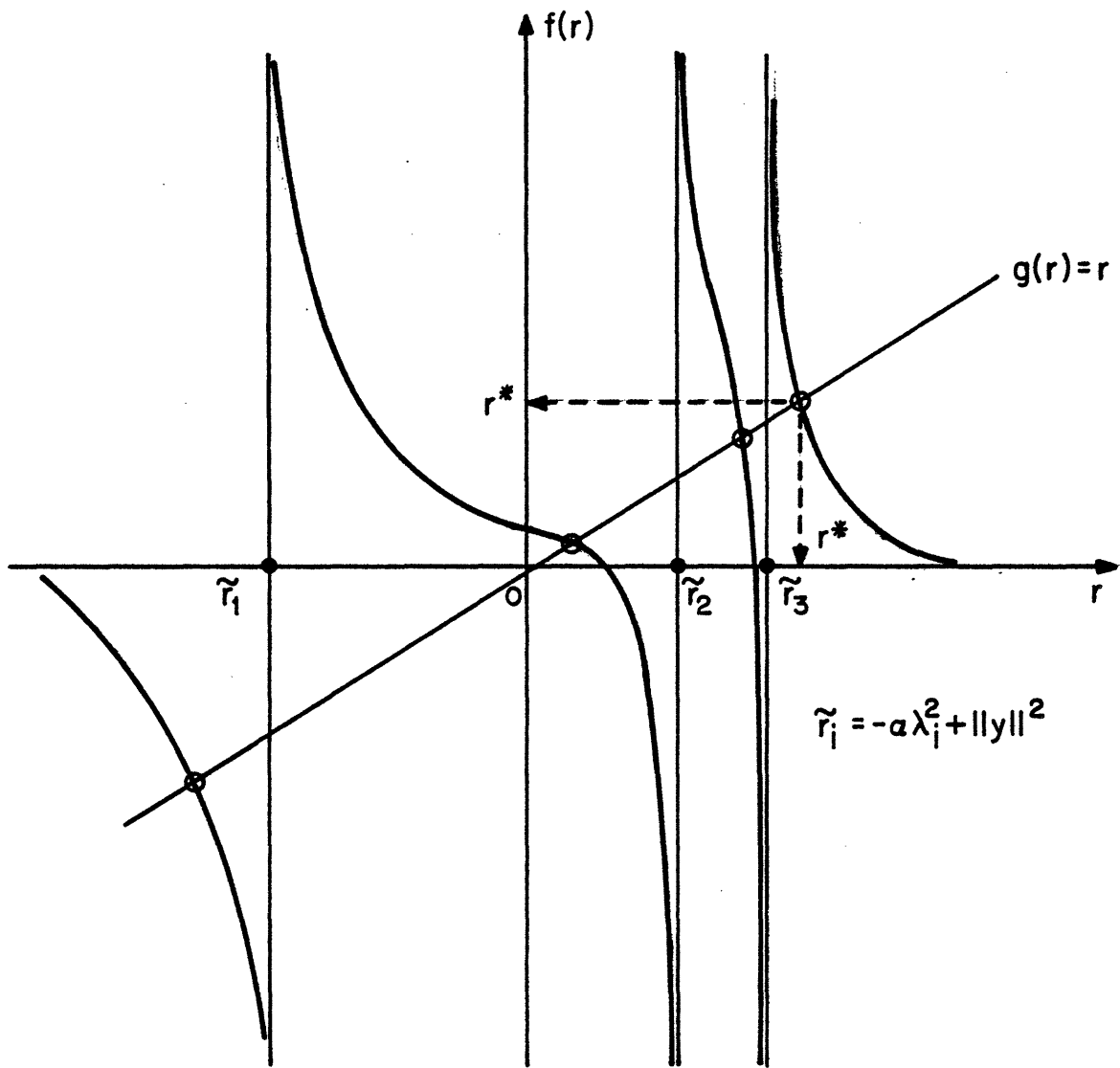


FIGURE 3.3.1

which is equal to:

$$\alpha \lambda_k^2 \quad \text{if } \gamma_k^2 \rightarrow \infty \quad \text{alone and}$$

$$\alpha \sum_{j=1}^M \lambda_j^2 \quad \text{if all } \gamma_j^2 \rightarrow \infty$$

Clearly the least value of such limit is $\min_j \alpha \lambda_j^2 = \alpha \lambda_{\min}^2$, therefore

$$\lim_{\|\underline{\beta}\| \rightarrow \infty} f(\underline{\beta}) \geq \alpha \lambda_{\min}^2 \quad (3.41)$$

which completes the proof.

3.3.1 - Explicit Solution of the Minimization Problem

In order to obtain all the elements of the matrix Z in $\ell(H, \underline{\beta})$, we should selectively excite each of the velocity groups in the nerve. This cannot be done in any simple way. As was described in paragraph 3.2.2 only one of the rows of Z can be measured directly, namely the one which is generated by a narrow population of nerve fibers all conducting at some reference velocity v_r :

$$\underline{z} = \underline{h}_r + \underline{w} \quad (3.42)$$

The remaining $M-1$ rows of Z - each corresponding to a measurement of the action potential due to one velocity group - are generated by observing that the ensemble average of Z , which is H , has its elements h_{ij} related as:

$$h_{ij} = h(v_j t_i) = h(v_r \frac{v_j}{v_r} t) = h(v_r t_k) \quad (3.43)$$

where $t_k = (v_j/v_r)t_j$, that is, the rows of H are discrete time versions of continuous functions $h(v_j t)$ of t which are "stretched" versions of some basic shape $h(v_r t)$. The j -th row of matrix Z is then obtained as:

$$z_{ij} = z(v_j t_i) = z(v_r \frac{v_j}{v_r} t_i) = a_k z_{\ell k} + (1-a_k) z_{\ell k+1} \quad (3.44)$$

$$k = \max\{n; 0 < n < (\frac{v_j}{v_r}) t_i\} \quad \text{and} \quad a_k = k - (\frac{v_j}{v_r}) i \quad (3.45)$$

for $i = 1 \dots N$.

where $\underline{z} = [z_{\ell 1} \dots z_{\ell N}]$, defined by (3.42). With the selection of the rows of Z according to the linear interpolation method indicated above, the resulting estimator is no longer the maximum likelihood estimate that the minimization of $\ell(H, \underline{\beta})$ generates when the noise processes have independent gaussian distributions.

If the conditions for the existence of a global minimum are satisfied, as discussed in the previous section, then the value of $\underline{\beta}$ which realizes the minimum can be computed using the necessary conditions. A quick calculation leads to the following expression for this $\underline{\beta}$:

$$\underline{\beta} = \left(\frac{r^* - Y'Y}{\alpha} I + Z'Z \right)^{-1} Z'Y \quad (3.46)$$

where r^* is a root of equation (3.28). As we have seen, only the maximum root of (3.28) gives a global minimum for $\ell(H, \underline{\beta})$, that is: $r^* = \max\{r; r \text{ is a root of (3.28)}\}$. The computation of this maximum is done in the following way: we know that $r^* > -(\alpha \lambda_{\min}^2 - y'y)$, so that the algorithm starts with some r^0 which satisfies this condition and keeps doubling it until r^i is less than the right hand side of (3.28). At this point, a rapidly converging binary scheme is used: for $j > i$,

$$\begin{aligned}
 r^{j+1} = & \begin{array}{l} r^j - r^i/2^{j+i} \text{ if right hand side of 3.28} < r^j \\ \text{stop search} \quad " \quad " \quad " \quad " \quad " \quad " \quad " = r^j \\ r^j + r^i/2^{j+i} \quad " \quad " \quad " \quad " \quad " \quad " \quad " > r^j \end{array} \quad (3.48)
 \end{aligned}$$

If exact convergence is not reached in 20 steps, the search is halted and the last value of r^j is used as the solution which is always accurate at least to six decimal places. The step-by-step algorithm to compute the estimate of $\underline{\beta}$ is the following:

1- From Z which was obtained by (3.44) and (3.45), and y , the matrix $Z'Z$, its eigenvalues and eigenvectors are computed; vectors $Z'y$ and $\underline{u} = \phi Z'y$ are also obtained.

2- Knowing the eigenvalues of $Z'Z$ and the elements of \underline{u} , the maximum root of (3.28) is then obtained according to the algorithm given in (3.48).

3- Finally, the vector $\underline{\gamma}$ is obtained according to (3.27) using the maximum root of (3.28) and then $\underline{\beta} = \phi \underline{\gamma}$ is determined.

In Appendix 4, this estimation procedure is evaluated by using a synthetic example. An evaluation of its performance using actual experimental data is presented in the next chapter.

CHAPTER 4

EXPERIMENTAL VERIFICATION OF THE TECHNIQUE

4.1 - INTRODUCTION

One of the basic motivations for the development of the technique described in this thesis was to produce an alternative to nerve biopsy in human subjects. The final electrophysiological technique and signal processing were consequences of a series of (most of the time) very simplified assumptions about nerve fibers, peripheral nerves and the electric fields they generate. In order to evaluate how accurate the generated results are, despite the built in weaknesses of the assumptions and of the whole model as well, we have to compare these results with those given by biopsy. Of course

the use of human subject for that purpose wouldn't be justified considering the extensive damage caused to the individual by such procedure. We decided then to use an animal, choosing a monkey because of the anatomical similarities of the fore limbs of this species to the human arms and hands. The result of such an experiment is described next.

4.2 - THE EXPERIMENT

The electrophysiological technique of estimating the distribution of conduction velocities described in the previous chapter was compared to standard histological techniques, using for this purpose a sensory branch of the ulnar nerve of a monkey (*rhesus macaca*). In healthy peripheral nerves, the conduction velocity of a fiber is proportional to its diameter as we have seen in paragraph 2.2.1.1, namely $v = K_v D$. The distribution of conduction velocities $\beta(v)$ was defined by (3.10) in terms of the fiber diameter histogram $S(D)$ as:

$$\beta(v) = K_v^2 S(v/K_v) \quad (4.1)$$

or in sampled data form:

$$\underline{\beta} = [\beta_1 \dots \beta_M]; \quad \underline{S} = [S_1 \dots S_M] \quad \text{with}$$
$$\beta_j = K_v^2 S_j \quad (4.2)$$

where $\beta_j = \beta(v_j)$, $S_j = S(v_j/K_v)$. In the experiment which is now described, $\underline{\beta}$ was determined using the electrophysiological method and also from the diameter histogram of the nerve using (4.2), and the two results were compared.

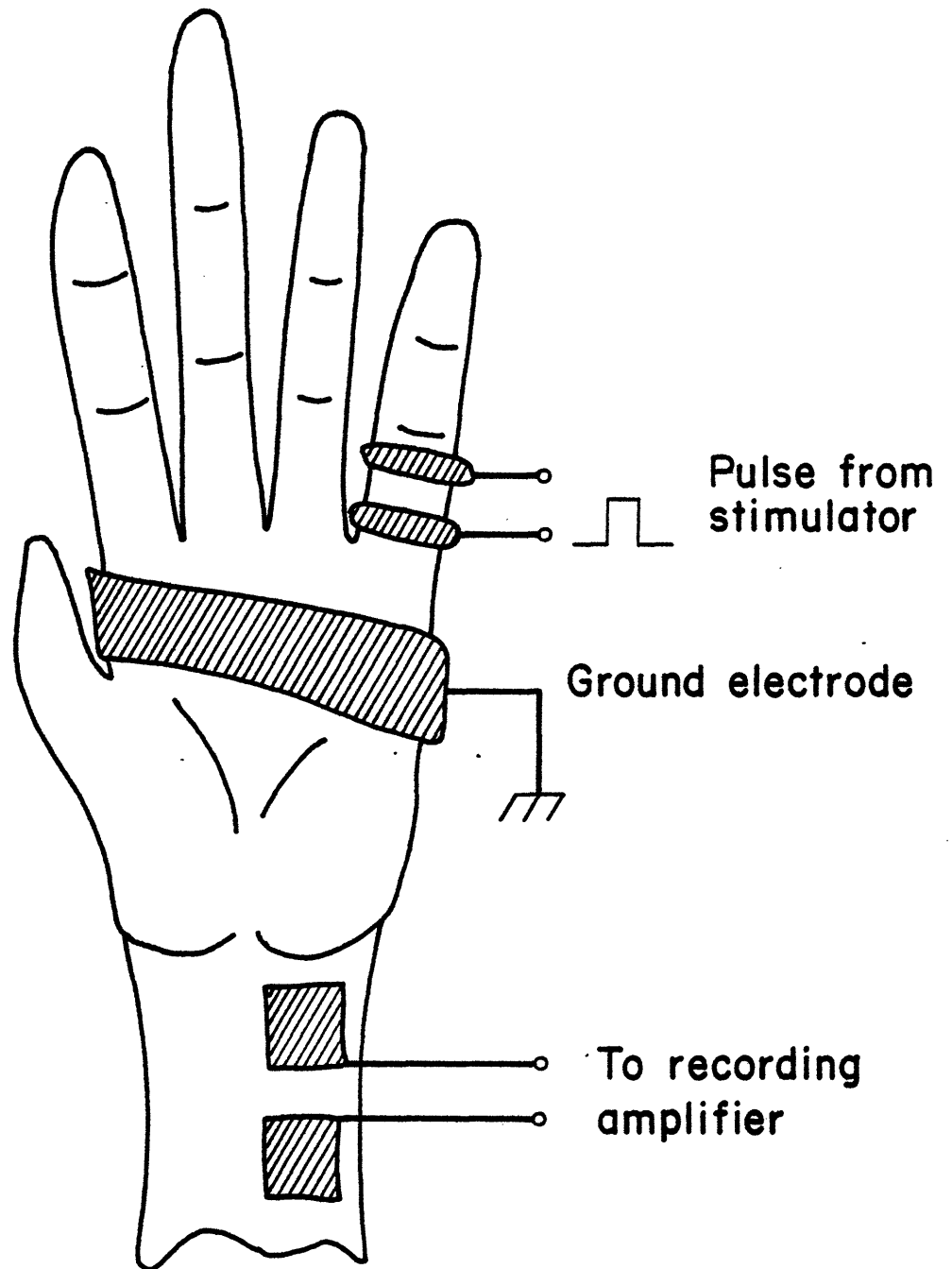
4.2.1 = Methods

4.2.1.1. - The Subject

The subject was a 2 year old healthy female rhesus macaca monkey. It was anesthetized with 1.5 cc of Nambuthal, and the same dosage was repeated 90 minutes later. The deep anesthesia assured complete relaxation of the muscles, so that no unwanted electromyographic signals corrupted the recorded nerve signals, as usually happened in human studies. The animal was laid in its right side, and the left arm was placed in the natural resting position. The electrophysiological testing lasted about 2 hours.

4.2.1.2. - Electrophysiological Procedures

A pair of ring electrodes was placed in the proximal phalanx of the left finger 5 - which is entirely innervated by a branch of the ulnar nerve - for the delivery of electrical stimulation. A layer of Teca electrode gel was placed between the electrodes and the skin to assure low electrode resistance . A large strap electrode soaked in sodium chloride was wrapped around the hand to be used as the ground of the preparation. The recording electrodes were a pair of large 1 sq.cm area square shaped lead pieces, placed above the ulnar nerve at the wrist, and separated by a distance of about .5 cm edge-to-edge. A layer of Teca electrode gel was used to improve the electrode contact. The arrangement is shown in



STIMULATING AND RECORDING ELECTRODE ARRANGEMENT

FIGURE 4.2.1

Figure 4.2.1.

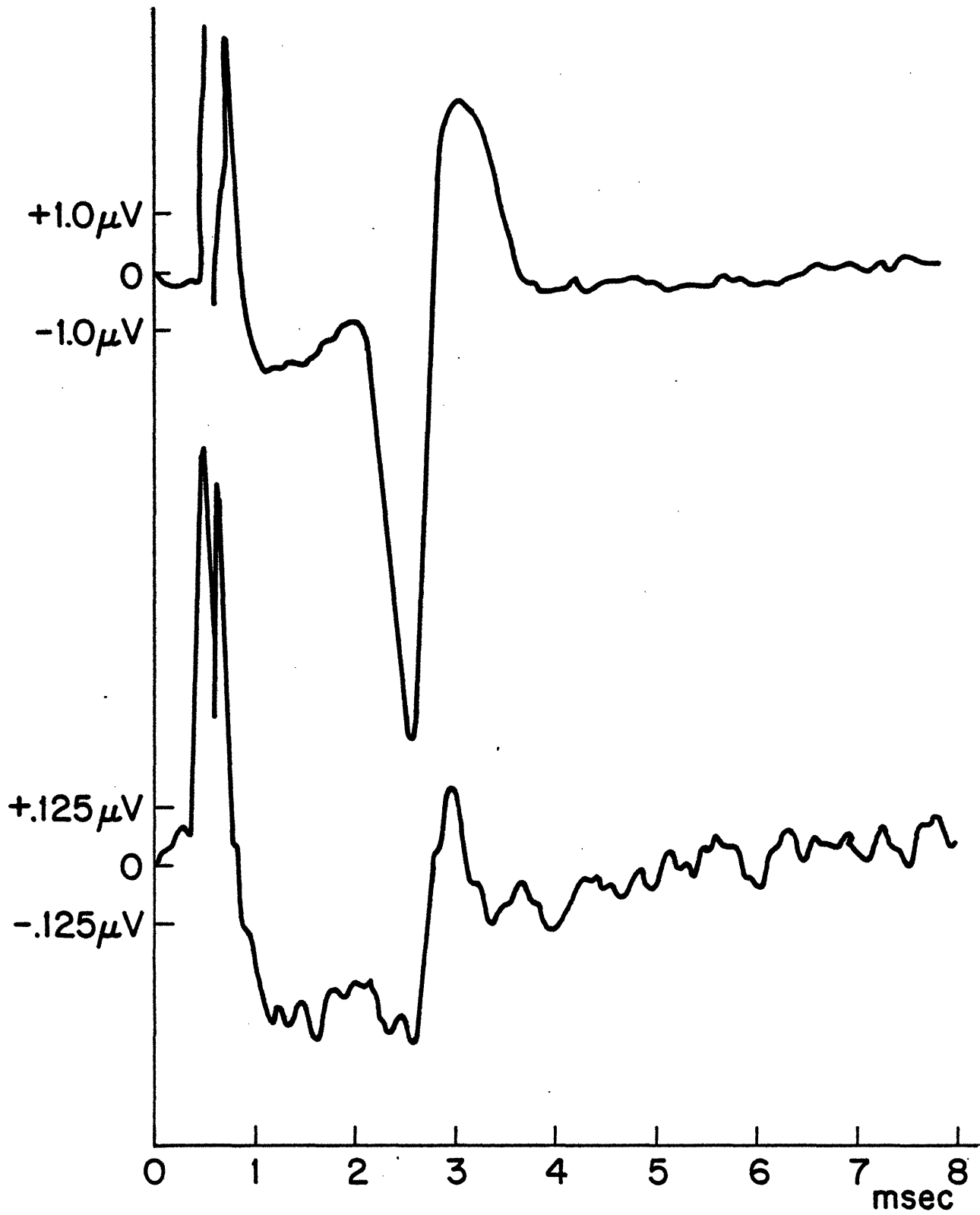
Electrical stimuli to the finger were delivered at the rate of 10 stimulus/second by a Grass stimulator and they were pulses of 50 microsec. duration. The reason for using such a short duration pulse was to maximize the synchronization between the action potentials from different fibers, and minimize the statistical dispersion of repeated action potentials in the same fiber as discussed in section 3.2.2.

The signal from the recording electrodes was amplified by a Grass amplifier and recorded on tape, with a stimulus marker recorded synchronously in another channel. The signal from the Grass amplifier was also fed into a digital averager in order to estimate the number of nerve responses needed for a good signal-to-noise ratio.

The intensity of the electrical pulse used as stimulus could be adjusted continuously over the range 0-200 Volts. The supramaximal stimulus intensity - that is the intensity which would evoke a action potential in nearly all myelinated fibers of the nerve - was determined by increasing the pulse strength until no further increase in the amplitude of the recorded compound action potential could be observed visually. The final value of the intensity used was about 20% above this critical intensity. Then 1024 responses were recorded and averaged. The adjustment for threshold stimulation was much more difficult and critical. First, the intensity was lowered to

the point where no nerve response could be observed on a single sample basis. Then, about 100 responses were averaged and if no response could be seen the amplitude was increased. If the presence of a signal from the nerve was evident, then the intensity was lowered. This process was repeated several times, until it was likely that only a narrow population of fibers were responding. If at any stage two or more individual peaks could be observed, indicating that two or more distinct populations of fibers were stimulated, the stimulating electrodes were repositioned. With the stimulus adjusted this way, 4096 samples were recorded and averaged. The recorded waveforms are shown in figure 4.2.2.

The baseline of both records is corrupted by what is known in electrophysiology as "shock artefact" or "stimulus artefact". It is a disturbance produced by the stimulating pulse and is synchronized to it. It is due to the transmission of the electrical pulse from the stimulating electrodes to the recording electrodes through the biological medium and electromagnetic radiation. The relative intensity of this artefact is for all practical purposes unpredictable. Some approximate models can be constructed for the artefact and it can be eliminated partially from the records. In Appendix 2, we describe in detail one such model and the algorithm used to estimate the parameters involved. The artefact-treated records were processed according to the signal processing described in paragraph 3.3.1 and



SIGNALS RECORDED FROM THE ULNAR NERVE

FIGURE 4.2.2

the estimate for the distribution of conduction velocities is shown in Figure 4.2.4.

4.2.1.3 - Histological Procedures

One week after the electrical data was gathered, the monkey was sacrificed, perfused with formaldehyde, the hands were chopped off above the wrist and fixed in formaldehyde for 3 days. After fixation, the fingers were removed with no damage to the proximal phalanges. The phalanx from the left finger 5 was placed in decalcifying solution for 4 days, until the bone was soft enough to be cut. It was then imbedded in parafin and cross-sections of about 6 to 8 μ thick were cut at about the medial region where the nerve was electrically stimulated in the electrophysiological experiment. The cross-sections were stained with Kultschisky blue dye - a myelin stain - for light microscope examination.

Under the microscope, 18 separate branches of different sizes could be identified. One contained as many as 250 myelinated nerve fibers, while another had only 7. Some of the branches were excessively oblique to the direction of the cut so that the diameters of the fibers on these branches couldn't be measured reliably. Oblique cuts were estimated to represent about 20% of the total number of fibers.

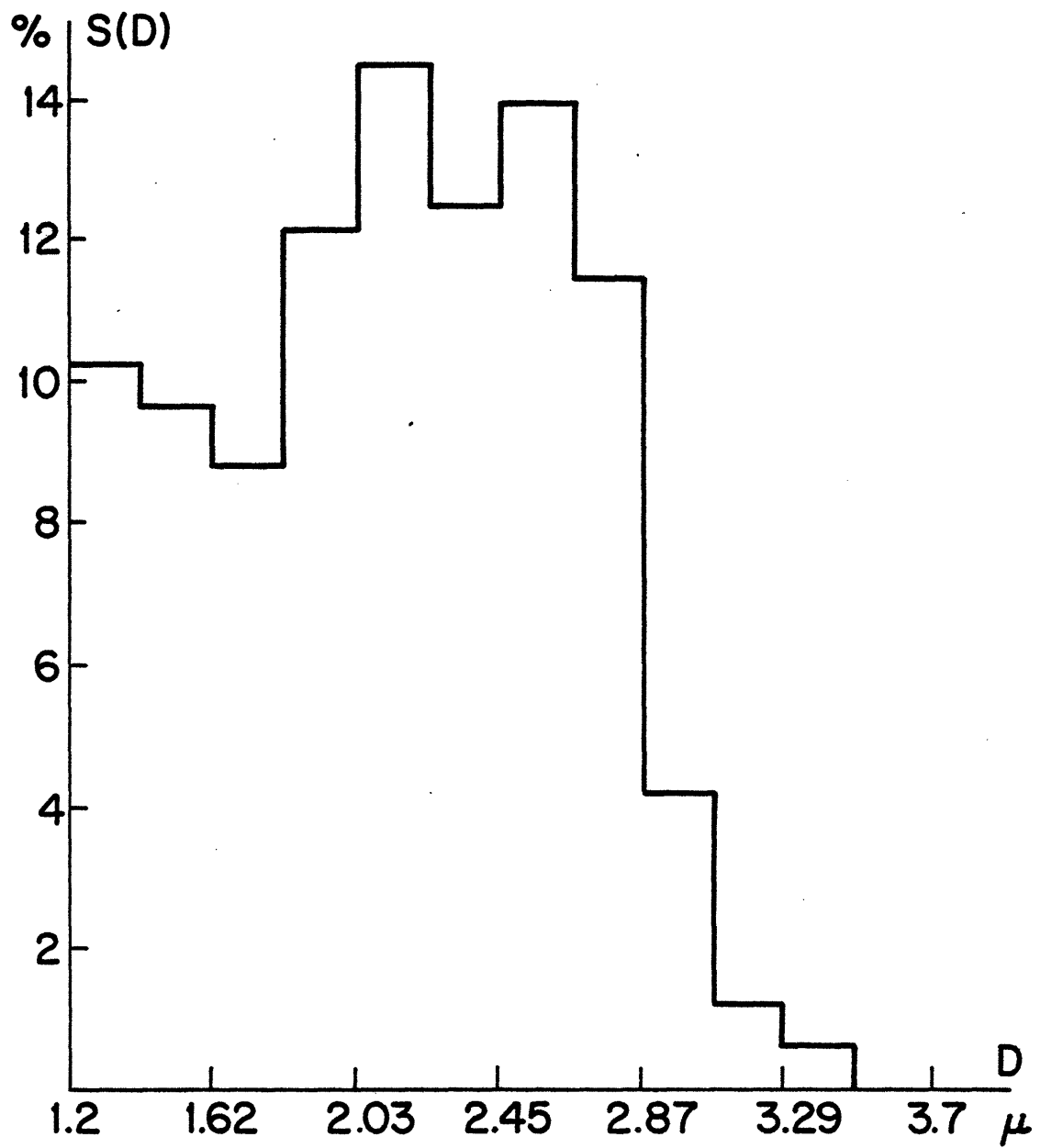
The prolonged decalcification of the finger dehydrated the

nerves causing them to shrink down to about only 30-35% of their original sizes. The amount of shrinkage was estimated by observing that the maximum measured diameter was about 3.5μ while the expected maximum diameter under normal - non dehydrated - conditions would be around 10μ . Also, the shrinkage could be deduced from the estimated value of K_v which turned out to be $19.3 \text{ m/sec} \cdot \mu$ while its usual value it is somewhere about 5 to $7 \text{ m/sec} \cdot \mu$.

Another problem, also due to dehydration, was the general departure of the fiber cross-sections from the circular shape, so that we had to define the diameter as the average of the maximum and the minimum measured diameter for each fiber.

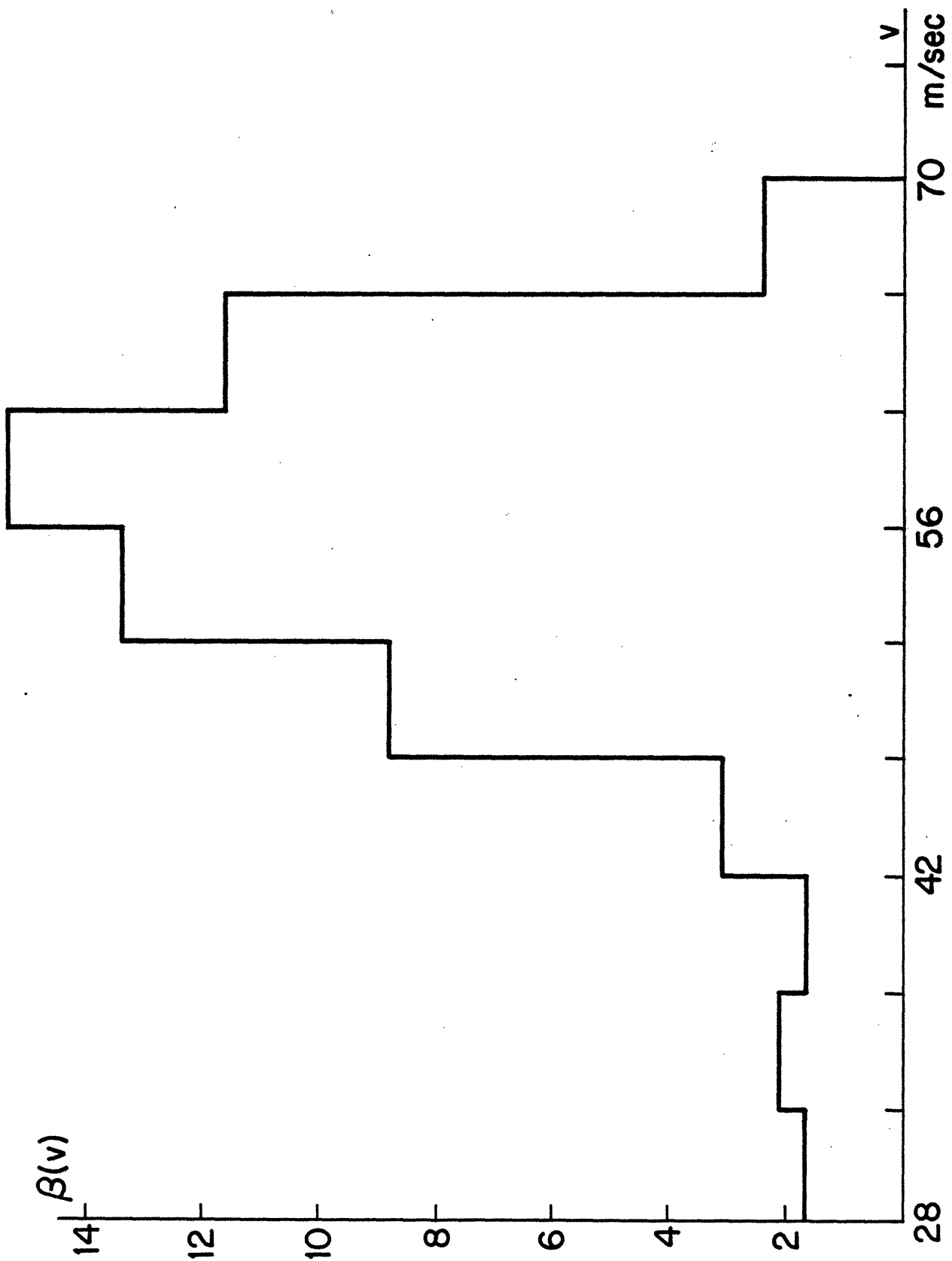
In order to measure the diameters, the sections were magnified 400 X and photographed. The photographs were printed with a 4 X enlargement so that the final magnification was 1600 X, which caused the boundaries of the myelin sheath of the fibers to blurr. This imposed the lower limit on the mesh size chosen to group the diameters, which was about $.21\mu$. The total diameter range of 1.2 to 3.5μ was divided into 11 subintervals

To minimize the effects of the blurring in the measurements of the diameters, the boundaries were enhanced by drawing them on an acetate sheet placed over the photographic print. The final measurements were taken from these drawings. The diameter histogram found this way is shown in Figure 4.2.3.

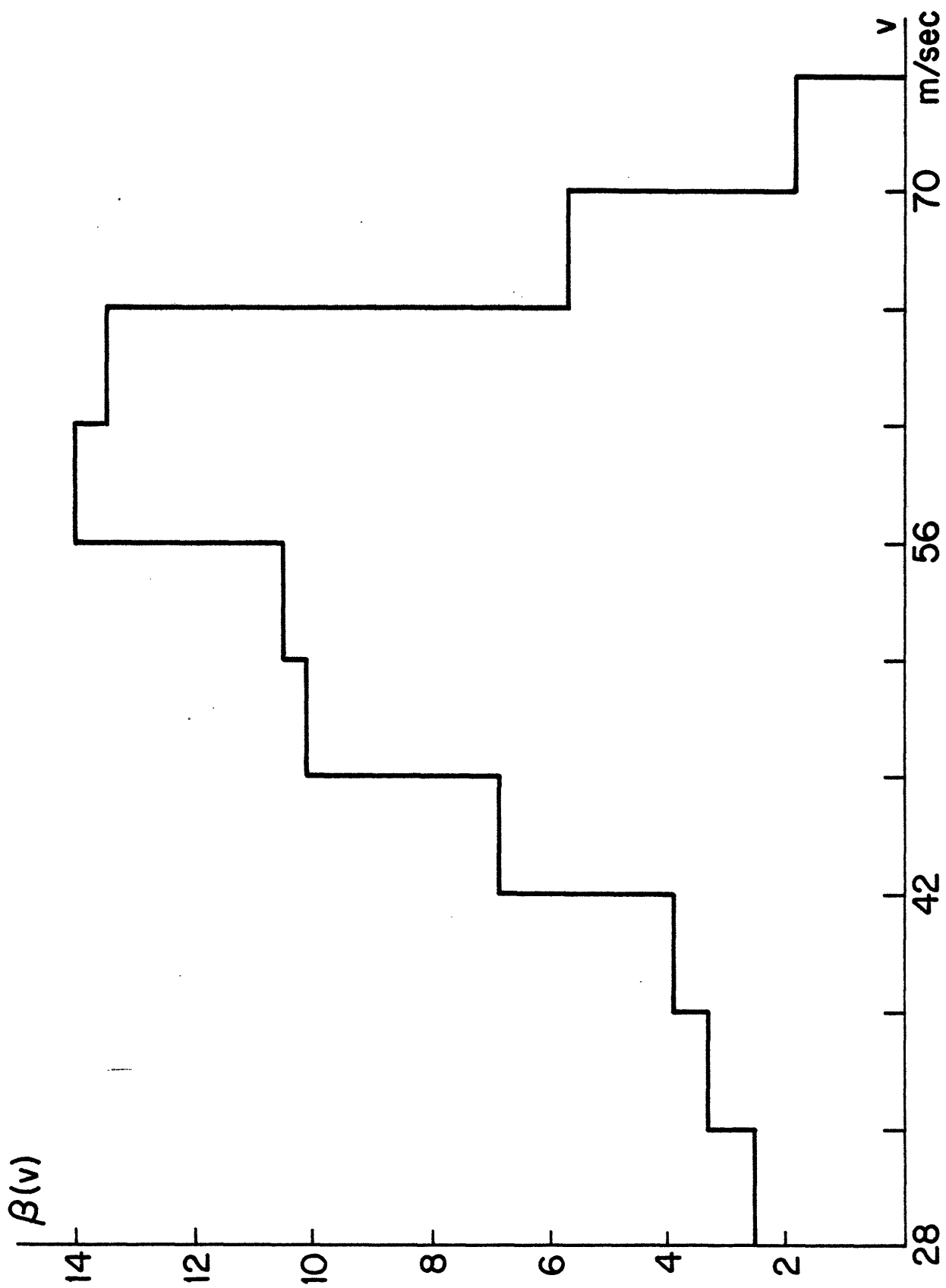


FIBER DIAMETER HISTOGRAM

FIGURE 4.2.3



DISTRIBUTION OF CONDUCTION VELOCITIES (ELECTROPHYSIOLOGICAL)
 FIGURE 4.2.4



DISTRIBUTION OF CONDUCTION VELOCITIES (HISTOLOGICAL)

FIGURE 4.2.5

4.2.2 - Results

The distribution of conduction velocities which resulted from the electrophysiological measurements is shown in Figure 4.2.4. and is referred to as $\beta_e(v)$. The distribution of conduction velocities obtained from the fiber diameter histogram $S(D)$ is referred to as $\beta_h(v)$ and it is shown in Figure 4.2.5. According to (4.1), the distribution $\beta_h(v)$ depends on $S(D)$ as:

$$\beta_h(v) = Kv^2S(v/K_v) \quad (4.3)$$

which means that we have to know the diameter to velocity conversion factor K_v in order to obtain $\beta_h(v)$. Since we couldn't measure it directly we had to estimate it somehow. We started assuming K_v^0 as the ratio of the maximum conduction velocity in $\beta_e(v)$ to the maximum diameter in $S(D)$. With this K_v^0 we found $\beta_h^0(v)$. Then we readjusted K_v until the best agreement between $\beta_h(v)$ and $\beta_e(v)$ was obtained. Finally, the coefficient K was chosen to minimize the mean square error between $\beta_h(v)$ and $\beta_e(v)$. The mean square error normalized to the squared norm of $\beta_h(v)$ resulted:

$$\epsilon^2 = \frac{||\beta_h(v) - \beta_e(v)||^2}{||\beta_h(v)||^2} = .017 \quad (4.4)$$

It can be said that the mean square error (or difference) between the two distributions is small. The electrophysiological mea-

measurements are very noisy in nature so a relatively large uncertainty associated with the estimate of $\beta_e(v)$ would be expected. The histological results are also corrupted by uncertainty because of problems associated to diameter measurement. It seems to us that the value of ϵ^2 is therefore reasonable.

In general, the diameter histogram of a nerve can be determined with a very good accuracy by following proper procedures, for instance as described by Boyd and Davey [B6]. These procedures do not include any processes which introduce large amounts of shrinkage or distortion, such as decalcification. Shrinkages of nerves processed properly are in general of the order of 10 to 20 %. But this applies to large or medium size nerve bundles which can be dissected and separated from the surrounding structures easily, which wasn't the case in our experiment. As we have said, 18 branches of the nerve were identified under the microscope and the largest had cross-section of 2mm. Finding and dissecting objects which are this small is a nearly impossible task.

In order to avoid decalcification we attempted the removal of the bone with minimum damage to the other structures. In the process, many of the branches which ran close to the bone were destroyed. It seems to us that under the constraints of this experiment one could hardly generate significantly better histological results.

CHAPTER 5

APPLICATIONS TO CLINICAL NEUROLOGY

5.1 - INTRODUCTION

Peripheral neuropathies are pathological changes which take place in peripheral nerves and interfere with their normal functioning. One of the most common and widespread neuropathies is the diabetic neuropathy. Clinically, different forms of diabetic neuropathies are distinguished, depending on the specific nerve and fiber groups affected. Diabetic sensory neuropathy affects sensory nerves, thus causing the loss of sensation mainly at the extremities of the limbs. There is clinical and histological evidence of changes in the fiber

content of the affected peripheral nerves [B16], [K1]. We decided to investigate this problem by estimating the distribution of conduction velocities in a population of 13 diabetic subjects and 14 neurologically normal subjects. Nearly 90 ulnar and median nerves were studied.

An approximate probabilistic model for the pathological changes in diabetic sensory neuropathy is proposed. The distortions caused by these pathological changes in the distribution of conduction velocities are examined, and the following interpretations are suggested: that either all fiber groups undergo uniform demyelination and remyelination; or, less significantly, that in such a neuropathy, the large fast conducting fibers are affected by segmental demyelination, remyelination and axonal degeneration.

5.2 - THE DISTRIBUTION OF CONDUCTION VELOCITIES IN DIABETIC NEUROPATHY

Before we describe in detail our methods and findings, let's briefly review the fundamental notions about peripheral neuropathies which will also give the minimum background for the subject. More detailed and extensive information on disease of peripheral nerves can be found in any good reference book in clinical neurology, such as Bradley's "Disorders of Peripheral Nerves" [B10] or volume 8 of the Handbook of Clinical Neurology [K1].

5.2.1 - Peripheral Neuropathies

Peripheral neuropathy is the generic term for any disease process which affects the normal functioning of a peripheral nerve. It is always associated with the abnormal conduction of the action potential by a subset of its component nerve fibers. Its causes probably run into several hundreds [B10]. The clinical characterization of neuropathies is usually done according to several criterions, such as:

- a) Rate of onset, it can be acute -that is present for a few days, or chronic when it is present for a long period of time.
- b) Distribution, it can be proximal- which means closer to the spinal cord where the nerve cell bodies are, or distal - that is closer to the extremities.

c) Type, it can be mainly motor, sensory or autonomic.

Many other criteria may be used for a more complete description. The pathological changes which occur in peripheral neuropathies are of two major kinds:

i) Degeneration and regeneration of the axons.

ii) Demyelination and remyelination of the nerve fibers.

Let's examine each of these changes in more detail.

Two kinds of degeneration are distinguished: 1) Wallerian degeneration which is localized and it is caused by the transection of the axon and 2) axonal toxic degeneration which is caused by some toxic substance entering the nerve fiber,

Wallerian degeneration - named after Waller who first described the changes following nerve transection in 1850 - usually occurs in entrapment neuropathies or when the nerves are cut accidentally. The transectioning of the nerve causes the distal part of the nerve to degenerate; that is, the axon is completely destroyed and absorbed by the organism. After a few days, the intact part of the fiber will start regrowing the axon, regenerating the nerve fiber over its whole extent. The regeneration is complete after about 12 months. In myelinated fibers the regenerated axon is wrapped by Schwann cells with a much smaller internodal length than the intact axon. We have seen in Chapter 2 that conduction velocity, fiber diameter and internodal length are more or less proportional to each other in heal-

thy fibers. There is some evidence that in regenerated fibers following Wallerian degeneration all the mentioned parameters including myelin thickness seem to return to normal, except the internodal length, as observed by Cragg and Thomas [C5]. This would suggest that internodal length is not a determinant factor for fiber conduction velocity. This question is not completely settled yet, and there is other experimental evidence suggesting that conduction velocity is in fact linearly related to internodal length [S2].

Toxic axonal degeneration is believed to affect the entire nerve including the cell body. It is not clear whether regeneration can occur in this case. The causes of toxic degeneration may be of metabolic origin or neurotoxins which somehow reach the nerve. We should also mention the not very well understood "dying back" degenerations which start at the extremities of the nerve fibers and progress toward the proximal regions.

Demyelination is a pathological process which affects only the Schwann cells but not the axons. It is thought to be the major factor in diabetic neuropathy by most workers in this field [B3]. It is patchy, affecting Schwann cells randomly along the whole extent of the fiber. It starts with the widening of the nodal gap caused by the retraction of the myelin. Eventually the Schwann cell in one internode dies completely, leaving the bare axon until adjacent Schwann cells divide and remyelinate that portion of the fiber. Usually two or three Schwann cells will replace one, that

is two or three internodes will replace one original internode.

In sensory neuropathies - such as the sensory diabetic neuropathy - the clinical symptoms are consistent with the abnormal conduction of a subset of nerve fibers in the peripheral nerve. The threshold for some sensory modalities - such as vibration sense or perception of pin prick - are raised or are completely lost. In some severe cases there is a loss of joint position sense and touch perception. Other symptoms are numbness, burning sensation and paraesthesia (sensation of pins and needles). The electrophysiological signs of these neuropathies are in general a decrease in the maximum conduction velocity and in the amplitude of the recorded compound action potential as noted by Lamontagne and Buchthal [L1]. The variability of these two electrophysiological parameters is relatively large among normals and it is also a function of age [K1]. Usually, a definite correlation between the lowered amplitude and conduction velocity of the recorded compound action potential and the presence of a peripheral neuropathy can be established only in the advanced stages of the disease. One would then expect to have a more complete picture about the state of the diseased nerve by looking at the distribution of velocities, which provides a quantitative measure of the activity of the fibers over a relatively wide velocity range.

5.2.2 - Experimental Procedures

5.2.2.1 - Subjects and Methods

A population of 27 subjects was studied; 14 had no diabetes while the other 13 suffered from that disease, presenting several degrees of sensory diabetic neuropathy. Of the 14 subjects with no diabetes, only 12 could be considered normals from the neurological point of view, since one had injured (cut) some of his peripheral nerves in a car accident (and will be considered apart), while another suffered from myotonia. Of the 13 subjects with diabetes, 4 had some other neurological disease so they cannot be included in the analysis of the diabetic population.

Sensory branches of the ulnar and median nerves were tested. Both nerves innervate the hand and for the sake of clarity they are shown in figure 5.2.1. Ideally we would like to have studied the two nerves on both sides of all of the subjects, but unfortunately not all of them came back after the first - sometimes unsuccessful - run to complete the testing. Most of the diabetic subjects were unavailable for repeat studies.

The subject was asked to wash his arms and was comfortably seated in an armchair. A pair of ring electrodes were applied to the proximal phalanx of finger 3 for the median nerve or finger 5 for the ulnar nerve. A strap on electrode was wrapped around the hand to ground

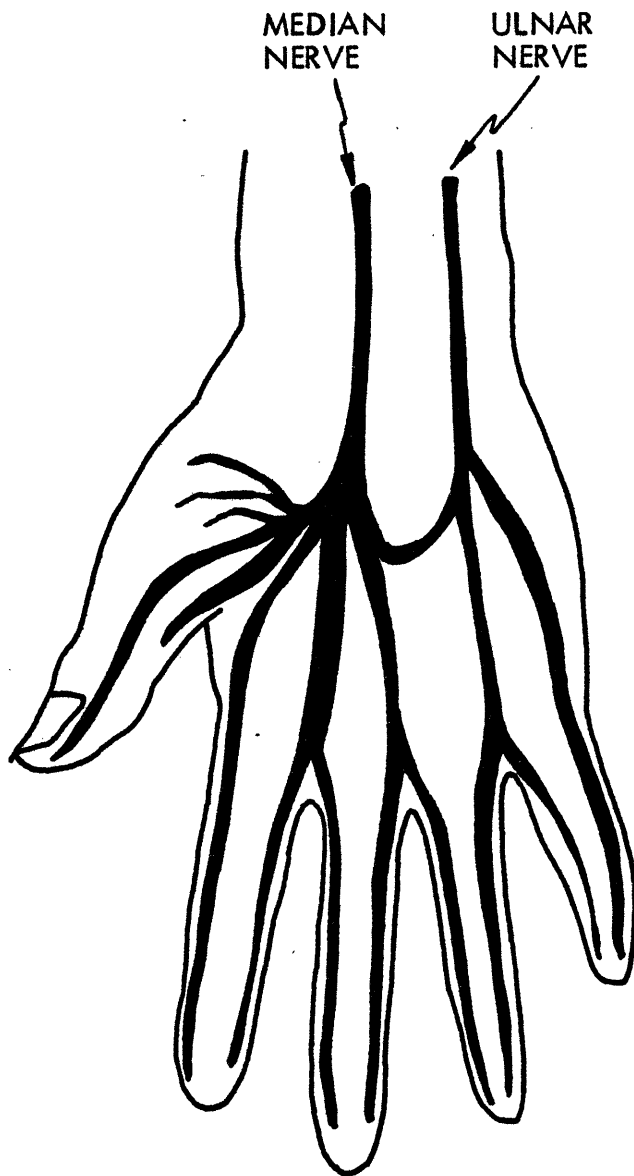


FIGURE 5.2.1

the subject. A pair of square shaped 1 by 1 cm lead electrodes were taped on the skin above the median nerve at the wrist or above the ulnar nerve at the elbow. A layer of Teca electrode gel was used between all electrodes and the skin to assure a good electrode contact.

The electrical stimulus was delivered by the stimulator of the TECA TE-4 EMG machine at the rate of 10 stimuli/sec. and it consisted of pulses of 50 microsec. duration. The signal from the recording electrodes was amplified and fed into a digital averager, where it was sampled at the rate of one sample each 50 microsec. A total of 1024 sample points were taken over a period of about 50 millisec. The averager was pre-triggered by the stimulator 3 to 5 milisec. before the stimulus was applied to the nerve, so that the stimulus artefact could be seen entirely in the records (to be used as a time marker). The detailed experimental set up is described in detail in Appendix 3. The signal picked up by the recording electrodes was in general heavily corrupted by EMG signals generated by muscles nearby. This interference represented the major part of the noise affecting the records. In some cases it could be significantly reduced by using "biofeedback", that is the recorded signal was displayed on an oscilloscope which the subject could watch and minimize his own muscle activity.

First a supramaximal stimulus was applied, The amplitude

of the pulse used was in general barely tolerable by the subject. A number of individual responses were averaged, usually in the range 128-1024, depending on the ability of the subject to reduce his EMG activity. The averaged compound action potential was sampled at 20×10^3 sp/sec. and could be fitted in a record consisting of 256 sample points. Such typical records are shown in Figures 5.2.2. and 5.2.4 for normal median nerves and Figure 5.2.6 for a diabetic ulnar nerve. The numerical values of the sample points were printed out for processing. The threshold stimulus was more difficult to determine and it was usually done with the help of the subject. The chosen pulse intensity was in the majority of the cases at a just noticeable level, as perceived by the subject. Again depending on the noise level, 1024 to 4096 individual nerve responses were averaged. Typical records for normals are shown in Figures 5.2.3 and 5.2.5 and for a diabetic ulnar nerve in Figure 5.2.7.

5.2.2.2 - Data Processing and Results

The numerical values of the data points of each record were transferred to paper tape for processing. Excluding a few exceptionally good records, the stimulus artefact had to be removed. The modeling of the stimulus artefact and the estimation of the parameters of the model are described in detail in Appendix 2. Basically, the artefact was modeled by $a(t) = A_1 + A_2(1 - \alpha t) \exp(-\alpha t)$ where the

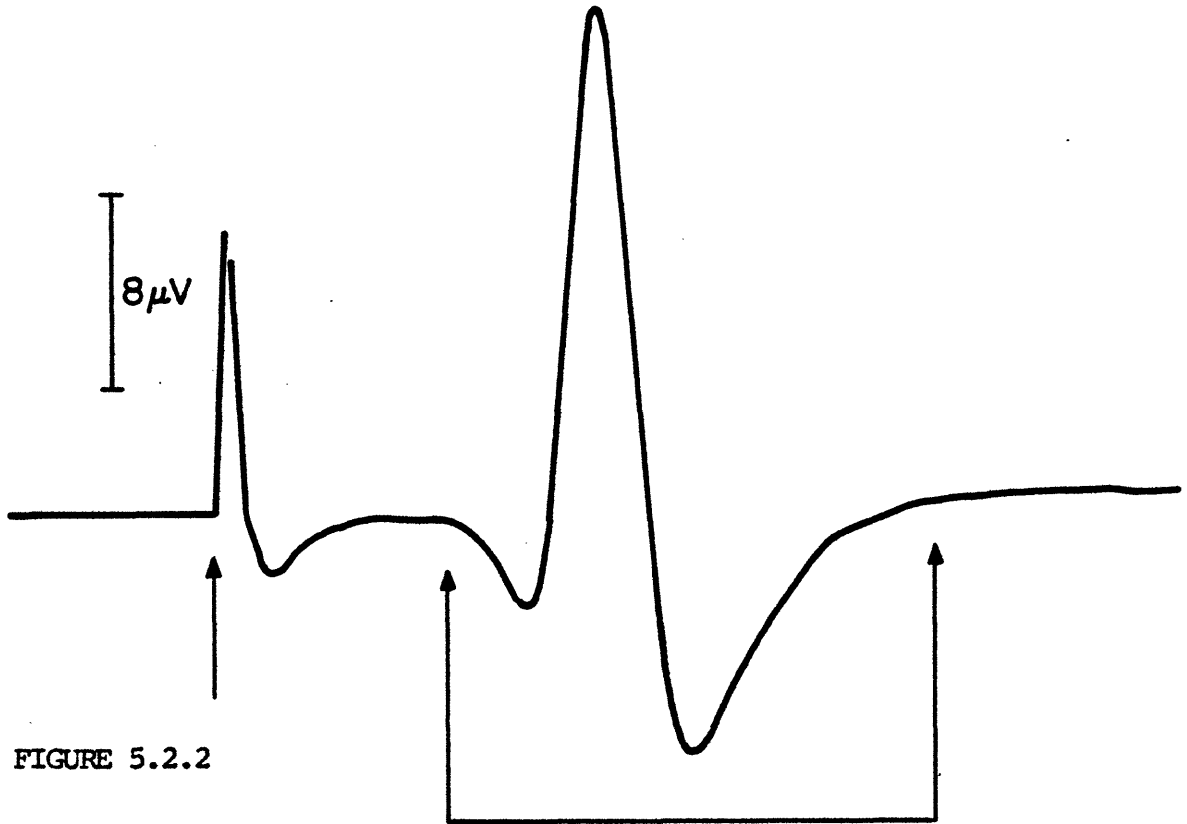


FIGURE 5.2.2

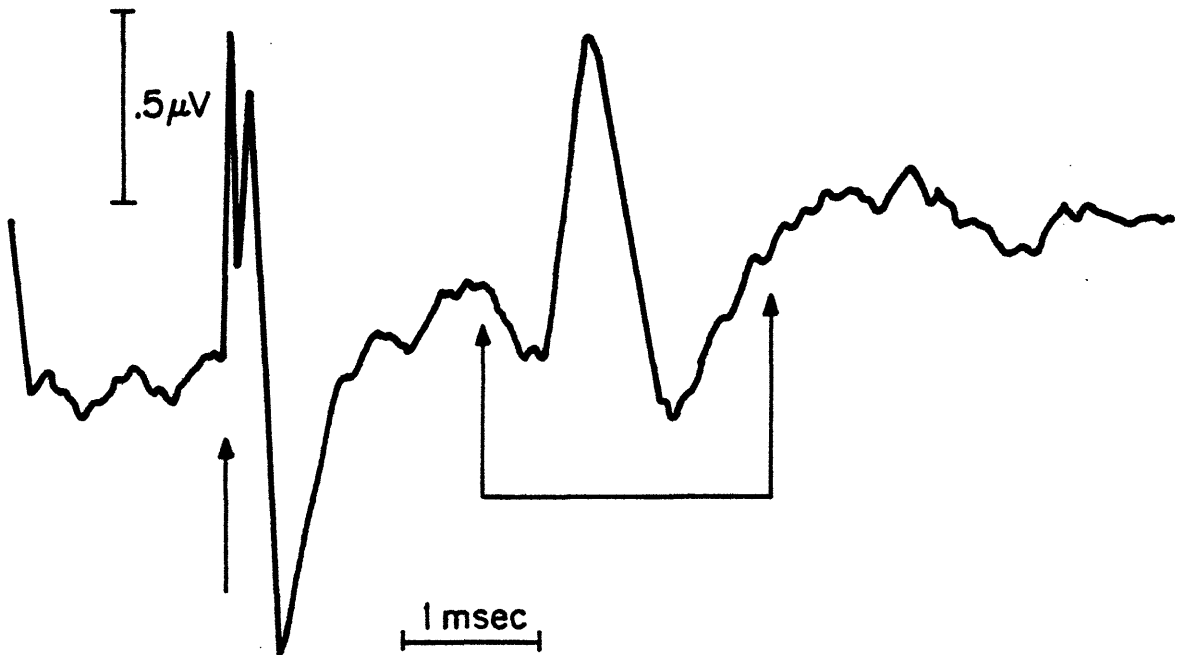


FIGURE 5.2.3 - Signals Recorded from a Normal Median Nerve.

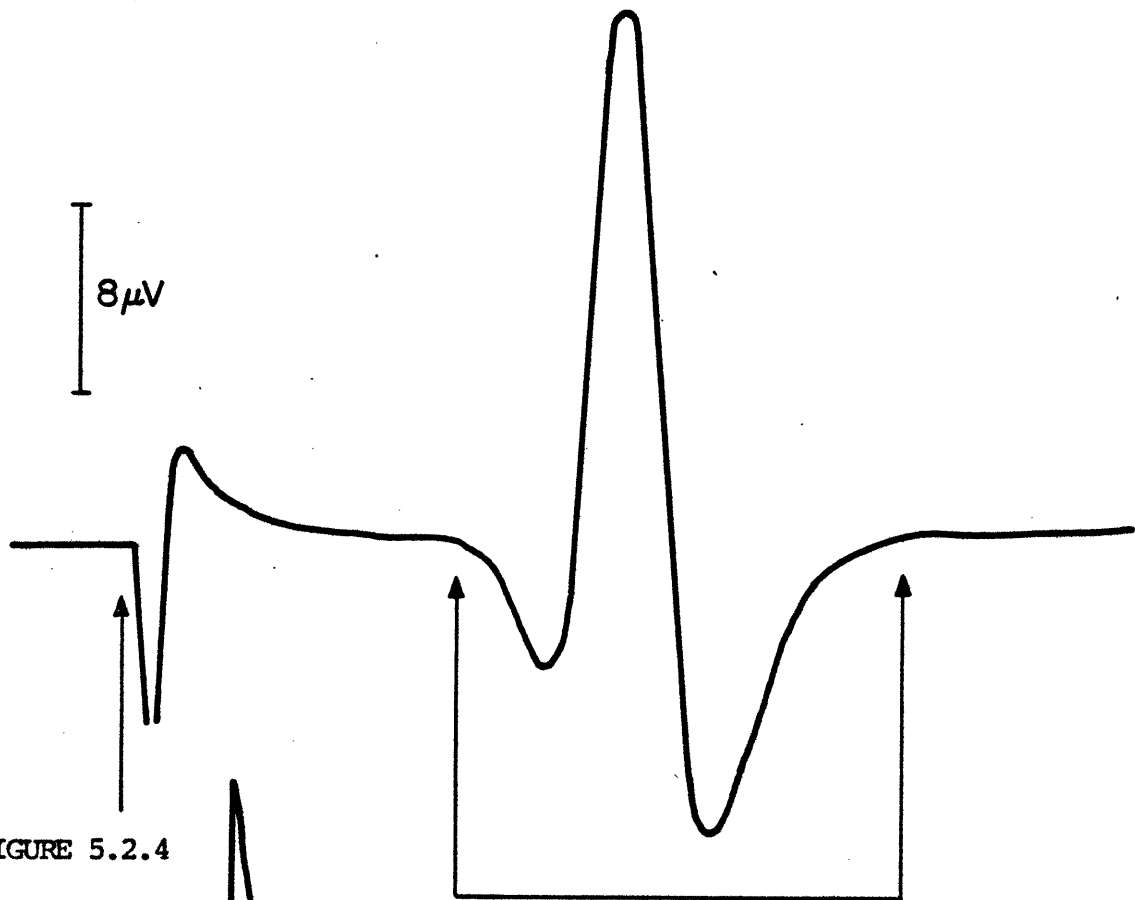


FIGURE 5.2.4

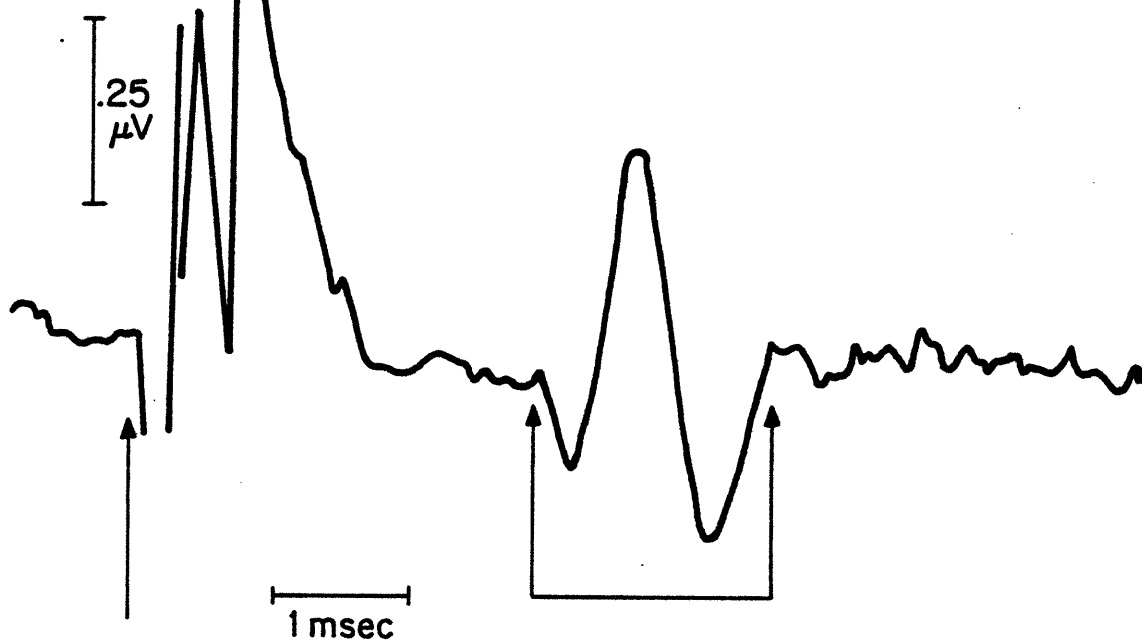


FIGURE 5.2.5 - Signals Recorded from a Normal Median Nerve.

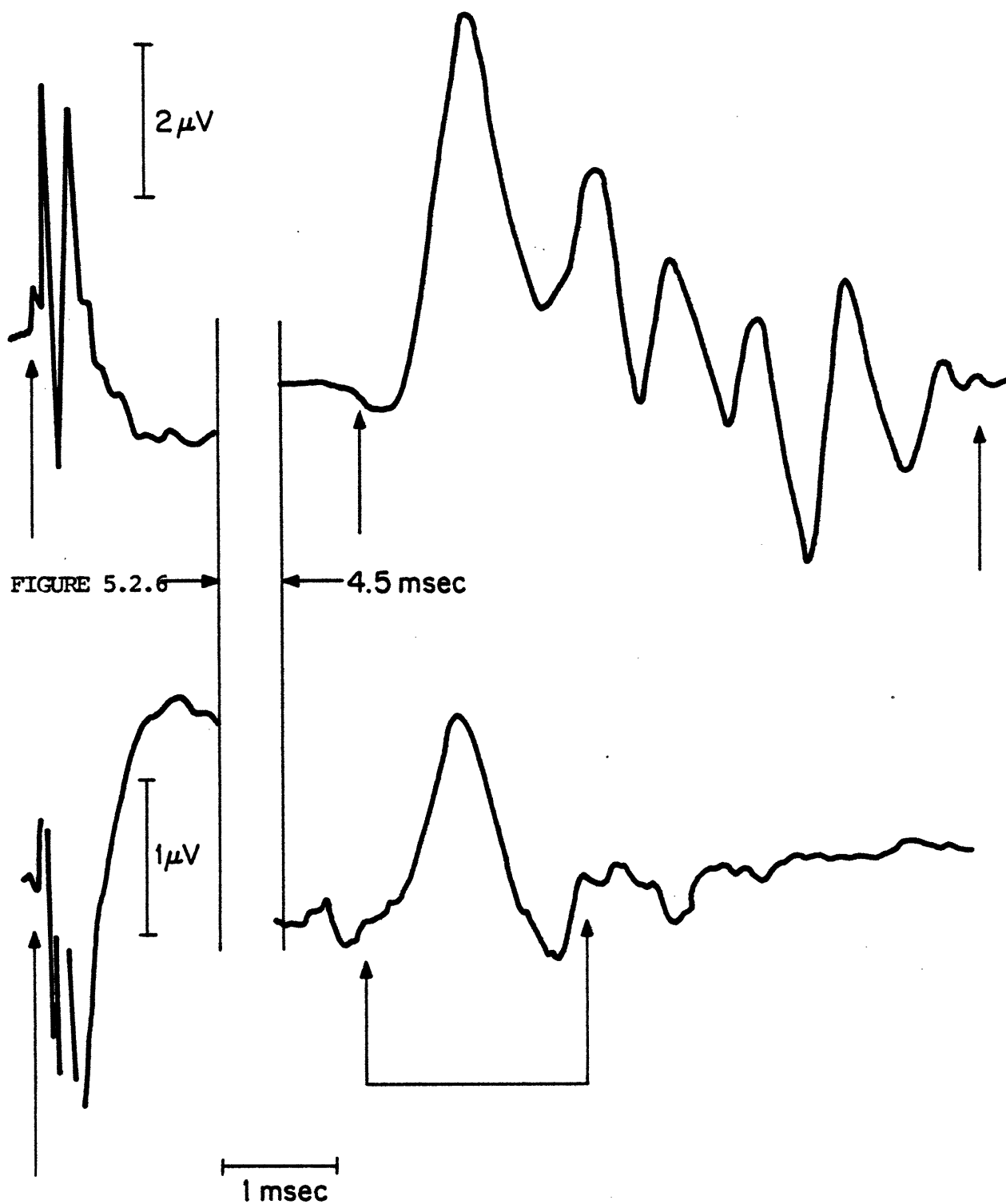


FIGURE 5.2.7 - Signals Recorded from a Diabetic Ulnar Nerve.

parameters A_1 , A_2 and α are least-squares estimated using the early portions of the records. The estimated artefact is then subtracted from the entire record, eliminating the major part of this disturbance. Finally a ramp $B + Ct$ was removed from the records according to the criterion that the signal must be zero - on the average - before and after the occurrence of the nerve response.

In order to compute the distribution of conduction velocities, we had to use the data from the instant $t=0$ which is when the stimulus is applied, up to a time $t = N$ when all the nerve responses had extinguished (or were so small that they could be considered extinguished). Due to the nonzero distance between the sites of stimulation and recording and to the finite maximum conduction velocity of the nerve, no response was recorded until a time $t = N_0$, which means that we have useful data only on the interval $[N_0, N]$. The records were therefore filled in with zeros from $t = 0$ to $t = N_0$. This was the format of the data used to estimate the conduction velocity distributions.

Not all of the distributions could be computed: in some instances the records were excessively noisy returning meaningless estimates, that is, distributions which had large negative valued peaks or clearly divergent behavior. From the total of 68 nerves examined (some were tested two or even three times), only 48 histograms were computed. Typical distributions in normal median and ulnar nerves are shown in Figure 5.2.8 A, B and C. All are from diffe-

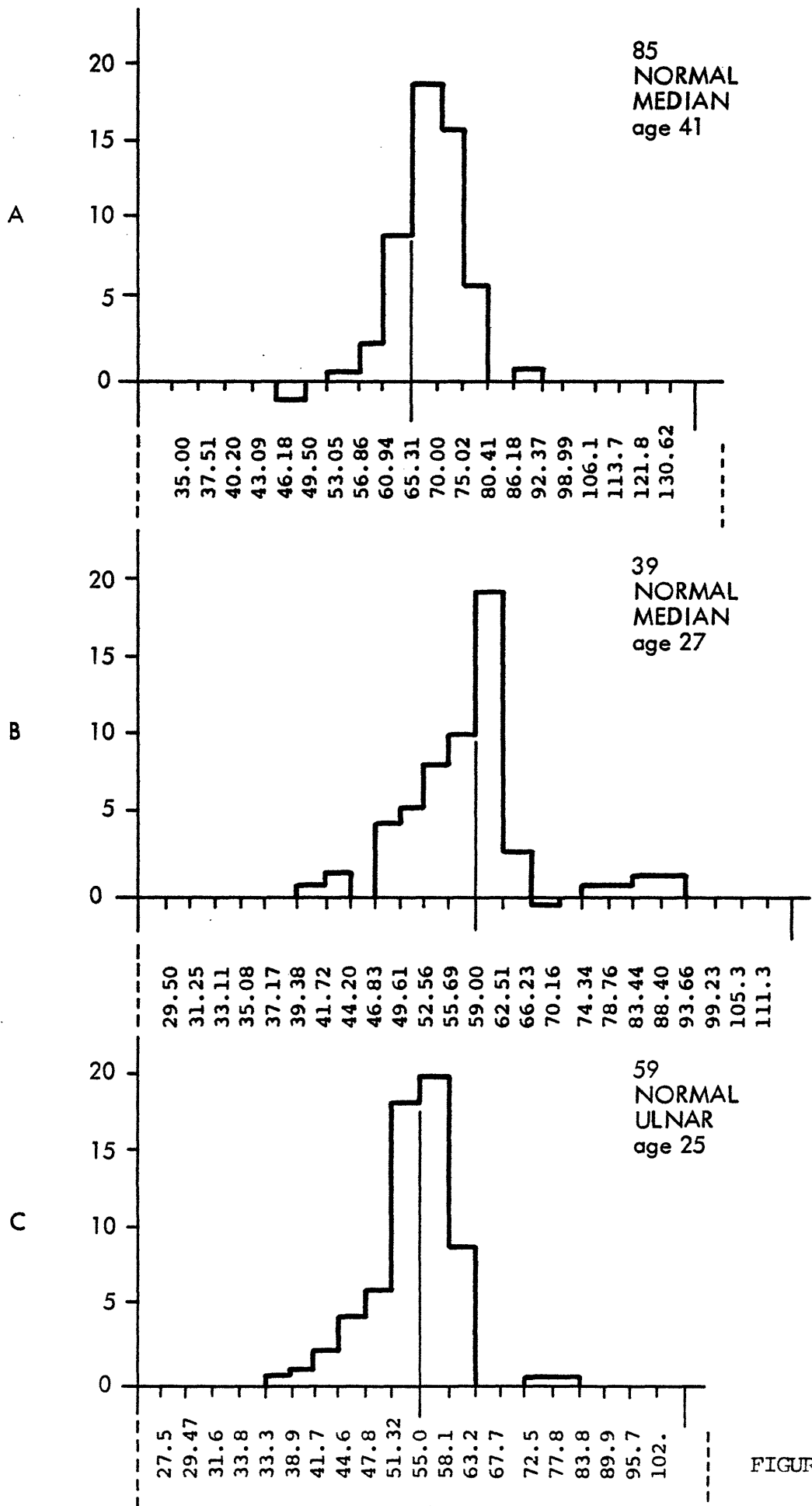


FIGURE 5.2.8

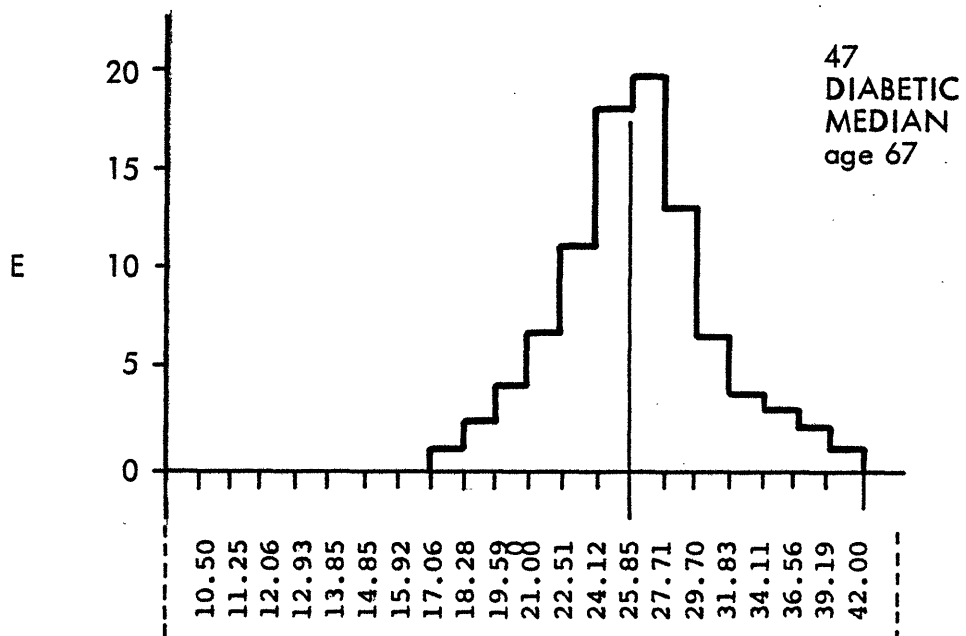
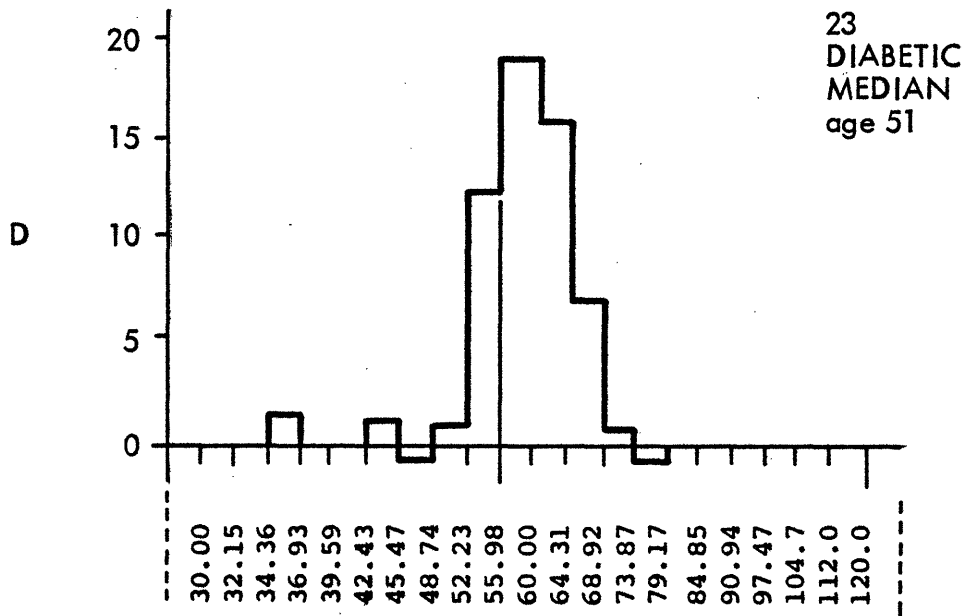


FIGURE 5.2.9

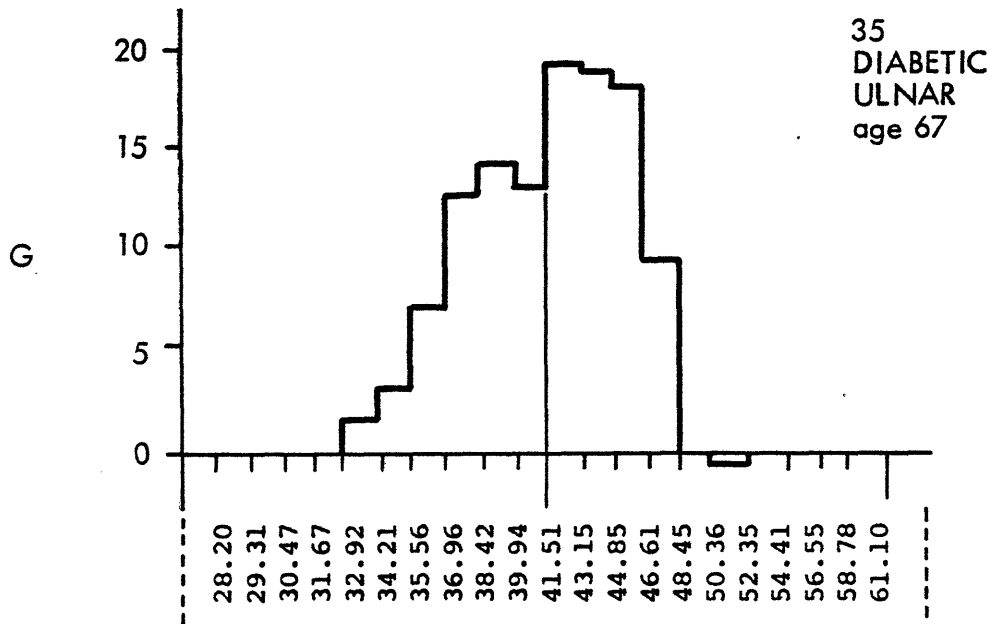
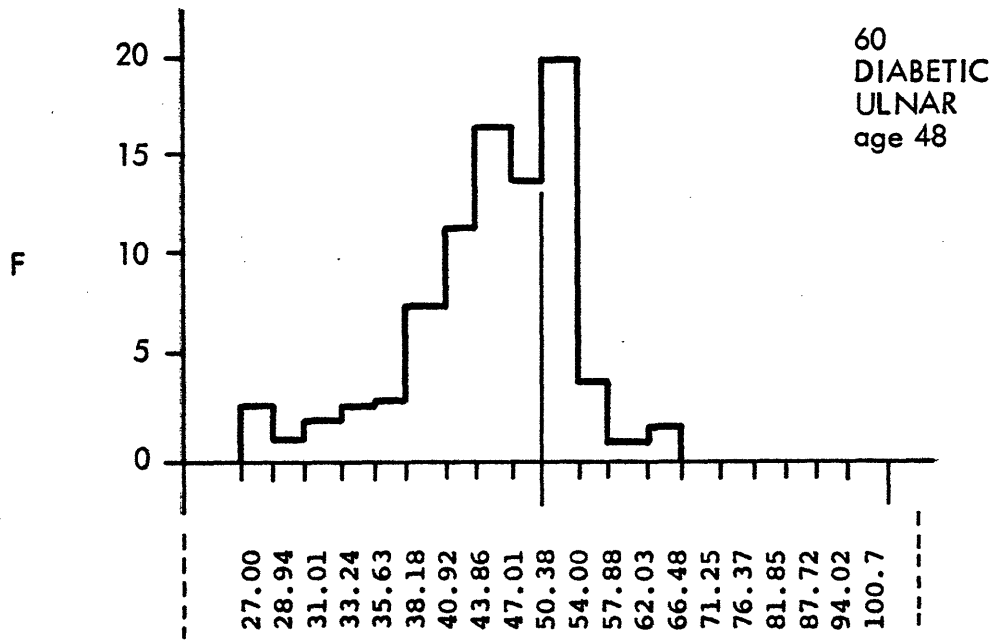


FIGURE 5.2.10

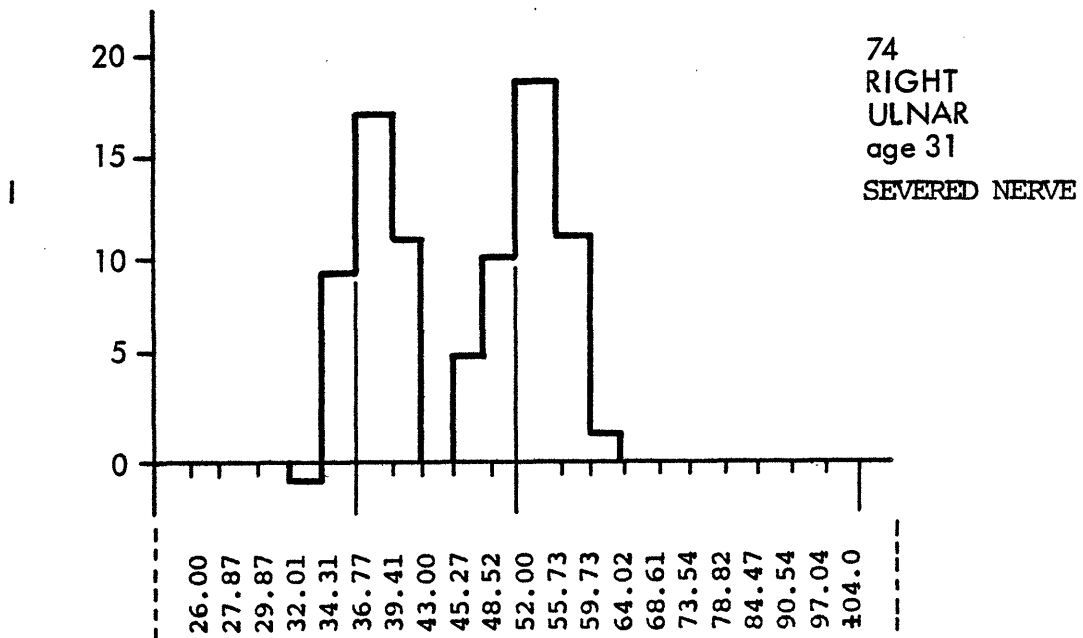
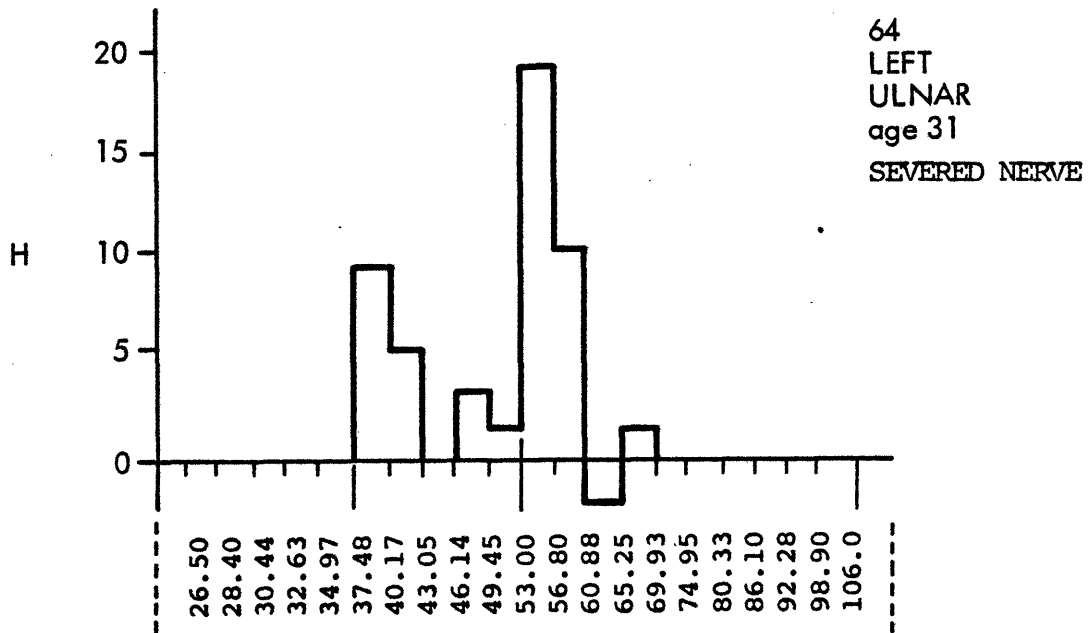


FIGURE 5.2.11

rent subjects. The variability of the distribution of conduction velocities in the group of normal subjects is represented by the pair B and C. The conduction velocity distributions in diabetic subjects are represented in Figures 5.2.9 and 5.2.10. The intersubject variability is much greater than in normals as this is evident from the pairs D,E and F,G. Distributions D and F are close to the normals, while E and G are significantly shifted toward a much lower velocity range. The apparent "fattening" of the distributions E and G as compared to D and F is due to the much finer velocity discretizations used to display them.

The distributions of conduction velocities of both ulnar nerves of a subject who suffered a car accident injuring these nerves are shown in Figure 5.2.11 . These distributions show the clustering of the fiber conduction velocities around two different means, one normal and the other about half of the normal. This feature was unique to this subject and was not found among normals nor the diabetics.

One obvious feature of the conduction velocity histogram in both normal and diabetic subjects is that it goes rapidly down to zero as the velocity decreases. This is a consequence of the fact that the conduction velocity distribution $\beta(v)$ is related to the fiber diameter histogram as $\beta(v) = Kv^2S(v/K_v)$. It reflects the inability of this technique to detect activity in the slow velocity ranges - a range which may be interesting to look at in some instances.

In order to analyze the differences and the similarities between the distributions, we have defined the following parameters:

- a) Maximum Conduction Velocity - which is the velocity above which the distribution of conduction velocities is less than 5% of its peak value.
- b) Minimum Conduction Velocity - which is the velocity below which the distribution of conduction velocities is less than 5% of its peak value.

The differences between these velocities is called the velocity range, which will be normalized to the maximum conduction velocity and called normalized velocity range. These parameters are shown for each computed histogram in the Tables 1 through 4.

We have also computed the average conduction velocity distribution for each nerve group: normal median, normal ulnar, diabetic median and diabetic ulnar. These are shown in Figures 5.2.12 and 5.2.13. The most striking difference between the average distributions of normals and diabetics is that the later have two peaks, indicating two clusters.

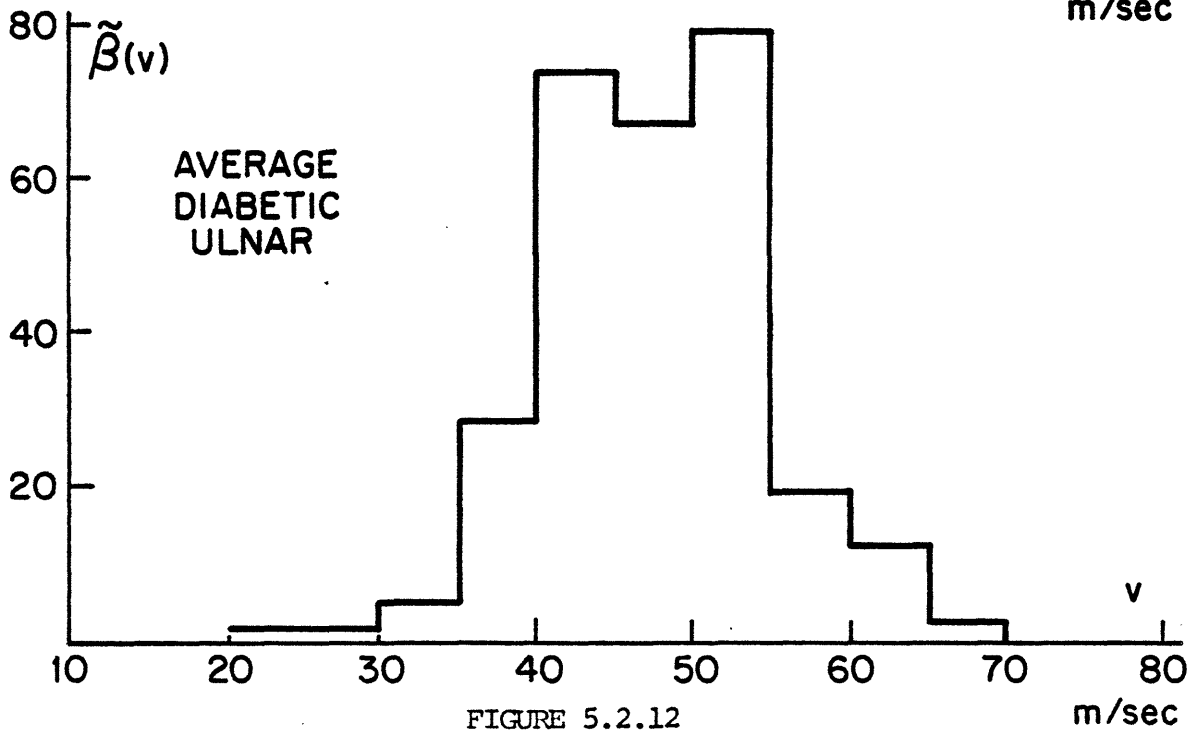
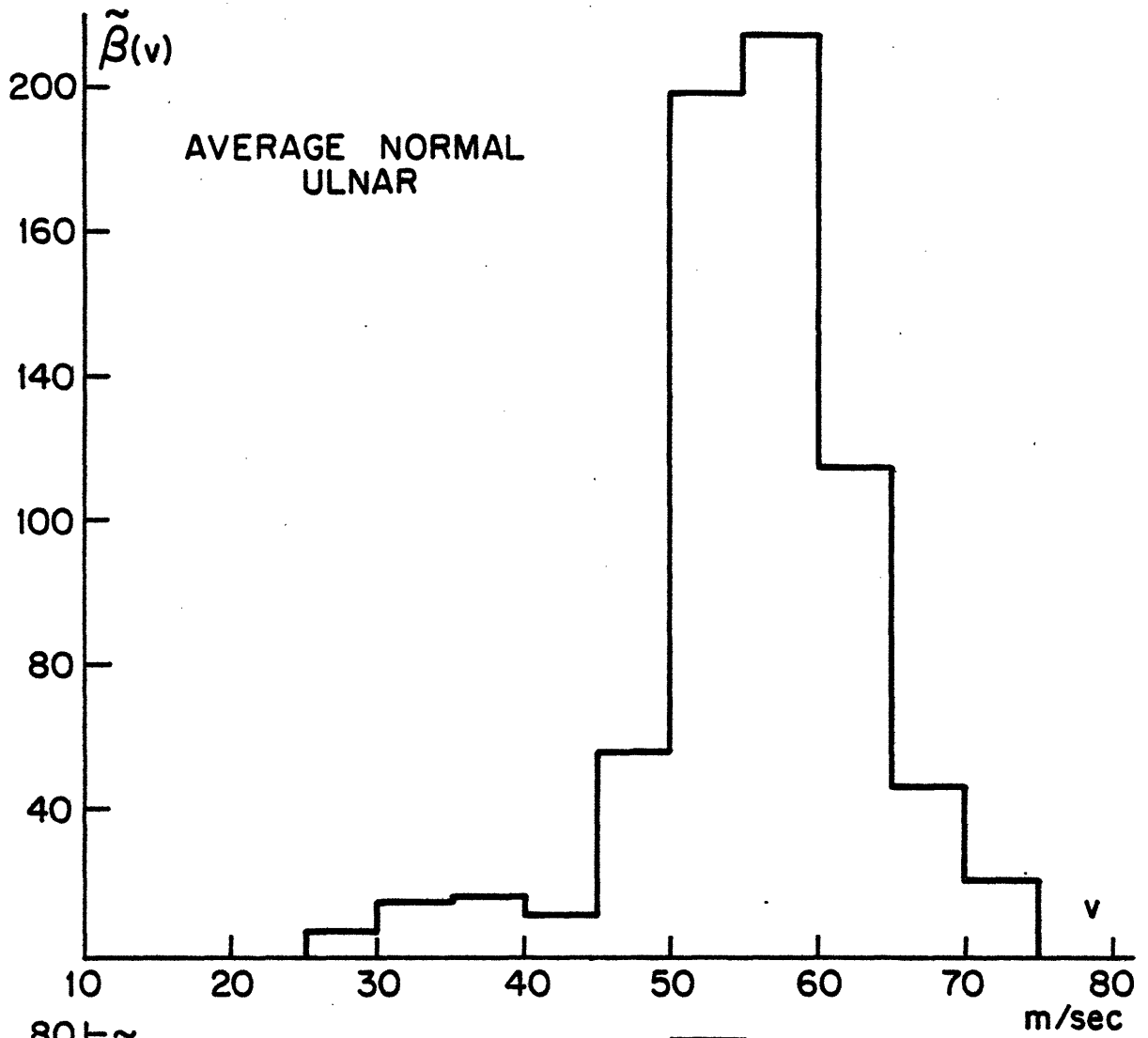


FIGURE 5.2.12

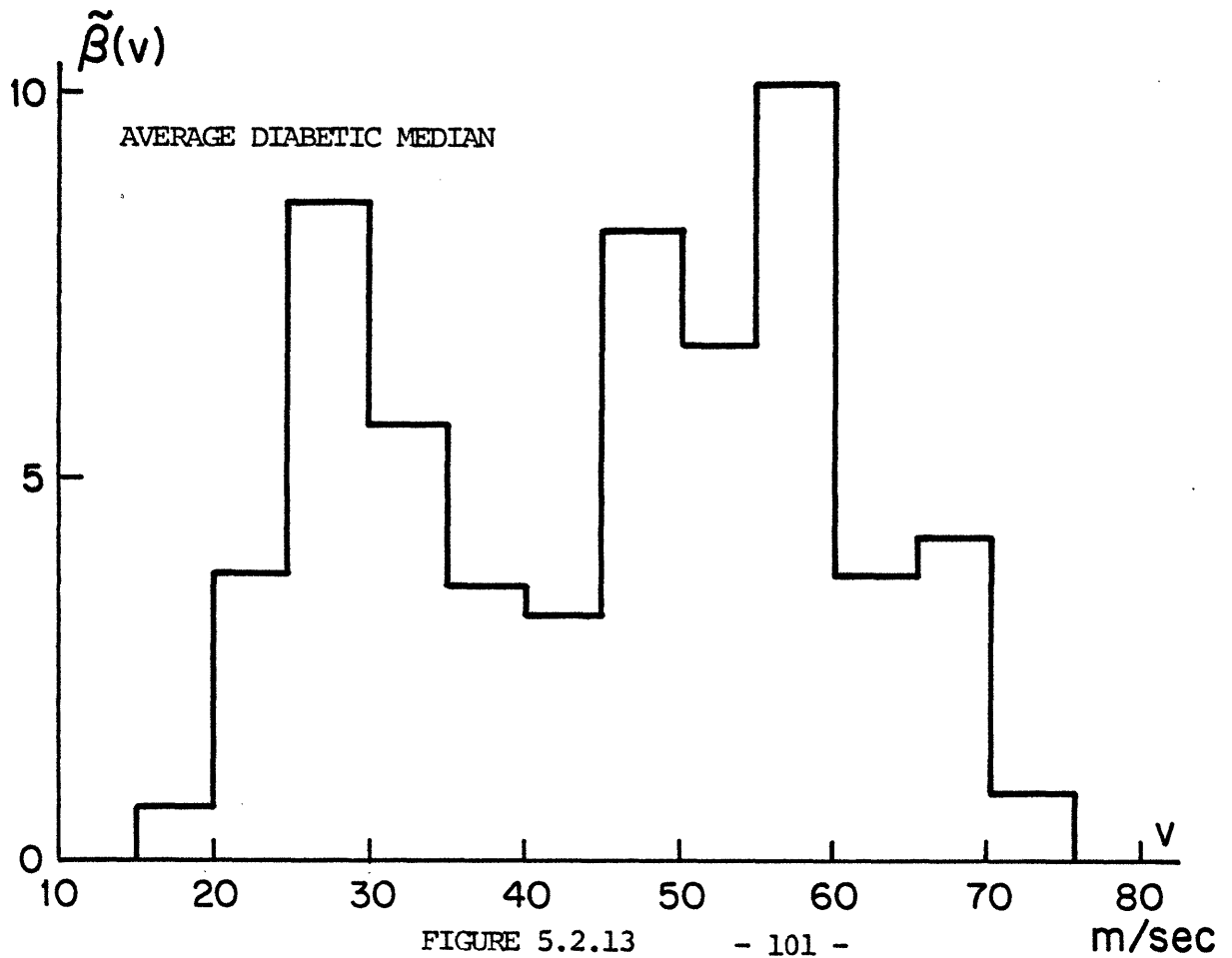
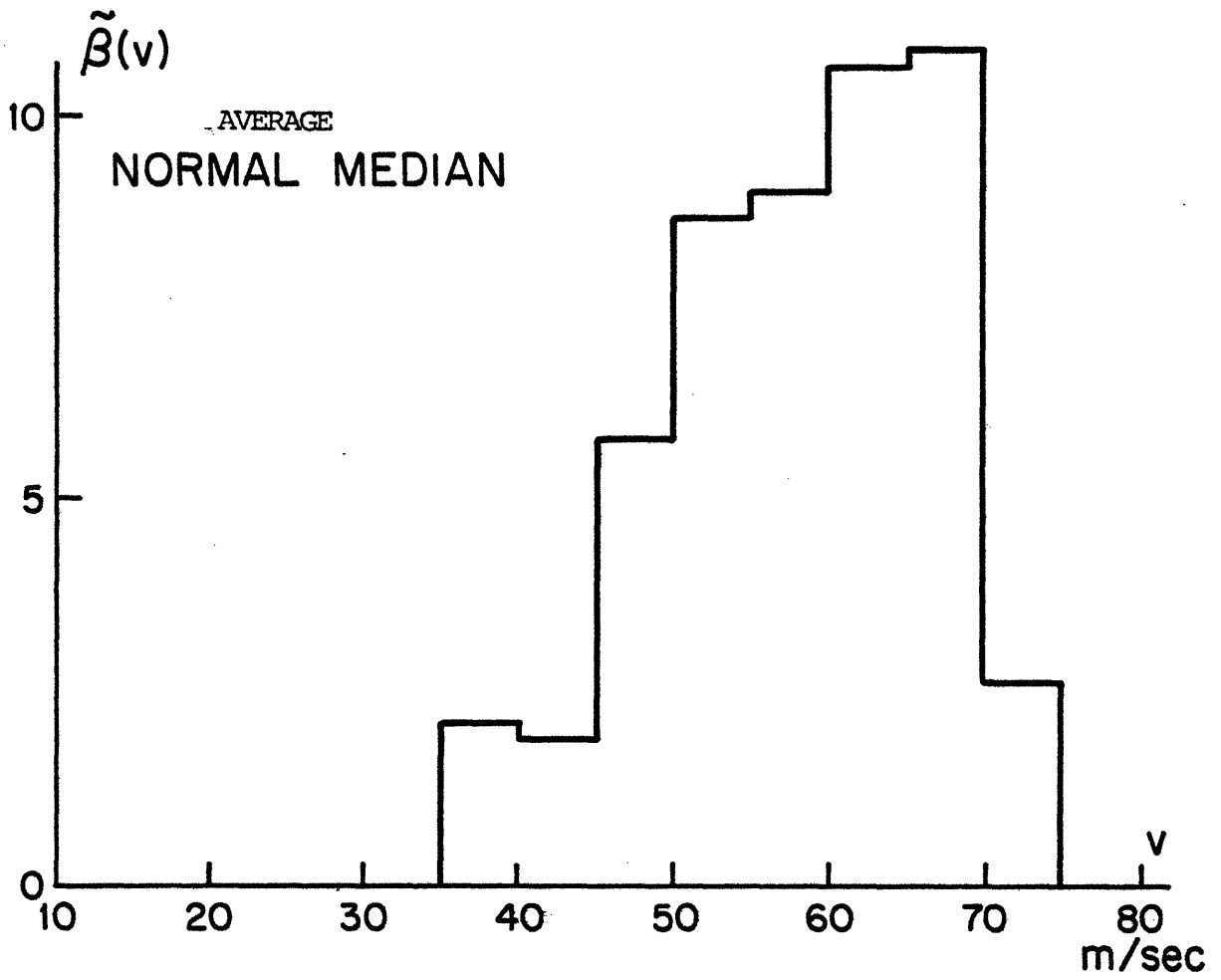


FIGURE 5.2.13

TABLE I - NORMAL MEDIAN

Number	MACV	MICV	Range	Nor. Range
18	74	58	16	.216
20	68	40	28	.411
27	78	46	32	.410
28	75	-	-	-
37	70	-	-	-
52	68	37	31	.455
56	66	46	20	.303
58	59	42	17	.288
62	58	33	25	.431
66	63	49	13	.209
70	64	32	32	.500
77	75	40	35	.466
80	80	-	-	-
82	74	-	-	-
85	80	53	33	.412
Average	70	43	25.6	.372

TABLE 2 - NORMAL ULNAR

Number	MACV	MICV	Range	Nor. Range
29	60	42	18	.300
32	60	-	-	-
33	66	45	21	.318
34	59	-	-	-
39	65	39	26	.400
40	67	37	30	.447
42	70	-	-	-
43	67	37	30	.447
44	67	37	30	.447
45	64	44	20	.312
46	65	26	38	.582
49	62	43	19	.306
50	61	31	30	.491
55	65	42	23	.353
59	63	39	24	.381
61	61	44	22	.333
67	65	-	-	-
69	70	56	14	.200
78	70	39	31	.442
79	74	47	27	.364
81	74	41	33	.446
83	71	36	35	.492
84	74	-	-	-
Average	65.9	40.5	26.1	.392

TABLE 3 - DIABETIC MEDIAN

Number	MACV	MICV	Range	Nor. Range
17	50	39	11	.220
19	73	50	23	.315
21	60	42	18	.300
22	60	41	19	.316
23	68	48	20	.294
24	20	-	-	-
25	71	54	17	.239
31	45	26	19	.422
36	44	-	-	-
47	42	16	26	.619
51	36	26	10	.277
54	56	36	20	.357
57	34	24	10	.294
68	64	35	29	.453
71	65	36	29	.446
72	65	-	-	-
76	43	-	-	-
Average	52.7	36.4	19.3	.350

TABLE 4 - DIABETIC ULNAR

Number	MACV	MICV	Range	Nor. Range
26	65	50	15	.231
30	48	-	-	-
35	48	32	16	.333
38	57	42	15	.263
41	51	-	-	-
48	51	38	13	.255
53	44	-	-	-
60	62	31	31	.500
63	58	31	27	.465
Average	57.3	37.3	19.5	.341

5.3 - MODELING THE DIABETIC NEUROPATHY

It has been established that segmental demyelination and remyelination do occur in diabetic neuropathy. Also there is some evidence of axonal loss or degeneration, probably in the most advanced stages of the disease [C3], [C4], although it is not completely settled that this occurs to a significant extent. Repeated cycles of de- and remyelination may cause the formation of so called "onion-bulbs"; that is, several Schwann cells wrapped around the same internodal segment, making the myelin thickness abnormally thick [B10]. During the demyelination and remyelination processes the conduction velocity of a nerve fiber can be slowed for the following reasons :

a) Complete loss of the myelin sheath in one or several internodal segments, leaving the bare axon which will conduct at a much slower velocity. Experimental evidence indicates that when the myelin is completely removed the conduction velocity decreases to about 10 % of its normal value [R5].

b) Change in the myelin thickness from its normal - and near optimal - value, either during demyelination or remyelination when it is thinner than normal, or when onion bulbs are formed making it thicker than normal. There are both theoretical [S3] and experimental [R5] reasons to believe that normal conduction velocity changes somewhat with myelin thickness. The optimal thickness seems to be around .3 of the external diameter. A \pm 50% change in this proportion will

cause the velocity to decrease to about 80% of its normal value.

c) After the de- and remyelination cycle is complete, and no bare axon is left and the myelin thickness has returned to normal, the internodal length is irreversibly reduced, sometimes to only one fourth of its normal value, causing a proportional reduction in the conduction velocity.

Axonal degeneration, if it is uniformly distributed over the whole diameter range, is expected to cause only a reduction in the amplitude of the recorded compound action potential, i.e. , the recorded potential and the distribution of conduction velocities are scaled down in amplitude. Distortion of the distribution of conduction velocities is only possible through a non-uniform axonal loss, for instance through a selective degeneration of the large and fast nerve fibers. The modeling of these pathological changes from the point of view of the distribution of conduction velocities is relatively simple, although the interpretation of the results is a more difficult task.

First we will model the effects of the demyelination and remyelination on the conduction velocity distribution. Let's consider a nerve fiber of total length L which is undergoing de- and remyelination. The portions of the fiber which have a complete myelin loss have a total length L_a ; the portions which have abnormal myelin thickness have a total length L_b and the portions which have abnor-

mal internodal length have total length L_c . The conduction velocities in each of the abnormal segments are given by:

$$v_a = C_a v_o \quad (5.1)$$

$$v_b = C_b v_o \quad (5.2)$$

$$v_c = C_c v_o \quad (5.3)$$

where v_o is the normal conduction velocity of the healthy segments of the nerve fiber. We note that while C_a is a constant and probably is the same for all nerve fibers, the factor C_b is an average over many different myelin thicknesses and the factor C_c is an average over different abnormal internodal lengths. Under these conditions, the conduction velocity measured over the whole length L of the fiber is:

$$v_f = Lv_o / (L + \frac{1 - C_a}{C_a} L_a + \frac{1 - C_b}{C_b} L_b + \frac{1 - C_c}{C_c} L_c) \quad (5.4)$$

Where $C_a = .1$ and $C_b > .5$ as we have already seen; $C_c = .63$, which was estimated in the following way: in normal nerve the proportionality factor between internodal length and diameter, is $.095 \text{ mm}/\mu$. In diabetes Thomas and Lascelles data [T1] gives $K_{\lambda \text{diab}} = .066 \text{ mm}/\mu$, and Chopra and Hurwitz [C4] data gives $K_{\lambda \text{diab}} = .0574$ and $.0576 \text{ mm}/\mu$ in two different populations of diabetic subjects. If we take $K_{\lambda \text{diab}}$ as the average of these three values, and if we assume that conduction velocity is proportional to internodal length, we obtain $C_c = K_{\lambda \text{diab}}/K_{\lambda}$ which is roughly $.63$.

In order to evaluate the significance of each term in the denominator of expression (5.4) , we have to consider the relative extent of each of the modeled pathological changes. Bare axon due to complete demyelination is relatively rare, and a typical value for L_a would correspond to three complete internodes; for a fiber 300 internodes long $L_a = .01L$; therefore

$$\frac{1 - C_a}{C_a} L_a = .1L \quad (5.5)$$

The sum of the lengths of onion bulbs and segments undergoing demyelination or remyelination can be assumed safely to be less than 30 internodes [B10]; that is, $L_b < .1L$ and it follows that:

$$\frac{1 - C_b}{C_b} L_b < .1L \quad (5.6)$$

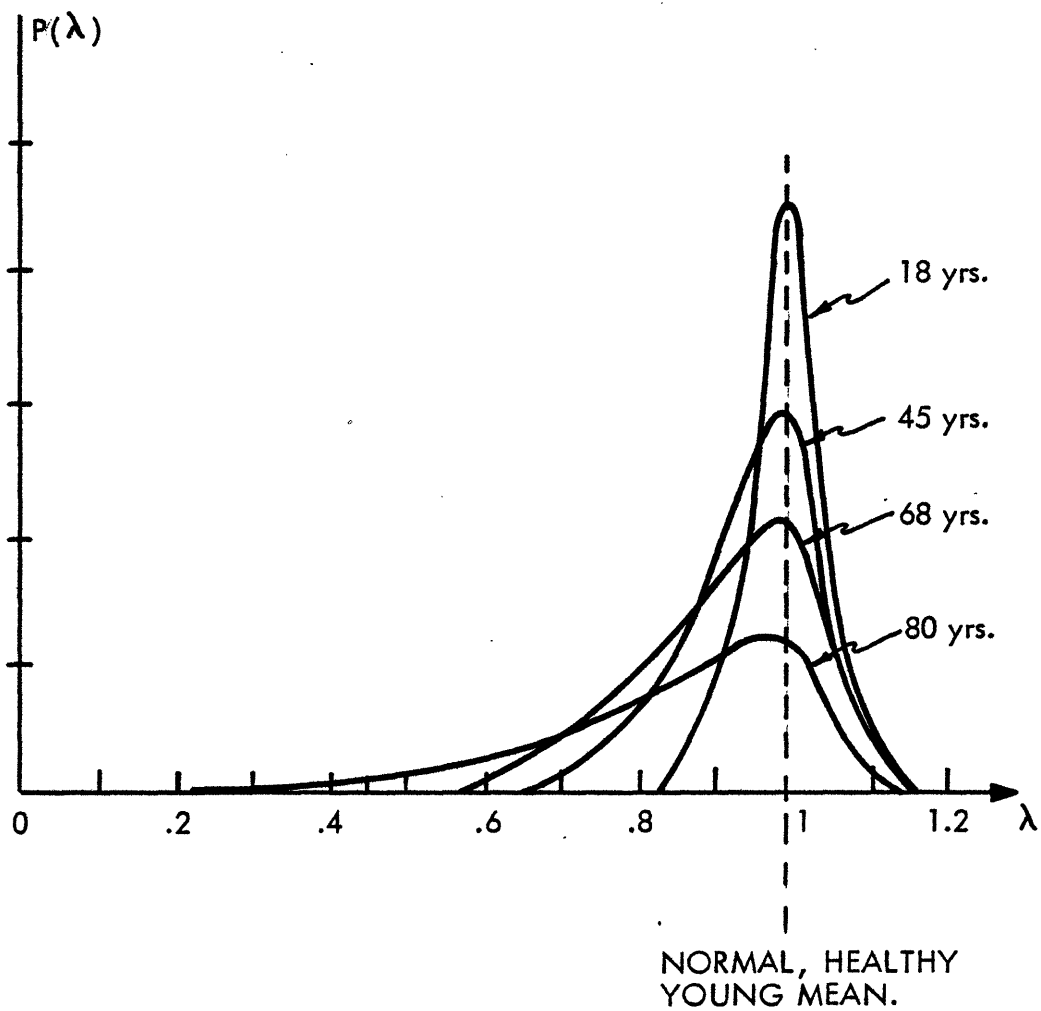
Finally, consider that the nerve over its whole extent has abnormal internodal length, that is $L_c = L$, and

$$\frac{1 - C_c}{C_c} L_c = .59L \quad (5.7)$$

which seems to be the dominant component in the slowing of the average conduction velocity. In our subsequent considerations we will assume that reduction in fiber conduction velocity is due only to reduction in internodal length. We note that this assumption may sometimes be far from reality.

Experimental evidence indicates that internodal length is a random variable along a fiber with diameter D , and has mean $\bar{\lambda} = K_{\lambda}D$. The variability of the internodal length has been shown to be very small in young and healthy individuals by Lascelles and Thomas [L2]. They have examined the sural nerve of a healthy 18 year old subject and found that $\bar{\lambda} = .100D$, and $\overline{(\lambda - \bar{\lambda})^2} = .0019D^2$. With increasing age, the variance of λ increases and its mean decreases. The important point is that with increasing age, more and more internodes of shorter than normal length show up, and internodes with a larger than normal length are seldom seen. Possible physiological explanations are that as the individual grows older, the nerve fibers are more likely to be exposed to some kind of mechanical or physiological trauma, or that a Schwann cell tends to die after a time and is replaced by more than one new Schwann cell. The variation of the probability density of the internodal length due to age, based on the data published in the work of Lascelles and Thomas [L2] is shown in Figure 5.3.1.

Let's see now how the conduction velocity is influenced by the variability on the internodal length. Suppose we have fibers of a certain diameter D and suppose that the probability density of the internodal lengths is given by one of the densities shown in figure 5.3.1. Further suppose that each fiber is N internodes long, so that its length L is a random variable since



BASED ON
DATA FROM THOMAS AND LASCELLES

FIGURE 5.3.1

$$L = \sum_{i=1}^N \lambda_i \quad (5.8)$$

Assuming that the action potential takes a fixed time τ to jump from one node to the next, independently of the size of the internode the expected value of the conduction velocity measured over the whole length of the fiber is:

$$\bar{v} = \bar{L} / N = N\bar{\lambda} / N\tau = \bar{\lambda} / \tau \quad (5.9)$$

and the variance of v is:

$$\sigma_v^2 = \sigma_\lambda^2 / N\tau^2 \quad (5.10)$$

This results in a standard-deviation to mean ratio for the velocity of

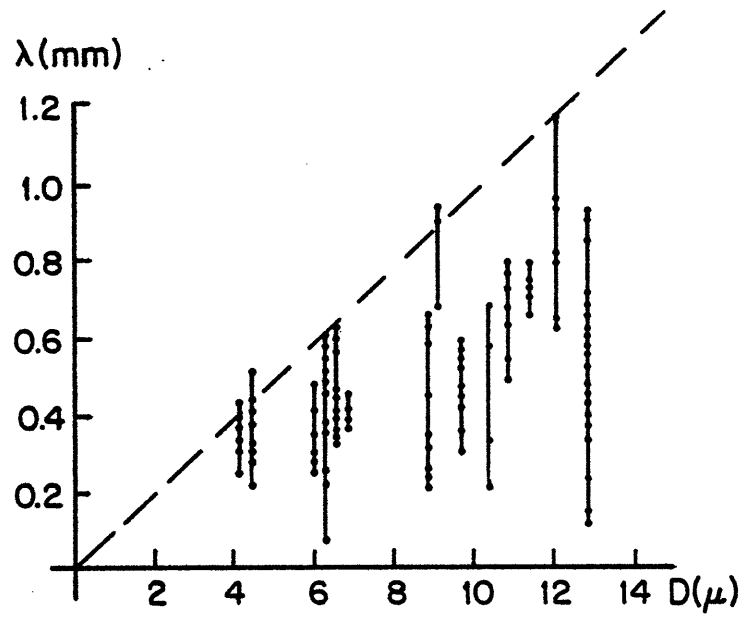
$$\sigma_v / \bar{v} = \sigma_\lambda / \bar{\lambda} \sqrt{N} \quad (5.11)$$

For $N = 300$ (say $\bar{L} = 30$ cm and $D = 10\mu$), this ratio is about 1/17 of the same ratio for the internodal length. Even if we consider the internodal length probability density for an 80 year old subject by assuming $\sigma_\lambda / \bar{\lambda} = .5$, we get a standard deviation to mean ratio for the velocity of .03, that is a $\pm 3\%$ deviation from the mean. This result is important to establish that in a normal subject, two fibers with the same diameter will exhibit essentially the same conduction velocity. Clearly if the mean internodal length decreases with age so will the conduction velocity of the nerve fiber as

established by several workers [K1].

Let's now examine the effect of repeated de- and remyelination which occurs in diabetic neuropathy on the distribution of conduction velocities. The available data on internodal length in diabetes from histological studies is relatively scarce and incomplete. The most extensive reports are those by Thomas and Lascelles [T1] and by Chopra and Hurwitz [C4]. The techniques used by them as well as the presentation of the results is essentially identical: they have taken by biopsy a sample about 3 cm long of the sural nerve and prepared longitudinal sections in order to measure internodal lengths and diameters. For each specimen, the result was presented in a graph of internodal length versus diameter (λ, D), such as shown in Figure 5.3.2. Each vertical line represents one single nerve fiber with the indicated diameter and each dot on the line indicates the length of one internode of the fiber. The dashed line - which was not published originally with the results - represents the normal λ -to-D ratio $K_\lambda = .095 \text{ mm}/\mu$. The situation seems to be the same as with aging: the randomness of the internodal length increases in diabetic neuropathy while the mean decreases. Based on the statistical information available in the mentioned works, let's formulate some consistent hypotheses and then examine if they agree with our findings.

Consider a healthy peripheral nerve composed of a large number of nerve fibers. These fibers are grouped according to con-



FROM CHOPRA AND HURWITZ.

FIGURE 5.3.2

duction velocity into M groups. The distribution of conduction velocities of this normal peripheral nerve is represented by β_{nor} , with its components given by $\beta_j = Kv_j^2 S_j$, where S_j is the total number of fibers in the j -th velocity group. Now suppose that this nerve undergoes repeated de and remyelination. Two hypothesis can be made:

- a) In each diameter group all fibers are equally affected, i.e., the probability density of the internodal lengths is the same for all fibers in the group. For clarity, suppose there are S_j fibers in the group with diameter in (D_j, D_{j+1}) , then according to this hypothesis:

$$p_{\lambda,i}(\lambda;D_j) = p_{\lambda,k}(\lambda;D_j) \text{ for all } i,k \in [1,S_j] \quad (5.12)$$

- b) The probability density of the internodal lengths is not the same for all nerve fibers in the same diameter group, i.e. :

$$p_{\lambda,i}(\lambda;D_j) \neq p_{\lambda,k}(\lambda;D_j) \text{ for some or all } j \neq k \quad (5.13)$$

Under hypothesis b) we could say that the mean internodal length of each fiber in the same group is a random variable over the ensemble of the fibers of the group with probability density $p_{\bar{\lambda}}(\bar{\lambda};D_j)$.

Both hypothesis are consistent with the published data and

it is impossible to decide which of them is correct. Assuming that hypothesis a) is true, we can consider either that:

a1) The de- and remyelination affects all fibers groups identically, that is:

$$\begin{aligned}
 p_{\lambda}(\lambda; D_j) &\stackrel{\Delta}{=} p_{\lambda_j}(\lambda) = p_{D_j}(\lambda) = \\
 &= \frac{D_k}{D_j} p_{\lambda_k}\left(\frac{D_k}{D_j} \lambda; D_k\right)
 \end{aligned}
 \tag{5.14}$$

To simplify the notation we define the random variable:

$$q_i = \frac{\lambda}{D_i} \tag{5.15}$$

then condition (5.14) becomes:

$$\begin{aligned}
 p_{q_j}(q; D_j) &= D_j p_{\lambda_j}(D_j q) = D_k p_{\lambda_k}(D_k q) = \\
 &= p_{q_k}(q; D_k)
 \end{aligned}
 \tag{5.16}$$

that is the statistics of the random variable q_i do not depend on the subscript i which identifies the diameter group.

a2) The effect of de- and remyelination is different for different fiber groups, namely:

$$p_{q_j}(q; D_j) \neq p_{q_k}(q; D_k) \text{ for some or all } j \neq k \tag{5.17}$$

that is the statistics of q_i depends on the diameter. The consequences of each of the above hypothesis on the distribution of conduction velocities is examined next.

Given a fiber of diameter D_i the probability that its velocity measured over a length L falls within some region $[v_j, v_{j+1})$ is given by:

$$P(v \in [v_j, v_{j+1}); D_i) = \int_{v_j}^{v_{j+1}} p_v(v; D_i) dv \quad (5.18)$$

where the probability density $p_v(v; D_i)$ is a function of the probability density of the internodal lengths $p_\lambda(\lambda; D_i)$ since:

$$v = (L/N_i \tau) \sum_{j=1}^{N_i} \lambda_j \quad (5.19)$$

Under hypothesis a), $p_\lambda(\lambda; D_i)$ is the same for all fibers in the i -th group, therefore the probability expressed by (5.18) is the same for all of them. Let's call $S(v_j, D_i)$ the number of fibers with diameter D_i which have velocity in the range $[v_j, v_{j+1})$. We have then:

$$\lim_{S(D_i) \rightarrow \infty} \left(\frac{S(v_j, D_i)}{S(D_i)} \right) = P(v \in [v_j, v_{j+1}); D_i) \quad (5.20)$$

For finite but large $S(D_i)$ we can say that:

$$S(v_j, D_i) \cong S(D_i) \int_{v_j}^{v_{j+1}} p_v(v; D_i) dv \quad (5.21)$$

In order to get the total number $S(v_j)$ of fibers which have conduction velocities in the j -th interval, we have to sum all $S(v_j, D_i)$ for all i from 1 to M , namely:

$$S(v_j) = \sum_{i=1}^M S(v_j, D_i) = \sum_{i=1}^M S(D_i) \int_{v_j}^{v_{j+1}} p_v(u; D_i) du \quad (5.22)$$

From the definition of $\beta_{\text{nor}}(v)$ we have that:

$$S(D_i) = (K \frac{D_i^2}{v_i})^{-1} \beta_{\text{nor}}(K \frac{D_i}{v_i}) \quad (5.23)$$

where the subscript "nor" stands for normal. Replacing (5.23) in (5.22) we obtain:

$$S(v_j) = \sum_{i=1}^M (K \frac{D_i^2}{v_i})^{-1} \beta_{\text{nor}}(K \frac{D_i}{v_i}) \int_{v_j}^{v_{j+1}} p_v(u; D_i) du \quad (5.24)$$

furthermore, because of (5.19) the probability density of v is given by:

$$p_v(u; D_i) = \text{conv}_{j=1, N_i} (N_i \tau p_{\lambda_j}(N_i u \tau)) \quad (5.25)$$

where the symbol "conv" stands for convolution of all probability densities $p_{\lambda_j}(N_i u \tau)$ from $j = 1$ to N_i . The relevant point here is that the first and second moments of this density are:

$$E(v; D_i) = \frac{1}{\tau} E(\lambda; D_i) = E(q) D_i / \tau = \bar{q} D_i / \tau \quad (5.26)$$

$$\sigma_v^2 = \sigma_\lambda^2 / N_i \tau \quad (5.27)$$

for large N_i the variance of v is always very small, as we have seen when we studied the effects of aging. We can consider then that $p_v(v;D)$ is entirely confined in the range $[v_j, v_{j+1})$ which contains its mean, that is:

$$\int_{v_j}^{v_{j+1}} p_v(v;D) dv = \begin{cases} 1 & \text{for } v_j \leq \bar{q}D/\tau < v_{j+1} \\ 0 & \text{otherwise} \end{cases} \quad (5.28)$$

Replacing this result in (5.24), we obtain:

$$S(v_j) = (K \frac{v_j^2 \tau}{\bar{q}^2})^{-1} \beta_{\text{nor}}(K_V \tau v_j / \bar{q}) \quad (5.29),$$

$$(5.30)$$

we can now find the abnormal distribution of conduction velocities $\beta_{\text{abn}}(v)$ of the diseased peripheral nerve by using the definition:

$$\beta_{\text{abn}}(v_j) = K v_j^2 S(v_j) = (\bar{q}^2 / \tau^2) \beta_{\text{nor}}(K_V \tau v_j / \bar{q}) \quad (5.31)$$

Since $K_V \tau / \bar{q} \leq 1$, this expression means that the conduction velocity

distribution for the diseased nerve under hypothesis a1) is shifted and compressed as shown in Figure 5.3.3. A direct consequence of (5.30) is that the normalized velocity range of $\beta_{abn}(v)$ is:

$$\begin{aligned}
 b_{abn} &= \frac{v_{\max,abn} - v_{\min,abn}}{v_{\max,abn}} = \\
 &= \frac{Cv_{\max,nor} - Cv_{\min,nor}}{Cv_{\max,nor}} = b_{nor} \quad (5.31)
 \end{aligned}$$

where $C = K_v \tau / \bar{q}$ and b_{nor} is the normalized velocity range for normal healthy nerve. We can summarize the consequences of hypothesis a1) on the distribution of conduction velocities as follows:

- i) the maximum conduction velocity $v_{\max,abn}$ is less than $v_{\max,nor}$,
- ii) the normalized velocity range b_{abn} is the same as b_{nor} .

Under hypothesis a2) according to which the de- and remyelination act selectively on the different fiber size groups, we can consider two cases:

- a2.1) The large fibers are primarily affected
- a2.2) The small fibers are primarily affected

In the first case, to fix ideas we can consider that the random variable $q_i = \lambda/D_i$ defined previously has mean \bar{q}

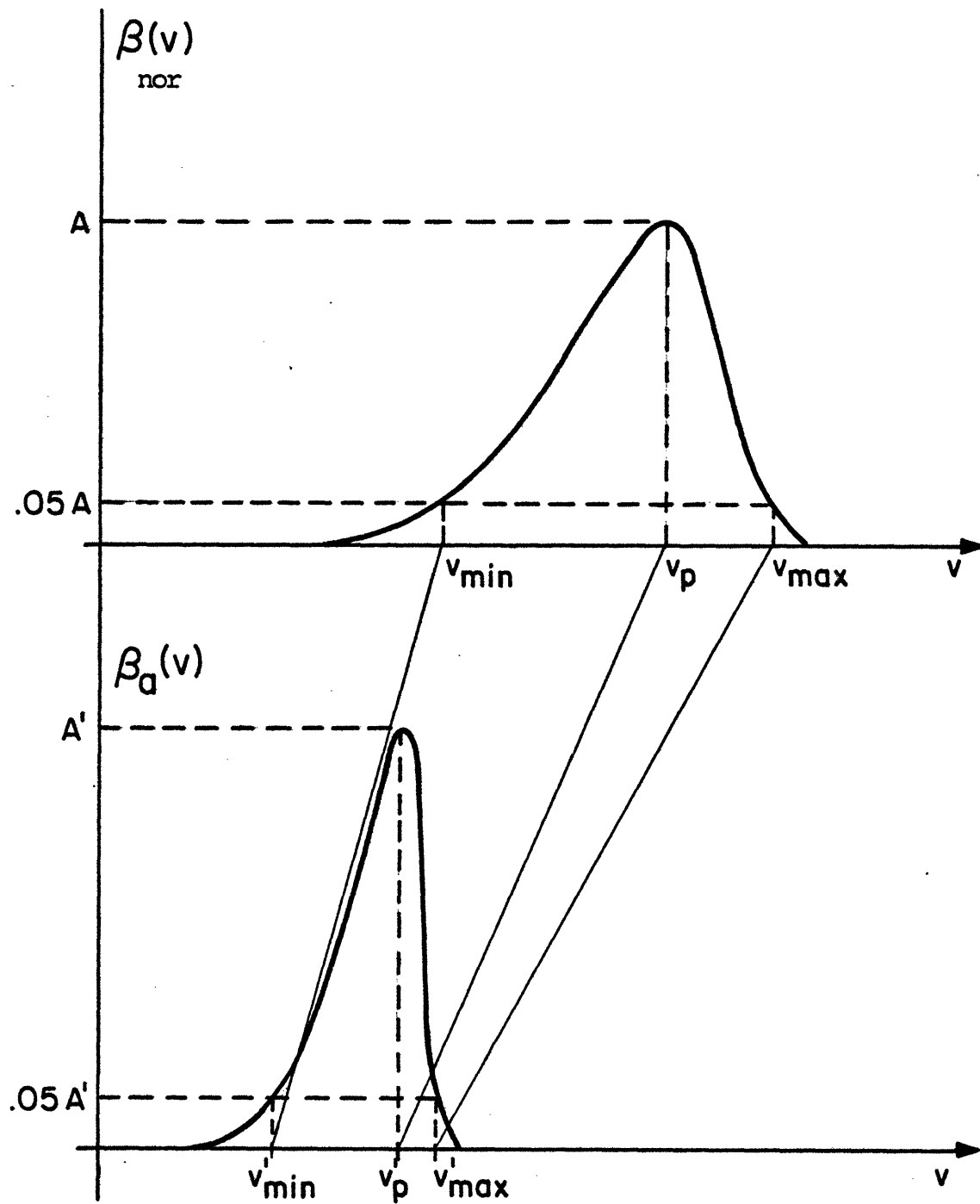


FIGURE 5.3.3

Distortion of the Distribution of Conduction Velocities when all fibers are affected identically.

which is equal to K_λ , i.e. the normal value, for all fibers which have diameter below some diameter D_1 and $\bar{q} < K_\lambda$ for all fibers which have diameter greater than $D_2 > D_1$. This is shown in Figure 5.3.4.a. The consequences of this assumption are that the distribution of conduction velocities is unaffected for all those fibers which have diameter less than D_1 while it is distorted for those with diameter greater than D_2 , according to hypothesis a1). The resulting distribution of conduction velocities is the superposition of these two portions and it is represented in Figure 5.3.4.b. We observe that $v_{\min,abn} = v_{\min,nor}$ while $v_{\max,abn} < v_{\max,nor}$, so that the normalized velocity range is:

$$\begin{aligned} b_{abn} &= (v_{\max,abn} - v_{\min,abn}) / v_{\max,abn} = \\ &= 1 - v_{\min,nor} / v_{\max,nor} < b_{nor} \end{aligned} \quad (5.32)$$

We can summarize the consequences of hypothesis a2.1 as:

- i) the maximum conduction velocity $v_{\max,abn}$ is less than $v_{\max,nor}$
- ii) the normalized velocity range b_{abn} is less than b_{nor} .

In the second case, that is when the small fibers are primarily affected by de- and remyelination, the mean \bar{q} as a function of dia-

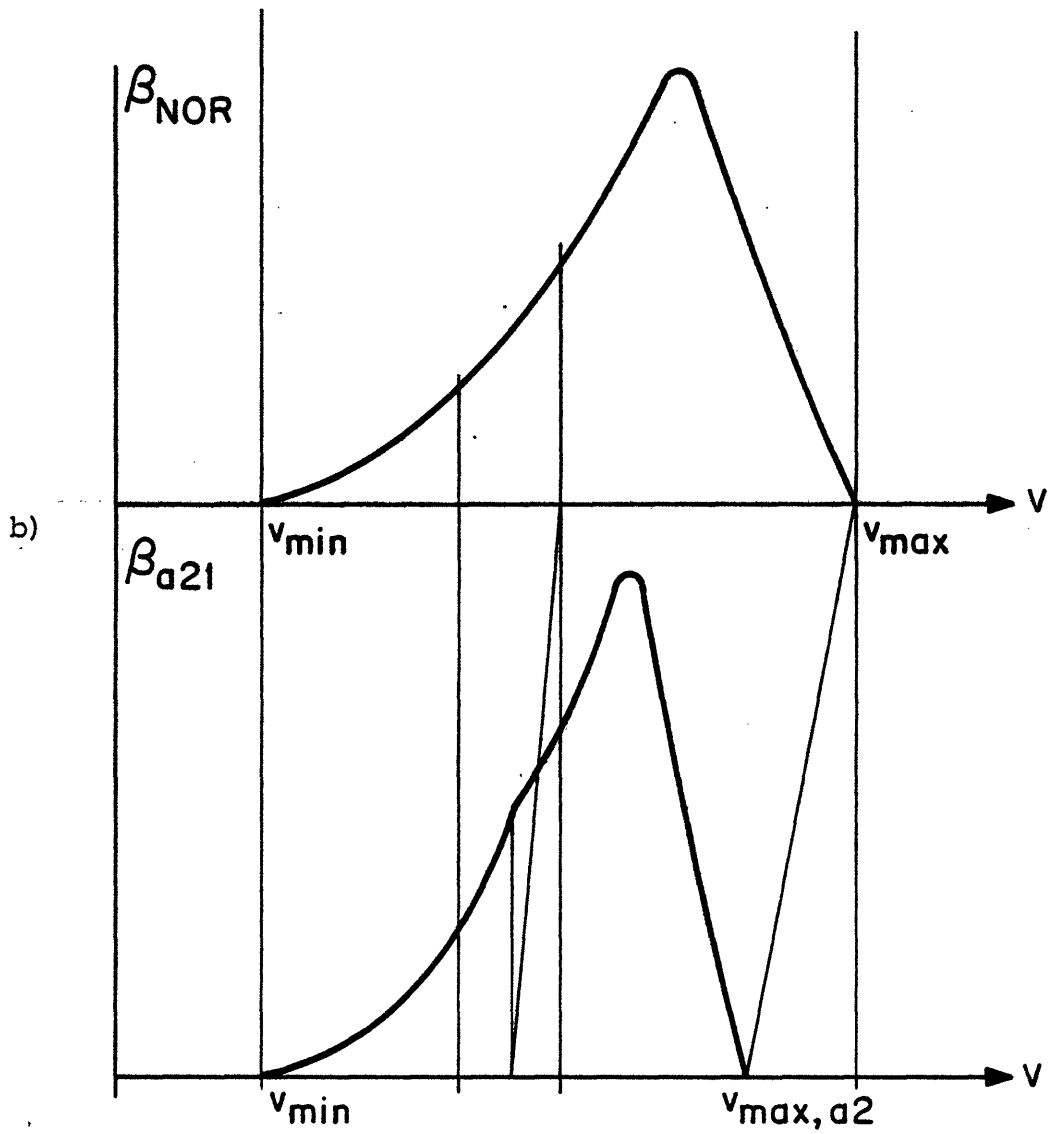
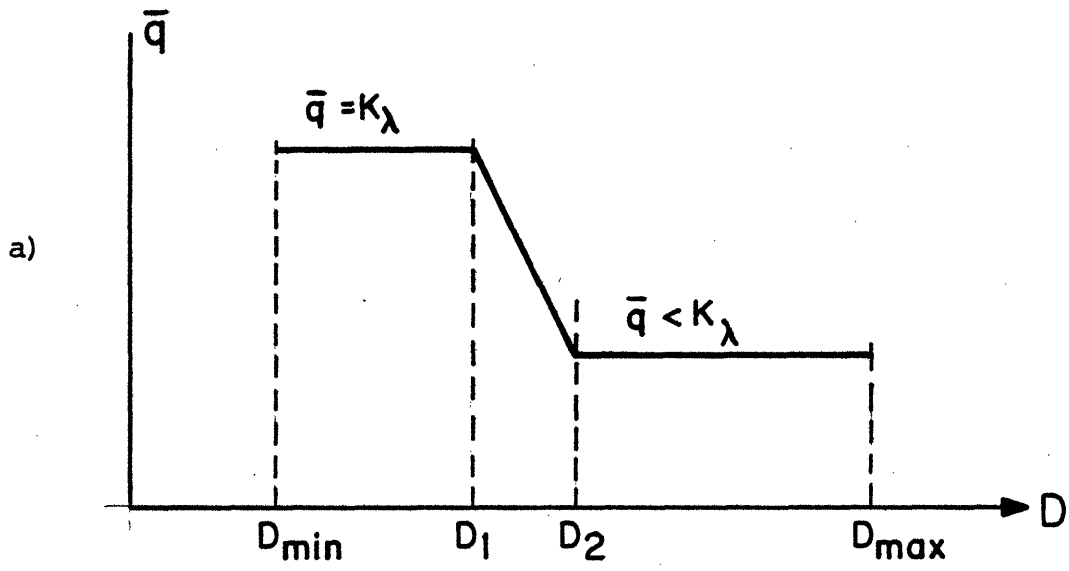


FIGURE 5.3.4

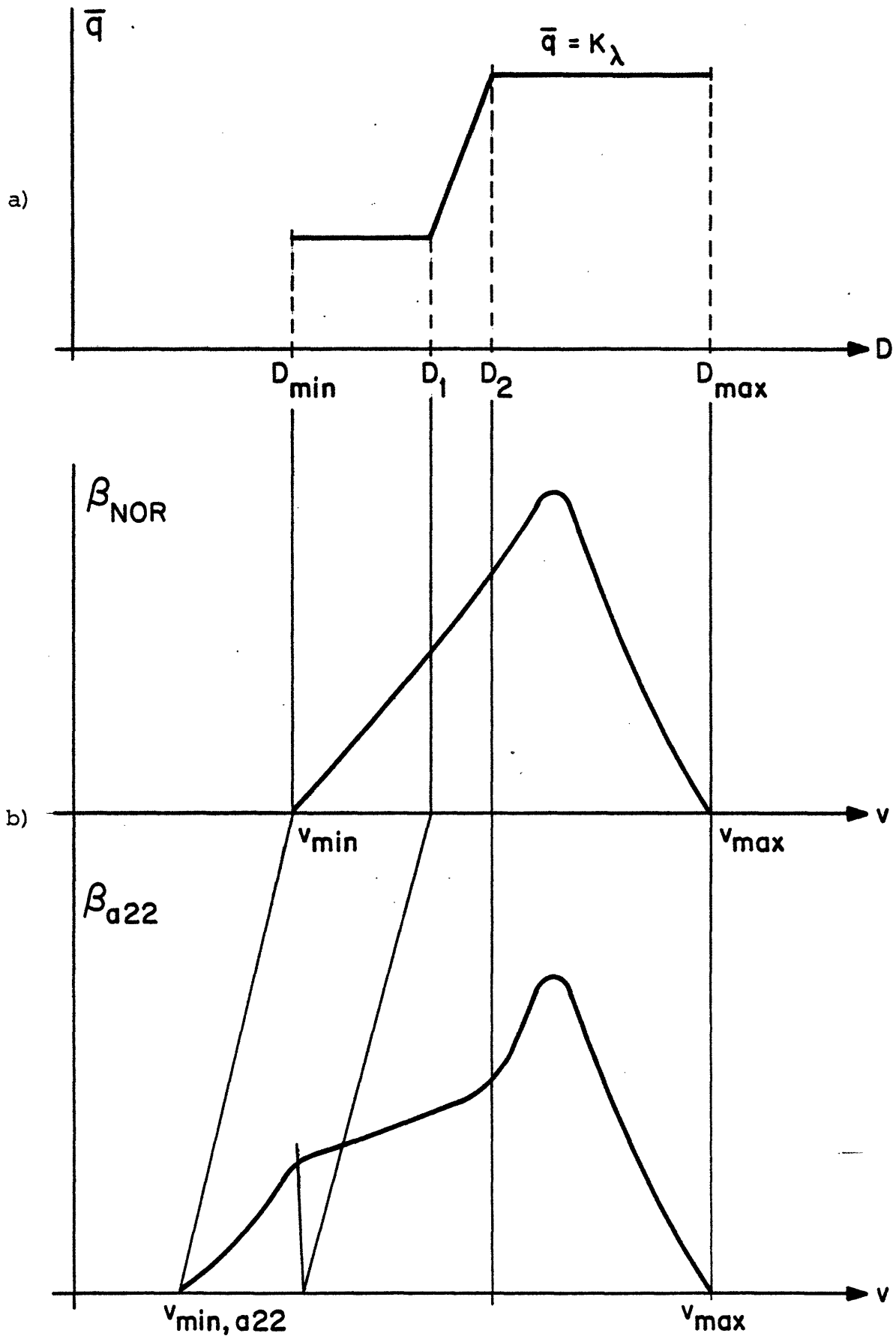


FIGURE 5.3.5

meter can be represented as in Figure 5.3.5.a and the resulting distribution of conduction velocities is shown in Figure 5.3.5.b. In this case we have that the normalized velocity range for the diseased fiber is:

$$b_{abn} = 1 - v_{\min,nor}/v_{\max,nor} > b_{nor} \quad (5.33)$$

The consequences of this hypothesis can therefore be summarized as:

- i) the maximum conduction velocity $v_{\max,abn} = v_{\max,nor}$
- ii) the normalized velocity range $b_{abn} > b_{nor}$.

Under hypothesis b) we have that the mean internodal length $\bar{\lambda}$ of each fiber is considered as a random variable over the ensemble of fibers in the same diameter group and it is distributed according to some probability density $p_{\bar{\lambda}}(\bar{\lambda}; D_i)$ (which has mean and variance independent of the number N_i of internodes in each fiber.) We have then that the conduction velocity of the k -th nerve fiber in the i -th diameter group is:

$$v_{k,i} = \frac{1}{N_i \tau} \sum_{j=1}^{N_i} \lambda_{j,k,i} \quad (5.34)$$

which has expected value $\bar{v}_{k,i} = \bar{\lambda}_{k,i}/\tau$. The random variable over the ensemble of fibers with diameter D_i has mean

$$E\{\lambda_{k,i}/\tau\} = E\{\lambda_{k,i}\}/\tau \triangleq \bar{\lambda}_i/\tau \quad (5.35)$$

and variance $\sigma_{v_i}^2$ which is not necessarily small. We can follow the same steps as in hypothesis a) to obtain the distribution of conduction velocities $\beta_{abn}(v_j)$ as a function of the distribution of conduction velocities in the normal nerve $\beta_{nor}(v)$. The result is:

$$\beta_{abn}(v_j) = C^{-1} \int_{v_0}^{v_1} \beta_{nor}(Cv) p_v(v_j;v) dv \quad (5.36)$$

where $C < 1$ depends on the statistics of the internodal length. The probability density $p_v(v_j;v)$ of the conduction velocity of a nerve fiber in the diseased nerve depends on the conduction velocity which that nerve fiber would have in a healthy nerve, that is v .

The substantial difference between this hypothesis and hypothesis a) is that under a) the probability density $p_v(v_j;v)$ was a function of the number of internodes in the nerve fibers and as long as this number was large, the standard deviation associated to $p_v(v_j;v)$ was always small. Under hypothesis b) this is no longer true and the standard deviation of $p_v(v_j;v)$ can be large. Assuming that $\beta_{nor}(v)$ and $p_v(v;v)$ are as represented in Figures 5.3.6.a and b, the resulting distribution of conduction velocities $\beta_{abn}(v)$ according to (5.36) is shown in Figure 5.3.6.c. We note that the maximum conduction velocity decreases while the normalized velocity range increases.

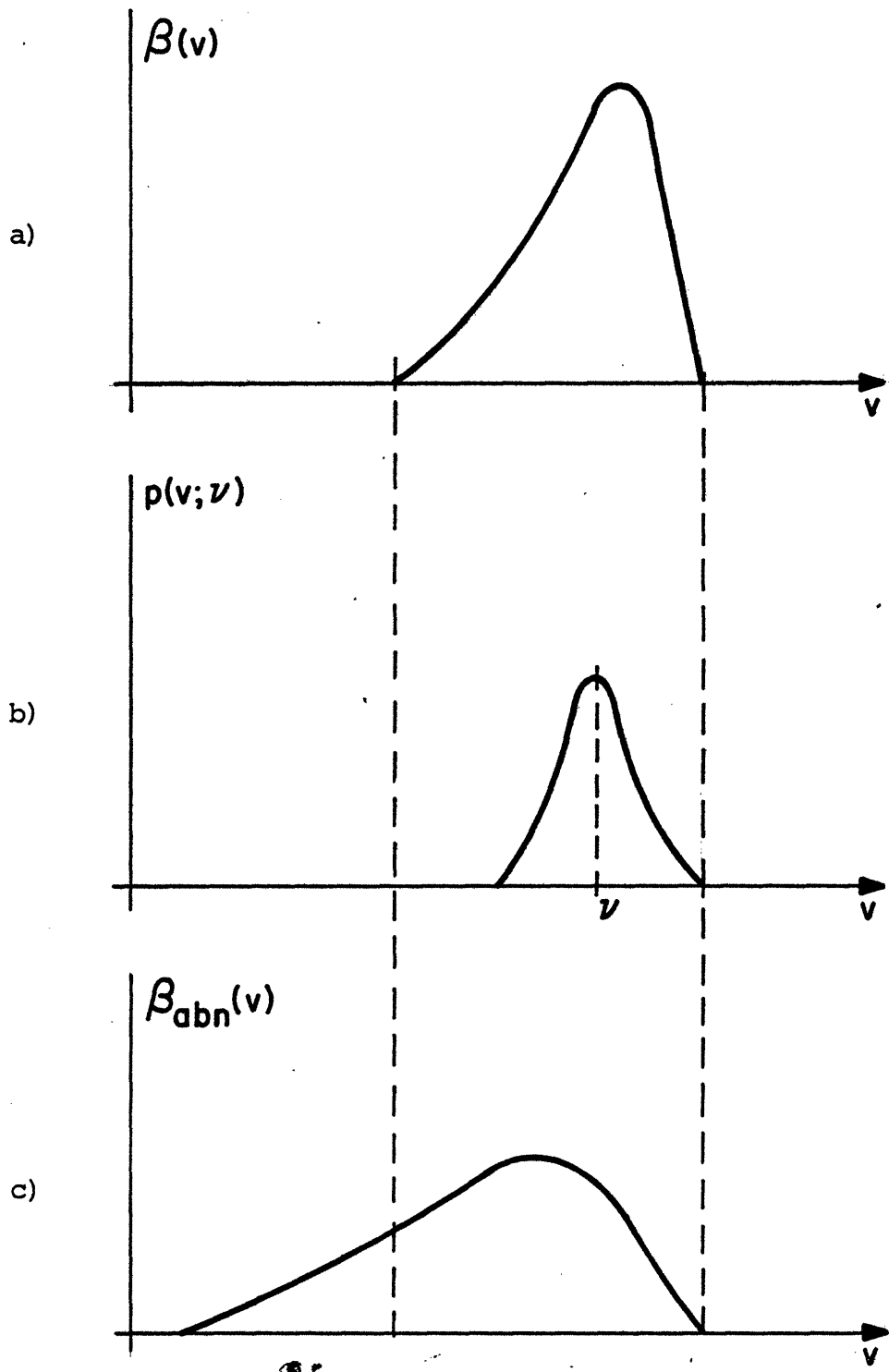


FIGURE 5.3.6

Axonal degeneration, if it is uniformly distributed over the whole fiber size range, is expected to cause only a reduction in the amplitude of the recorded compound action potential. Distortion of the distribution of conduction velocities from the normal is only possible through a non-uniform axonal loss. If large, fast conducting fibers are affected primarily then a reduction in the maximum conduction velocity and the normalized velocity range would be expected. If small fibers are affected primarily then the maximum conduction velocity should remain at its normal value but the normalized velocity range would be reduced.

The results of this discussion on segmental demyelination and axonal degeneration are summarized in Table 5.

The experimental data presented in the previous section suggests quite clearly that in diabetic sensory neuropathy the maximum conduction velocity is reduced and with less significance that the normalized velocity range is the same as is in normals. The maximum conduction velocities and normalized velocity ranges with the associated standard deviations in the median and ulnar nerves in both populations are:

- Normal Median, $v_{\max} = 70$ m/sec, $b = .372$, $\sigma_b = .096$
- Diabetic Median, $v_{\max} = 52.7$ m/sec, $b = .350$, $\sigma_b = .105$
- Normal Ulnar, $v_{\max} = 65.9$ m/sec, $b = .392$, $\sigma_b = .089$
- Diabetic Ulnar, $v_{\max} = 53.7$ m/sec, $b = .341$, $\sigma_b = .105$

TABLE 5

(b)	De- and Remyelination				Axonal Loss		
	hyp. a)	al.1	al.2	b)	uniform	large	small
$> b_{nor}$			X	X			
$= b_{nor}$	X				X		
$< b_{nor}$		X				X	X
(v_{max})							
$< v_{max,nor}$	X	X		X		X	
$= v_{max,nor}$			X		X		X

Hyp. a) Segmental Demyelination affects all diameter groups equally.

al.1) Large diameter groups are affected primarily.

al.2) Small diameter groups are affected primarily.

b) All diameter groups are affected, but fibers in the same group may be affected differently.

The standard deviation for all groups is roughly $\sigma = .1$, and the largest difference between normalized velocity ranges is $b_{\text{nor,ul}} - b_{\text{diab,ul}} = .051 \approx \sigma/2$, suggesting that in fact b does not change significantly with diabetes. The only consistent explanation according to Table 5 is then that uniform demyelination and remyelination (that is, which affects all fibers in the same way) is the major pathological change in diabetic neuropathy. The other possibility is that b is slightly less than normal in diabetes which according to Table 5 would indicate that mainly large fibers are affected either by segmental demyelination or by axonal degeneration, or both. Both possibilities are consistent with the clinical picture of sensory diabetic neuropathy.

Due to the relatively large intersubject variability of the maximum conduction velocity and of the normalized velocity range, it seems that it is unsafe to express any opinion with respect to the pathological changes according to Table 5 for any individual case.

CHAPTER 6

CONCLUDING REMARKS AND SUGGESTIONS FOR FURTHER RESEARCH

An electrophysiological and statistical technique for estimating the distribution of conduction velocities in peripheral nerves from the compound action potential recorded by surface electrodes has been proposed, developed and analyzed. The method is appealing for clinical studies of human peripheral neuropathies because it is non invasive and it can be applied to most of the peripheral nerves. On the other hand, because it uses measurements which in general have very low signal-to-noise ratios, it may present relatively large uncertainties associated with the estimates. Also, because the intensity of the recorded action potentials from peri-

pheral nerve fibers depends quadratically on the fiber diameter, the technique has an "intrinsic" limitation for measuring the activity in the small fibers, and is therefore restricted to the study of the upper half of the fiber size spectrum (approximately from 5μ on.).

The technique was compared to standard histological techniques for obtaining the same information and the results were in good agreement. This evaluation could be further improved by using more sophisticated histological processes which result in less shrinkage and distortion of the nerve fibers. The electrophysiological procedure, however, seems to be close to its optimum performance and better results could possibly be obtained only by changing the recording technique, using for instance needle recording electrodes. The restriction of this would be that the technique could be used in humans only by a qualified physician.

The signal processing technique is relatively simple but is suboptimal. Two different further directions could be investigated. One, toward an optimal processor which (if it exists) seems to have huge computational complexity and may not result in significantly better estimates. The second path to follow, would be toward a simpler signal processing scheme which would require less computation, even sacrificing accuracy if necessary.

Diabetic sensory neuropathy was studied with this technique. We think that some interesting insights into the underlying

pathological changes could be obtained. After this first stage, the study could be extended to more carefully selected and controlled populations and a correlation between the severity of the neuropathy as defined by clinical standards and the distribution of conduction velocities could be attempted. Other neuropathies, such as alcoholic neuropathy or neuropathies of toxic origin could also be studied and compared.

Only sensory peripheral nerves have been studied with this technique. Its extension to the study of motor nerves which innervate skeletal muscles is complicated by the fact that when the muscle fibers contract due to the stimulation of the motor nerves, the records of the nerve action potentials are disturbed by the much larger muscle action potential. In general, the action potential from the nerve is completely buried in the evoked EMG signal. This problem can be corrected in part by recording from the nerve at points which are relatively far from the innervated muscle. For mixed motor and sensory nerves, we have a similar problem with respect to the motor portion of the nerve.

It should also be mentioned that the method offers no simple means of separating efferent from afferent activity since it is not based on the natural stimulation of the nerves through the sensory receptors or motor structures they innervate.

Finally, we should note that the technique is obviously

not restricted to the study of human neuropathies. In any recording situation from nerves for which the linear superposition of the individual action potentials holds and in which only noise corrupted measurements can be made, the proposed estimation technique can be applied. Among such recordings situations are the recordings made from excised nerves which are commonly used in animal studies and basic research in physiology.

APPENDIX 1

THE ESTIMATOR EQUATIONS

We will show here that if H and β are solutions of the system of equations:

$$\alpha(H - Z) + (H\beta - y)\beta' = 0 \quad (\text{A1.1})$$

$$H'H\beta - H'y = 0 \quad (\text{A1.2})$$

then β will also be the root of the quadratic vector equation

$$\beta\beta'Z'y + (\alpha Z'Z - y'yI)\beta - \alpha Z'y = 0 \quad (\text{A1.3})$$

In fact, from (A1.1) we have that:

$$H(\alpha I + \beta\beta') = \alpha Z + y\beta' \quad (\text{A1.4})$$

the matrix $(\alpha I + \beta\beta')$ is always invertible for $\alpha \neq 0$ and its inverse is given by:

$$(\alpha I + \beta\beta')^{-1} = (\alpha^2 + \alpha\beta'\beta)^{-1}((\alpha + \beta'\beta)I - \beta\beta') \quad (\text{A1.5})$$

which can be verified easily. Let's call $k = \alpha + \beta'\beta$. Replacing (A1.5) in (A1.4) we obtain:

$$H = k^{-1}(kZ + y\beta' - Z\beta\beta') \quad (\text{A1.6})$$

Expression (A1.2) can be written as:

$$H'(H\beta - y) = 0 \quad (\text{A1.7})$$

From (A1.6) we get the following equality:

$$H\beta - y = k^{-1}(Z\beta - y) \quad (\text{A1.8})$$

which replaced in (A1.7) gives:

$$(kI - \beta\beta')Z'Z\beta - (kI - \beta\beta')Z'y + \beta\beta'Z'y - y'y\beta = 0 \quad (\text{A1.9})$$

multiplying this equation by $(\alpha I + \beta\beta')$ and using the identity (A1.5), we obtain:

$$\alpha k Z'Z\beta - \alpha k Z'y + (\alpha I + \beta\beta')\beta\beta'Z'y - (\alpha I + \beta\beta')y'y\beta = 0 \quad (\text{A1.10})$$

which after rearranging the terms and using the definition of k , reduces to:

$$\beta\beta'Z'y + (\alpha Z'Z - y'yI)\beta - \alpha Z'y = 0 \quad (\text{A1.11})$$

which is the desired result.

APPENDIX 2

THE STIMULUS ARTEFACT

The nerve response $r(t)$ in (3.18b) starts only at some time $t_f = d/v_{\max}$ after the application of the stimulating pulse, where d is distance between the recording and stimulating electrodes and v_{\max} is the maximum conduction velocity of the nerve. Therefore, for $t \in [0, t_f)$ we have only the stimulus artefact plus noise, namely:

$$y(t) = A(1 - \alpha t)\exp(-\alpha t) + n(t), \quad t \in [0, t_f) \quad (\text{A2.1})$$

and we want A and α such that the mean square error:

$$L = \int_{t_0}^{t_f} (y(t) - A(1-t)e^{-t})^2 dt \quad (\text{A2.2})$$

is minimum. The initial time t_0 is chosen such that the initial transient has settled and the model matches the artefact. If such A and α exist, they must be among the solutions of the necessary conditions for minima:

$$\frac{\partial L}{\partial A} = 0 \quad (\text{A2.3})$$

$$\frac{\partial L}{\partial \alpha} = 0 \quad (\text{A2.4})$$

while the second component is minimized by shielding all cables.

The hypothesis about the composition of the stimulus artefact is consistent with the experimental observation that the stimulus artefact grows linearly with stimulus intensity. This is now briefly reported

The experimental set up was the same as for measuring the compound action potential from the median nerve and it is described in detail in Appendix 3. The electrical stimulus, consisting of an electrical pulse of 50 microseconds duration was increased from 0 to 84 Volts and measurements were taken at 13 different intensities. At each of these intensities, the stimulus artefact was measured by averaging 1024 individual responses, and one such average response is shown in Figure A2.1. The peak-to-peak values were plotted against stimulus intensity. The linear regression line of the peak-to-peak values versus stimulus intensity was computed using least-squares and it is shown in Figure A2.2.

The linear nature of the artefact suggested the following solution - soon discarded for obvious reasons - to eliminate it from the action potential records: First, using a very small stimulus intensity, so that no nerve fiber in the trunk is stimulated the artefact is measured:

$$y_1(t) = a(t) + n_1(t), \quad t \in [0, T] \quad (A2.1)$$

where $n_1(t)$ is measurement noise with zero mean and spectral density

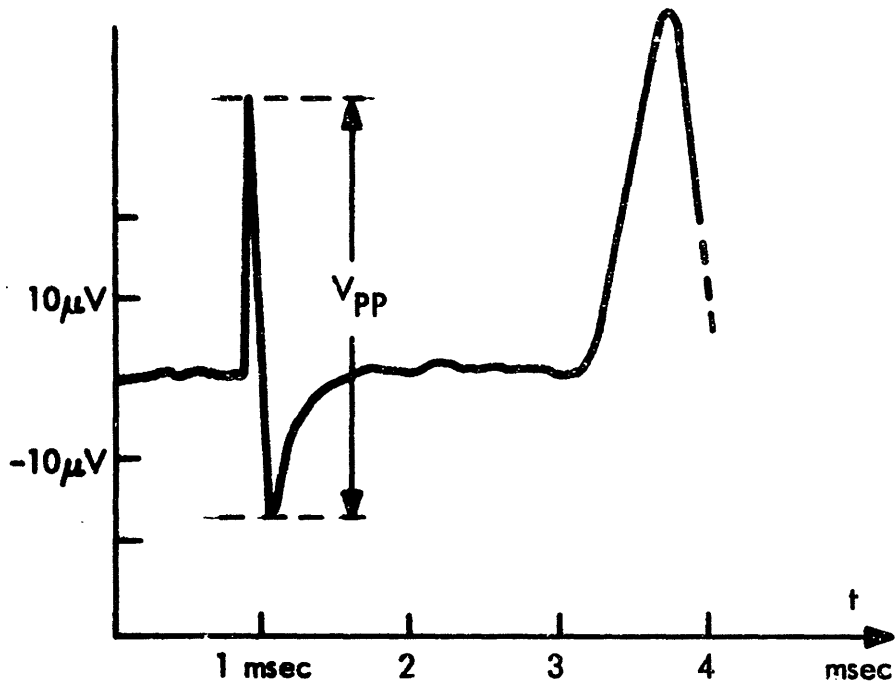


FIGURE A2.1

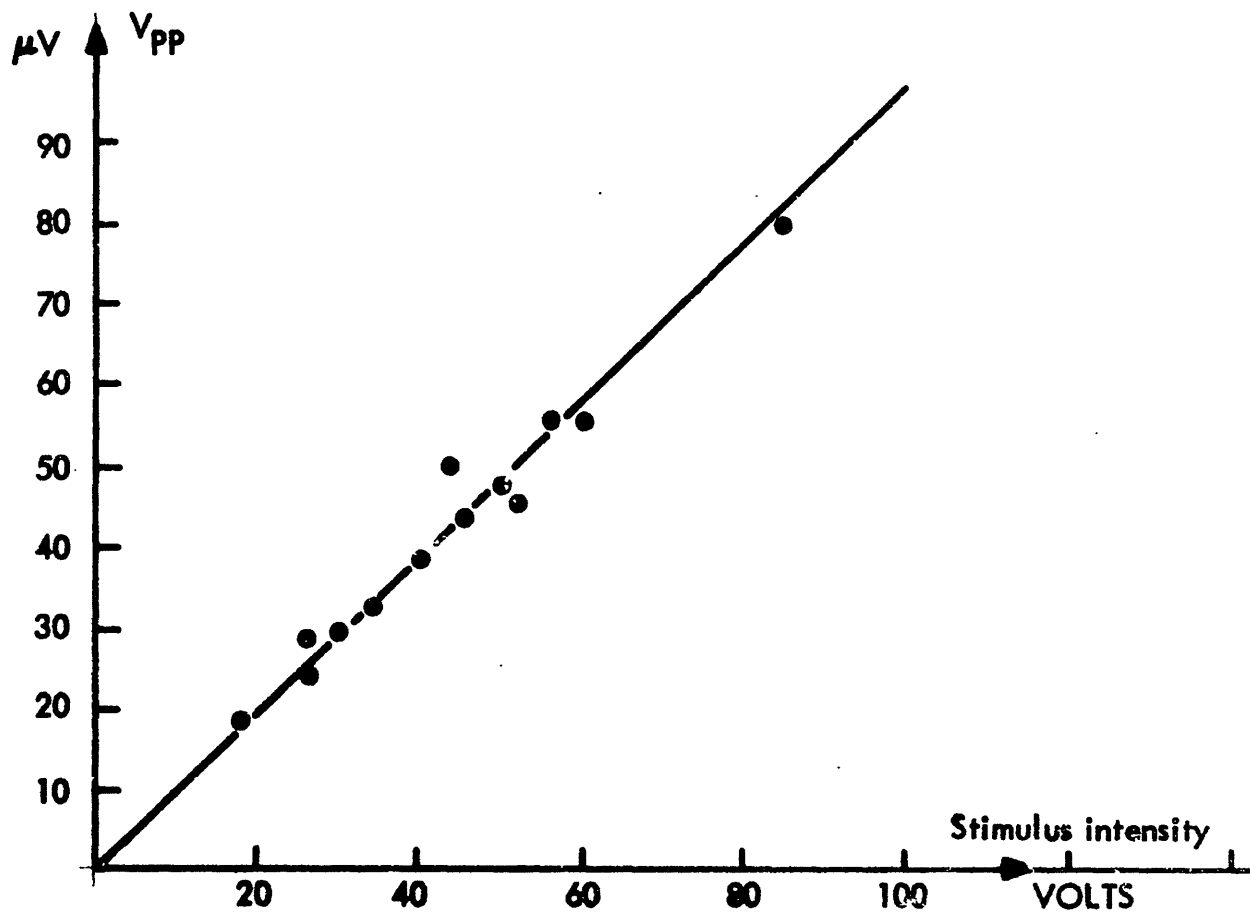


FIGURE A2.2

σ_1^2 . Then the compound action potential is measured:

$$y_2(t) = r(t) + Ka(t) + n_2(t), \quad t \in [0, T] \quad (\text{A2.2})$$

where $r(t)$ is the signal from the nerve, and $n_2(t)$ is zero mean noise with spectral density σ_2^2 . The scaling factor K is estimated by the ratio of the stimulus intensities used to obtain $y_1(t)$ and $y_2(t)$. The artefact free signal is then obtained by:

$$\begin{aligned} y_2(t) &= y_2(t) - Ky_1(t) = \\ &= r(t) + n_2(t) - Kn_1(t) = \\ &= r(t) + n(t) \end{aligned} \quad (\text{A2.3})$$

where the noise $n(t)$ has spectral density $\sigma_n^2 = \sigma_2^2 + K^2\sigma_1^2$. Clearly, we need a very small σ_1^2 in order to have σ_n^2 reasonably small because K is in general large. We have calculated that under typical conditions ($K = 10$, $\sigma_n^2 = 2\sigma_2^2$, and $y_2(t)$ obtained by averaging 1024 responses at the rate of 10 stimulus/sec) $y_1(t)$ should be the average of about 10^5 individual responses which would take about 3 hours of averaging. This approach was abandoned. The following solution to eliminate the artefact was finally used:

It was realized that the artefact could usually be modeled with a very good accuracy by the following function:

$$\begin{aligned} a(t) &= A(1 - at)\exp(-at) && t > 0 \\ &= 0 && \text{otherwise} \end{aligned} \quad (\text{A2.4})$$

In the actual artefact the discontinuity at $t = 0$ is obviously non-existent, therefore there is always a large error between the model and the actual signal in the neighborhood of $t = 0$. Otherwise the model matches the artefact quite well. The least-squares estimation of A and α is now described.

The nerve response $r(t)$ in (A2.2) starts only at some time $t_f = d/v_{\max}$ after the application of the stimulating pulse, where d is distance between the recording and stimulating electrodes and v_{\max} is the maximum conduction velocity of the nerve. Therefore, for $t \in [0, t_f)$ we have only the stimulus artefact plus noise, namely:

$$y(t) = A(1 - \alpha t)\exp(-\alpha t) + n(t), \quad t \in [0, t_f) \quad (\text{A2.5})$$

and we want A and α such that the mean square error:

$$L = \int_{t_0}^{t_f} (y(t) - A(1 - \alpha t)e^{-\alpha t})^2 dt \quad (\text{A2.6})$$

is minimum. The initial time t_0 is chosen such that the initial transient has settled and the model matches the artefact. If such A and α exist, they must be among the solutions of the necessary conditions for minima:

$$\frac{\partial L}{\partial A} = 0 \quad (\text{A2.7})$$

$$\frac{\partial L}{\partial \alpha} = 0 \quad (\text{A2.8})$$

which gives:

$$\frac{1}{\epsilon} \int y(t) (2t - \alpha t^2) e^{-\alpha t} dt = A \Psi(\alpha, \epsilon) \quad (\text{A2.5})$$

$$\frac{1}{\epsilon} \int y(t) (1 - \alpha t) e^{-\alpha t} dt = A \frac{1}{\epsilon} \int (1 - \alpha t)^2 e^{-2\alpha t} dt \quad (\text{A2.6})$$

where

$$\Psi(\alpha, \epsilon) \triangleq \chi(\alpha) - \epsilon^2 \chi(\alpha \epsilon) \quad (\text{A2.7})$$

$$\chi(\alpha) \triangleq (1 - (1 + 2\alpha - 6\alpha^2 + 4\alpha^3) e^{-2\alpha}) / 8\alpha^2 \quad (\text{A2.8})$$

and

$$\epsilon \triangleq t_0 / t_f \quad (\text{A2.9})$$

The algorithm which will be used to solve the above set of equations in A and α , depends on the monotonicity of the function $\Psi(\alpha, \epsilon)$ in the neighborhood of the solution. First, we will show that $\chi(\alpha) = \Psi(\alpha, 0)$ is strictly monotonically decreasing. In fact, for $\alpha > 0$, $\chi(\alpha)$ is strictly monotonically decreasing if and only if:

$$\frac{d\chi(\alpha)}{d\alpha} < 0 \quad \text{for } \alpha > 0 \quad (\text{A2.10})$$

we note that

$$\frac{d\chi(\alpha)}{d\alpha} = \frac{(4\alpha^4 - 8\alpha^3 + 2\alpha^2 + 2\alpha + 1)e^{-2\alpha} - 1}{4\alpha^3} \quad (\text{A2.11})$$

is strictly negative for positive α if

$$4\alpha^4 - 8\alpha^3 + 2\alpha^2 + 2\alpha + 1 < e^{2\alpha} \quad (\text{A2.12})$$

We note that for any given polynomial, making α sufficiently large $e^{2\alpha}$ can be made larger than that polynomial. This assures that the inequality (A2.12) is always true for sufficiently large α . Expanding $e^{2\alpha}$ in series, (A2.12) becomes:

$$(\alpha - 2) < 2 \sum_{i=0}^{\infty} (2\alpha)^i / (i+3)! \quad (\text{A2.13})$$

Now, we note that for $\alpha < 2$ the left hand side is always non-positive while the right hand side is strictly positive. We have the inequality then verified for $0 < \alpha < 2$. For $\alpha > 2$, we proceed as follows:

The right hand side of (A2.13) can be written as

$$\begin{aligned} 2 \sum_{i=0}^{\infty} (2\alpha)^i / (i+3)! &= 1/3 + \alpha/6 + \alpha^2/15 + \alpha^3/45 + \\ &+ 2 \sum_{i=4}^{\infty} (2\alpha)^i / (i+3)! \\ &\triangleq p(\alpha) + \xi(\alpha) \end{aligned} \quad (\text{A2.14})$$

If we now show that

$$p(\alpha) > (\alpha - 2) \quad \text{for } \alpha \geq 2 \quad (\text{A2.15})$$

then because $\xi(\alpha) > 0$ for $\alpha > 0$ and $\xi(\alpha) > 0$ for $\alpha > 0$, we have (A2.13) verified for all positive α .

We have that:

$$p(\alpha) = \frac{\alpha^3 + 3\alpha^2 + 7.5\alpha + 15}{45} \quad (\text{A2.16})$$

and

$$\frac{dp(\alpha)}{d\alpha} = \frac{3\alpha^2 + 6\alpha + 7.5}{45} \quad (\text{A2.17})$$

which are both monotonically increasing for positive α , and $p(\alpha)$ is a convex function in any closed interval $[0, x]$ in that region.

We have therefore that for any α_0 and α , $\alpha > \alpha_0$:

$$p(\alpha) - p(\alpha_0) \geq (\alpha - \alpha_0) \dot{p}(\alpha_0) \quad (\text{A2.18})$$

In particular for $\alpha_0 = 3.444$ for which $\dot{p}(\alpha_0) = 1$ and $p(\alpha_0) = 2.6$, we have that

$$p(\alpha) > \alpha - .844 > \alpha - 2 \quad (\text{A2.19})$$

and inequality (A2.13) is verified for all positive α .

We will show now that for certain values of ϵ , the function $\Psi(\alpha, \epsilon)$ is non-monotonically decreasing in a certain range of positive α . In fact, $\Psi(\alpha, \epsilon)$ is strictly monotonically decreasing if and only if:

$$\left. \frac{d\Psi}{d\alpha} \right|_{\alpha_0} = \left. \frac{d\chi}{d\alpha} \right|_{\alpha_0} - \epsilon^3 \left. \frac{d\chi}{d\alpha} \right|_{\epsilon\alpha_0} < 0 \quad (\text{A2.20})$$

but,

$$\frac{dx}{d\alpha} = \frac{Q(\alpha)e^{-2\alpha} - 16}{64\alpha^3} \quad (\text{A2.21})$$

where $Q(\alpha)$ is a polynomial. Condition (A2.20) implies then that:

$$Q(\alpha)e^{-2\alpha} > Q(\alpha\varepsilon)e^{-2\alpha\varepsilon} \quad (\text{A2.22})$$

for all $\varepsilon \in (0,1)$. This can be satisfied if and only if $Q(\alpha)e^{-2\alpha}$ is monotonically decreasing, that is if:

$$\frac{d}{d\alpha} Q(\alpha)e^{-2\alpha} = \{\dot{Q}(\alpha) - 2Q(\alpha)\} e^{-2\alpha} < 0 \quad (\text{A2.23})$$

or

$$\dot{Q}(\alpha) - 2Q(\alpha) < 0 \quad (\text{A2.24})$$

In terms of the roots of $\dot{Q}(\alpha) - 2Q(\alpha)$ we obtain that:

$$\dot{Q}(\alpha) - 2Q(\alpha) \begin{cases} < 0, & \text{for } \alpha \in (0, (5-\sqrt{5})/2) \cup ((5+\sqrt{5})/2, \infty) \\ > 0, & \text{for } \alpha \text{ elsewhere} \end{cases} \quad (\text{A2.25})$$

Therefore we can guarantee the uniqueness of the inverse of $\Psi(\alpha, \varepsilon)$ only if ε is restricted to one of the intervals for which (A2.24) is satisfied. Under this restriction, the system of equations (A2.25) and (A2.26) which gives the least squares estimates of the parameters of the artefact is then solved in the following way:

We start with some α_0 and obtain A_0 from (A2.25), and

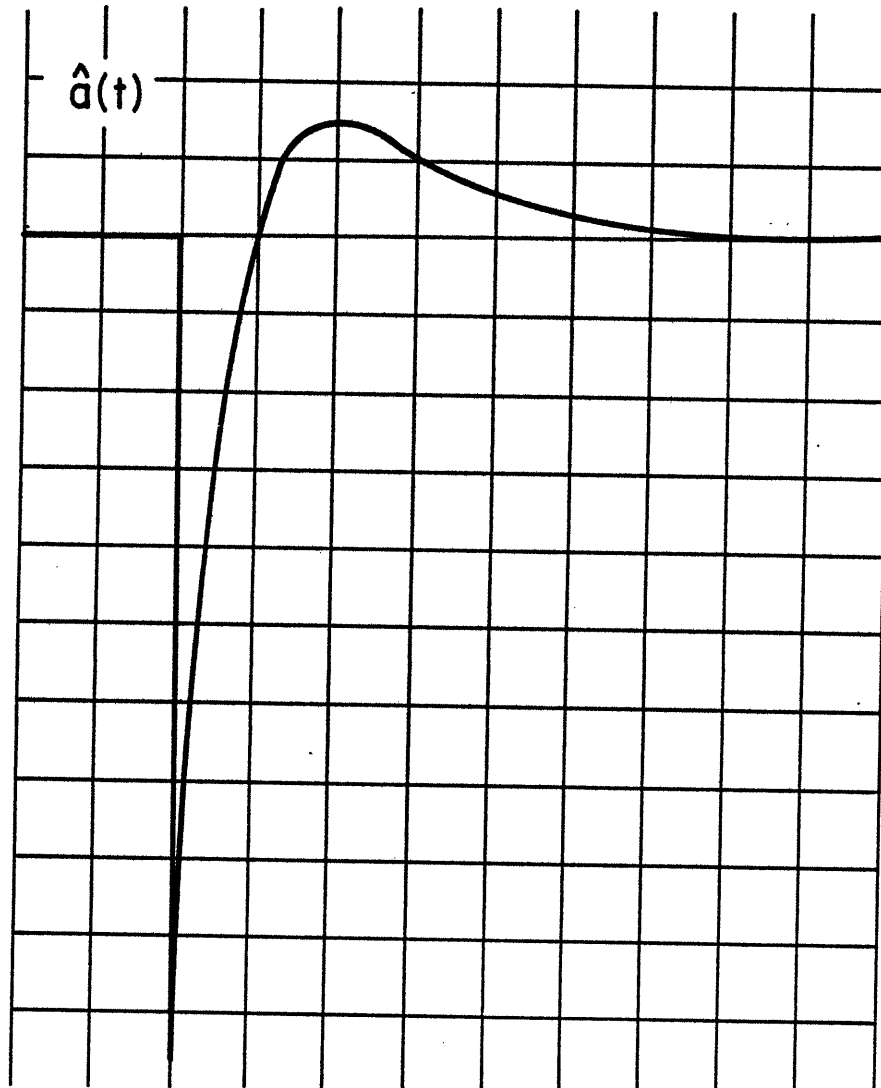
the next iterated value α from (A2.9) as long as $\Psi(\alpha, \epsilon)$ is uniquely invertible for that α_1 . At the n-th iteration, we have that:

$$A_n = \left\{ \int_{\epsilon}^1 y(t) (1-\alpha_n t) e^{-\alpha_n t} dt \right\} / \left\{ \int_{\epsilon}^1 (1-\alpha_n t)^2 e^{-2\alpha_n t} dt \right\} \quad (\text{A2.26})$$

$$\Psi(\alpha_{n+1}, \epsilon) = A_n^{-1} \left\{ \int_{\epsilon}^1 y(t) (2t - \alpha_n t^2) e^{-\alpha_n t} dt \right\} \quad (\text{A2.27})$$

which converges to the solution provided that $\Psi(\alpha_n, \epsilon)$ is invertible for all α_n .

This algorithm was implemented in Fortran and it is listed in Appendix 5. Only in a very few cases convergence couldn't be obtained, and those corresponded in general to situations in which the artefact was unusually large and the true value of α was outside the range for which convergence can be guaranteed. The algorithm was extensively tested with real data obtained under typical circumstances; one such result is shown in Figure A2.1.



FIGURE

A2.1

APPENDIX 3

INSTRUMENTATION AND TESTING PROCEDURES

We have collected data on 90 peripheral nerves (median and ulnar), in a total of 27 subjects, 13 were diabetic male subjects with ages ranging from 26 yrs. to 71 yrs.; 9 were non-diabetic male subjects with ages from 19 yrs. to 62 yrs. and 5 were normal female subjects with ages from 18 yrs. to 38 yrs. The experimental set up as well as the instruments used were changed during the course of the four month testing period, so not all of the 90 experiments are comparable in this sense.

We started by using the TECA TE-4 EMG machine for delivering the stimulus as well as for recording the nerve response.

The responses were averaged with a FABRITEK DIGITAL AVERAGER. In many situations the nerve responses were as small as .1 microvolts peak-to-peak, so that 1024 to 4096 individual responses had to be averaged in order to get an acceptable signal-to-noise ratio. The problem with this set up was that the recording channel of the TECA TE-4 was corrupted by a stimulus-locked digital noise and was enhanced together with the nerve response by the averaging process. This noise was probably generated inside the stimulator, and it was about .1 microvolt peak-to-peak. Many of the records done under these circumstances couldn't be used for the estimation of the distribution of conduction velocities. The problem was solved by using the TECA TE-4 preamplifier with separate batteries and the vertical channel of a Tektronix oscilloscope as amplifier.

The stimulus artefact was most of the time excessively large, that is of the order of 1 Volt peak-to-peak, while the largest nerve response recorded was about 60 microvolts. We found that most of the artefact was primarily radiated by the cables which connected the stimulating electrodes to the stimulator, and picked up by the wires of the recording electrodes. This problem was satisfactorily solved by shielding all signal cables. The stimulus artefact was lowered to the 5 to 20 microvolt range, which was excellent when the nerve responses were of the order of 60 microvolts, but still poor when they were in the fractions of micro-

volts.

The worst kind of noise of physiological origin in this study was the EMG signal generated by the muscles near to the recording electrodes. Few subjects had the ability to turn off voluntarily all their motor units in the arm under study for a longer period of time. We decided then to provide a "feedback" to the subject through an oscilloscope, so that he could watch his own EMG signal and learn how to turn it off. With this arrangement almost all subjects were able in a few minutes to relax their arms completely. The final set-up, used from experiment number 50 on, is shown in Figure A3.1.

The subjects were asked to wash their arms with soap in order to remove any saline layer of low resistivity which might be present on the surface of the skin. They were seated comfortably in an armchair. The ground strap electrode was attached and the best position for placing the recording electrodes was determined. This was done by stimulating different spots on the skin until the nerve was maximally stimulated. All median nerve responses were recorded at the wrist and all ulnar nerve responses at the elbow. The recording electrodes were made of lead and measured 1 by 1 cm. The ring electrodes used for stimulation were placed in the appropriate finger : finger 3 for the median nerve and finger 5 for the ulnar nerve.

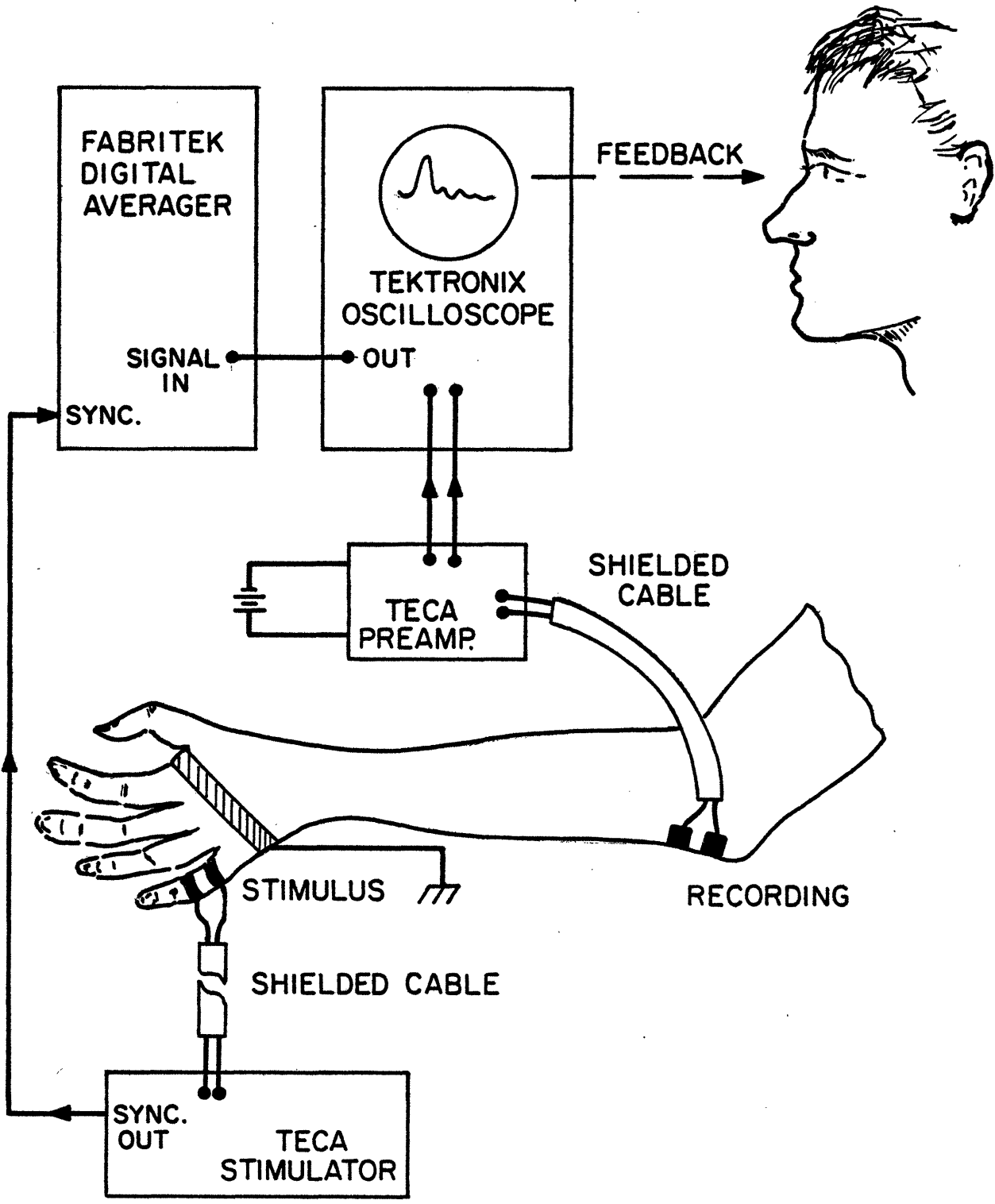


FIGURE A3.1

The electrical stimulus was delivered by the stimulator of the TECA TE-4 EMG machine at the rate of 10 pulses/sec. and it consisted of pulses of 50 microsec. duration. We started by stimulating the nerve supramaximally, just below the threshold for pain. Then, after the compound action potential was measured, we applied the threshold stimulation, usually below the threshold for sensation. In the first case, usually 512 to 1024 individual nerve responses were averaged while in the second case 1024 to 4096 nerve responses were used. In many instances, the second part was repeated two or three times until the smallest nerve response could be obtained.

APPENDIX 4

EVALUATION OF THE ESTIMATOR USING SYNTHETIC COMPOUND ACTION POTENTIAL

The estimator described in chapter 3, was evaluated using synthetic data, in the following way:

The basic action potential $h(v_r t)$ was assumed to have some realistic shape as shown in Figure A4.1.a. The distribution of conduction velocities $\beta(v)$, was assumed to be the one shown in Figure A4.2, represented by the black dots. The compound action potential was then generated according to:

$$y(t) = \sum_{j=1}^{14} \beta_j h_j(v_j t) \quad (\text{A4.1})$$

This compound action potential is shown in Figure A4.1.c. Finally, random noise was added to $h(v_r, t)$ as shown in Figure A4.1.b, in such a way that $\sigma_n^2 / \|h\|^2 = .108$, and to the compound action potential $y(t)$ in the proportion $\sigma_{ny}^2 / \|y\|^2 = .01$. This data was used to estimate the distribution of conduction velocities. The computed estimate $\hat{\beta}(v)$ is shown in Figure A4.2 and is represented by the bars. The mean-square error normalized to the squared norm of the true distribution of conduction velocities resulted:

$$\epsilon^2 = (\|\beta - \hat{\beta}\|^2) / \|\beta\|^2 = .0055$$

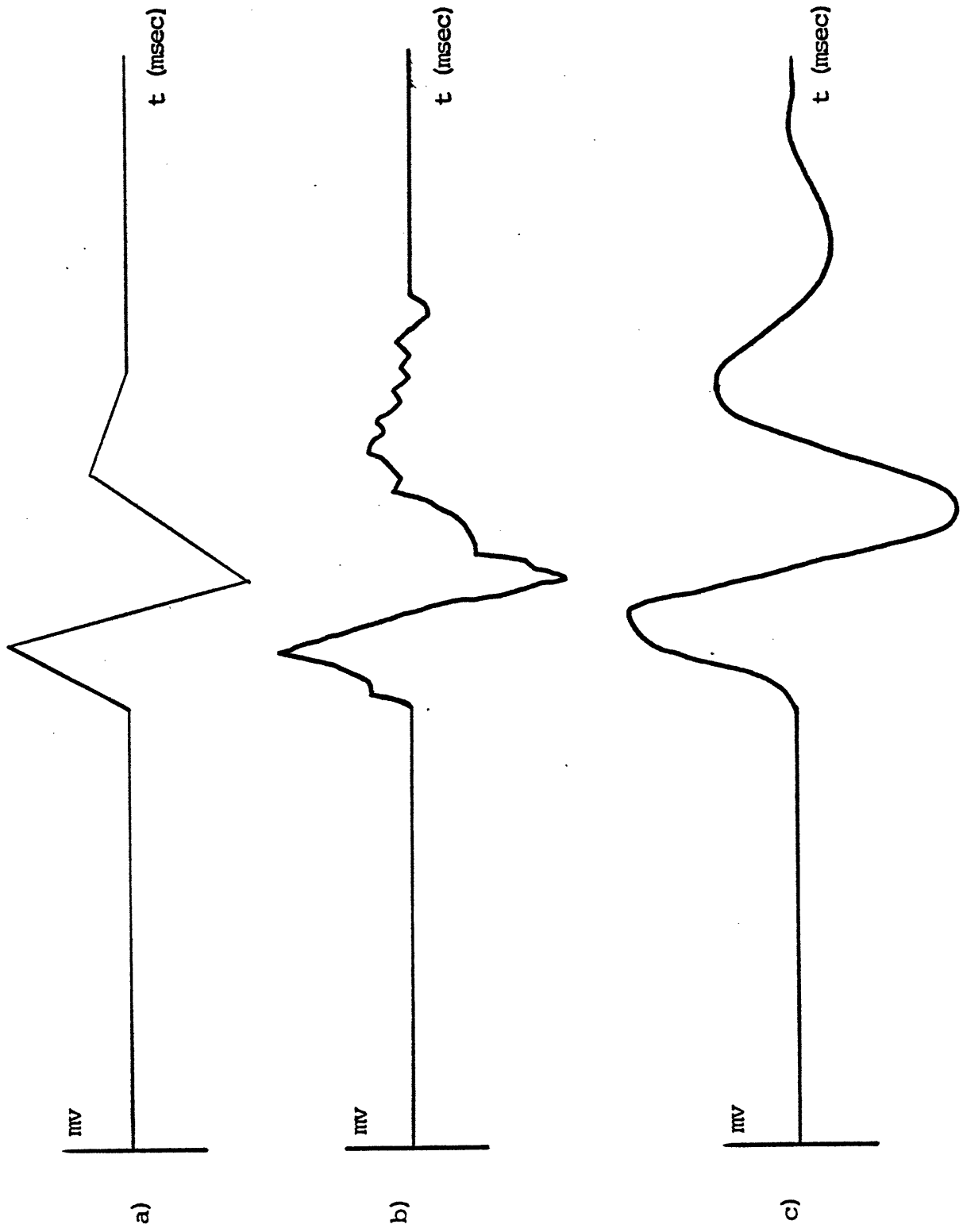


FIGURE A4.1

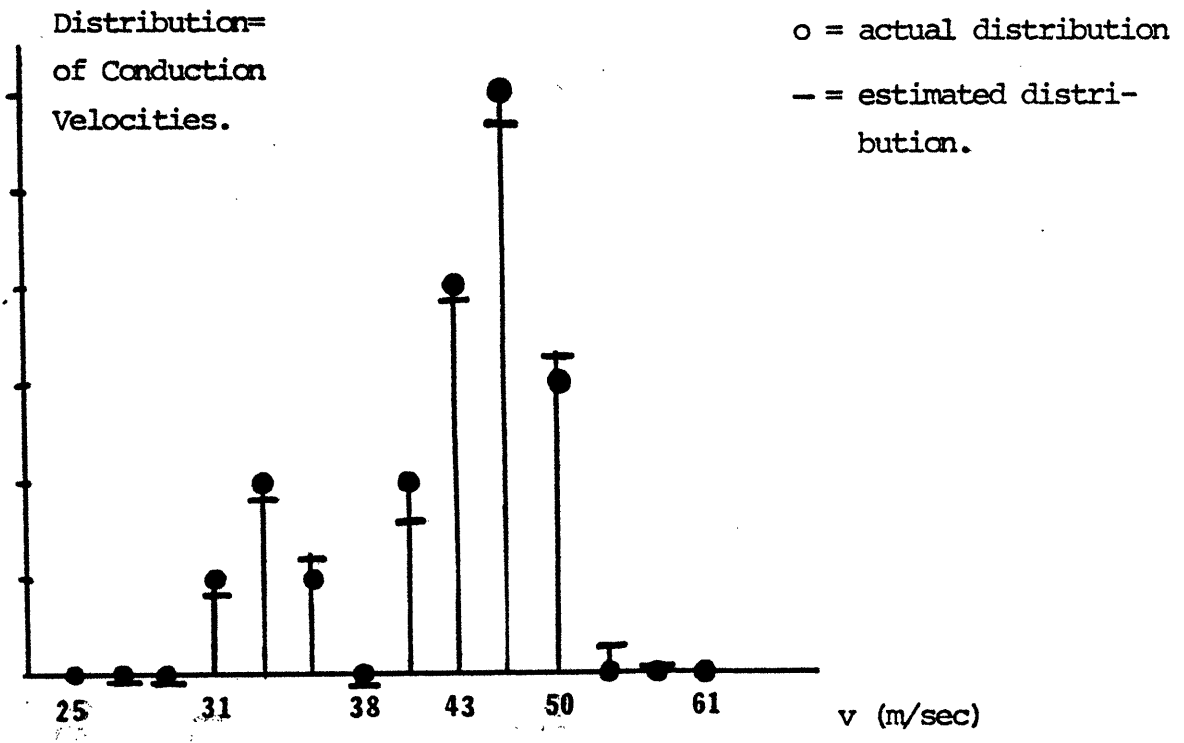


FIGURE A4.2

APPENDIX 5

COMPUTER PROGRAM LISTINGS

Program Name: VELDIS

Purpose: Compute the least-squares estimate of the Distribution of conduction velocities from the artefact-free nerve signals.

Sequence:

1- Reads in relevant data parameters and the data; namely:

N = the total number of sample points, that is the total length of the data. It must not exceed 400.

M = The number of discrete velocities. It must not exceed 24.

Z = Is the recorded nerve response to threshold stimulus. (Artefact-free)

Y = Is the recorded nerve response to supramaximal stimulation. (Artefact-free)

LZ, LY = Are the number of leading zeros in Z and Y respectively; that is, the number of sample points between the stimulus and the onset of the nerve response.

NZ, NY = Are the actual number of data points in Z and Y.

AZ, BZ and AY, BY = Are the parameters of the baselines to be subtracted from Z and Y.

EXTREME VELOCITIES = Are the normalized extreme velocities.

SCALE = The conduction velocity corresponding to Z. The above mentioned extremes are normalized to this number.

ALPHA = The ratio between the variance of the noise in Y and the variance of the noise in Z.

2 - ENERGIES = The squared norms - of Z and Y are computed and the ratio XSC is printed out.

- 3- VELOCITIES - From the given normalized velocity range and the total number of discrete velocities M , the normalized value of each velocity is computed.
- 4- MATRIX H - Using the vector Z and the discrete velocities calculated in (3), the elements of the matrix Z are computed by linear interpolation as indicated by expressions (3.44) and (3.45) of Chapter 3.
- 5- EIGENVALUES - The eigenvalues of $Z'Z$ and the orthonormal matrix θ are computed.
- 6- VECTOR U - The vector $u = \theta'Z'y$ defined in Chapter 3 is calculated.
- 7- ORDERING - All eigenvalues are reordered in an increasing order.
- 8- SEARCH - The eigenvalues of $Z'Z$ and the elements of the vector U are relabeled (re-indexed).
- 9- ROOT - The maximum root of (3.28) is determined.
- 10- OUTPUT - Vectors γ and β corresponding to the maximum root of (3.28) are calculated and the estimate of the distribution of conduction velocities (β) is displayed in an appropriate format.

```

C AS OF AUGUST 14,1976
C ***** VELDIS *****
C * N = TOTAL LENGHT OF THE DATA, IT MUST NOT *
C * EXCEED 400. *
C * M = NUMBER OF DISCRETE VELOCITIES, MUST NOT *
C * EXCEED 24. *
C * Z = IS THE RECORDED RESPONSE TO THRESHOLD STI- *
C * MULATION. *
C * Y = IS THE RECORDED RESPONSE TO SUPRAMAXIMAL *
C * STIMULATION. *
C * LZ,NZ = ARE THE NUMBER OF LEADING ZEROS AND *
C * THE NUMBER OF ACTUAL DATA POINTS IN Z. *
C * LY,NY = ARE THE NUMBER OF LEADING ZEROS AND *
C * THE NUMBER OF ACTUAL DATA POINTS IN Y. *
C * AZ,BZ = ARE THE PARAMETERS OF THE BASELINE TO *
C * BE SUBTRACTED FROM Z. *
C * AY,BY = ARE THE PARAMETERS OF THE BASELINE TO *
C * BE SUBTRACTED FROM Y. *
C *****
C
C
$NDM
DIMENSION Z1(350),Y1(350)
C
DIMENSION AM(25),IR(25)
DIMENSION A(25,25)
DIMENSION V(25,1),S(25)
DIMENSION H(25,25)
DIMENSION T(25,25)
DIMENSION Z(400,1),Y(400,1),U1(400),U2(400)
DIMENSION BTA(25,1)
PRINT,"N,M="
READ,N,M
PRINT,"Z="
READ,Z1
PRINT,"LZ,NZ="
READ,LZ,LX
PRINT,"Y="
READ,Y1
PRINT,"LY,NY="
READ,LY,NY
2PRINT,"EXTREME VEL'S"
READ,VMIN,VMAX
PRINT,"AZ,BZ="
READ,AZ,BZ
DO 5 I=1,LX
L=LZ+I
Z(L,1)=.0001*(Z1(I)-AZ-BZ*(I-1))
5CONTINU E
DO 7 I=1,LZ
Z(I,1)=0
7CONTINU E

```

```

PRINT,"AY,BY="
READ,AY,BY
DO 10 I=1,NY
L=LY+I
Y(L,1)=.0001*(Y1(I)-AY-BY*(I-1))
10CONTINUE
DO 11 I=1,LY
Y(I,1)=0
11CONTINUE
C
**ENERGIES**
ENY=0
ENZ=0
DO 12 I=1,N
ENY=ENY+(Y(I,1)/N)**2
ENZ=ENZ+(Z(I,1)/N)**2
12CONTINUE
XSC=SQRT(ENY/ENZ)
PRINT,"XSC="
PRINT 250,XSC
C
**VELOCITIES**
C
XMAX=ALOG(VMAX)
XMIN=ALOG(VMIN)
DEL=(XMAX-XMIN)/M
M=M+1
DO 20 I=1,M
V(I,1)=EXP(XMIN+(I-1)*DEL)
20CONTINUE
C
**MATRIX H**
C
DO 25 J=1,M
V1=V(J,1)
CALL INTPOL(U1,V1,Z,M,N)
DO 21 I=J,M
V2=V(I,1)
CALL INTPOL(U2,V2,Z,M,N)
T(I,J)=0
DO 21 L=1,N
T(I,J)=T(I,J)+U1(L)*U2(L)
21CONTINUE
S(J)=0.
DO 23 L=1,N
S(J)=S(J)+U1(L)*Y(L,1)
23CONTINUE
25CONTINUE
DO 27 J=1,M
DO 26 I=J,M
T(J,I)=T(I,J)
26CONTINUE

```



```

C          **ROOT**
C
L=K
102XS=-S(L)
IF(XS) 110,105,110
105L=L-1
GO TO 102
110X=XS+ABS(XS)
XFU=0.
115DO 120 J=1,M
XFU=XFU+(ALP*V(J,1)**2)/(X+S(J))
120CONTINUE
IF(XFU-X)130,130,125
125X=X+ABS(XS)
GO TO 115
130A1=XS
A2=X
CALL ROOT(A1,A2,V,S,X,K,ALP)
C=X
C
C          **OUTPUT**
C
PRINT," "
I=K
185DO 186 J=1,K
BTA(J,1)=ALP*V(J,1)/(C+S(J))
186CONTINUE
CALL PRODMA(H,BTA,Y,M,M,1)
PRINT 250,C
PRINT," "
CALL GRAPH(M,1,Y,XMIN,DEL,SCA)
PRINT,"CONTINUE=1,STOP=0"
190READ(50,,ERR=190) IAB
IF(IAB)192,192,37
192PRINT,"CHANGE PARAMETERS=1"
READ,JANS
M=M-1
IF(JANS)193,193,2
193PRINT 200,(Y(I,1),I=1,M)
200FORMAT(2X,5(E10.4,2X))
210FORMAT(1X,"VELOCITIES",//)
220FORMAT(1X,"EIGENVALUES",//)
230FORMAT(1X,"VECTOR U",//)
240FORMAT(1X,"EIGENVECTORS",//)
250FORMAT(1X,E10.4)
END
C *****INTPOL*****
C * SUBROUTINE INTPOL(H,VI,Z,M,N),DESIGNED TO *
C * GENERATE A WAVEFORM H WHICH IS ESSENTIALLY *
C * Z TRAVELLING AT A LOWER SPEED VI.M IS DUMMY *
C * N MUST BE LESS THAN 100. *

```



```

C *****
C
SU BROUTINE INTPOL(H,V1,Z,M,N)
DIMENSION Z(400,1),H(400)
H(1)=Z(1,1)
IF(V1-1)10,10,30
10K=0
DO 29 I=2,N
CR=-(K+1)/V1+(I-1)
IF(CR) 27,27,26
26K=K+1
27K1=K+2
K2=K+1
H(I)=(Z(K1,1)-Z(K2,1))*V1*(I-1-K/V1)+Z(K2,1)
29CONTINUE
GO TO 50
30DO 35 I=2,N
X=I*V1
J=1*X
L=J+1
IF(L-N)32,31,31
31J=N
L=N
32TAU=X-J
H(I)=Z(J,1)+(Z(L,1)-Z(J,1))*TAU
35CONTINUE
50CONTINUE
RETURN
END
SUBROUTINE EIG1(A,B,N,EPS,AM,IR,NA,NB)
DIMENSION A(25),B(25),AM(25),IR(25)
IJSF(I,J)=N*(I-1)+J-(I*(I-1))/2
IJDF(I,J)=NA*(J-1)+I
1 EN=N
3 IF(NA-1)7,5,7
5 MF=1
GO TO 10
7 MF=0
10 IF(EPS)601,11,12
11 SE=1.0E-12
GO TO 15
12 SE=SQRT(EPS)
15 DO 60 I=1,N
DO 50 J=1,N
IJ=NB*(J-1)+I
50 B(IJ)=0.
AM(I)=0.
II=NB*(I-1)+I
60 B(II)=1.0
80 DO 90 J=2,N
K=J-1

```

```

DO 90 I=1,K
IF(MF) 601,82,83
82 L=IJDF(I,J)
GO TO 84
83 L=IJSF(I,J)
84 T=ABS(A(L))
IF(T-AM(J))90,85,85
85 AM(J)=T
IR(J)=I
90 CONTINUE
100 BA=0.
DO 125 J=2,N
IF(AM(J)-BA) 125,120,120
120 BA=AM(J)
L=IR(J)
M=J
125 CONTINUE
IF(MF)601,126,127
126 LM=IJDF(L,M)
MM=LM-L+M
LL=IJDF(L,L)
GO TO 138
127 LM=IJSF(L,M)
LL=LM-M+L
MM=IJSF(M,M)
138 IF(EN*ABS(A(LM))-SE)590,150,150
150 LMI=L-1
LPI=L+1
MMI=M-1
MPI=M+1
200 R=SQRT((A(LL)-A(MM))**2+4.*A(LM)*A(LM))
T=A(LL)-A(MM)
400 C=SQRT(.5*(1.+ABS(T)/R))
S=-A(LM)/(R*C)
IF(T) 401,402,402
401 S=-S
402 SS=S*S
CC=C*C
SC=S*C
P=2.*A(LM)*SC
A(LM)=AM(L)=AM(M)=0.
IF(LMI) 411,450,411
411 DO 440 I=1,LMI
IF(MF) 601,412,413
412 IL=IJDF(I,L)
IM=IJDF(I,M)
GO TO 414
413 IL=IJSF(I,L)
IM=IL-L+M
414 TE=A(IL)
A(IL)=A(IL)*C-A(IM)*S

```

```

A(IM)=A(IM)*C+TE*S
TEM=ABS(A(IL))
IF(TEM-AM(L)) 430,415,415
415 AM(L)=TEM
IR(L)=I
430 TEM=ABS(A(IM))
IF(TEM-AM(M)) 440,435,435
435 AM(M)=TEM
IR(M)=I
440 CONTINUE
450 IF(LP1-M) 451,500,451
451 DO 490 K=LP1,MM1
IF(MF) 601,462,463
462 LK=IJDF(L,K)
LT=LK-L
KM=IJDF(K,M)
GO TO 464
463 LK=IJSF(L,K)
KM=IJSF(K,M)
464 TE=A(LK)
A(LK)=A(LK)*C-A(KM)*S
A(KM)=A(KM)*C+TE*S
IF(IR(K)-L) 465,470,465
465 TEM=ABS(A(LK))
IF(TEM-AM(K)) 480,467,467
467 AM(K)=TEM
IR(K)=L
GO TO 480
470 AM(K)=0.
KM1=K-1
DO 475 IT=1,KM1
IF(MF) 601,471,472
471 ITK=LT+IT
GO TO 473
472 ITK=IJSF(IT,K)
473 TEM=ABS(A(ITK))
IF(TEM-AM(K)) 475,474,474
474 AM(K)=TEM
IR(K)=IT
475 CONTINUE
480 TEM=ABS(A(KM))
IF(TEM-AM(M)) 490,485,485
485 AM(M)=TEM
IR(M)=K
490 CONTINUE
500 IF(M-N) 511,580,511
511 DO 540 J=MP1,N
IF(MF) 601,512,513
512 LJ=IJDF(L,J)
LT=LJ-L
MJ=LT+M

```

```

GO TO 514
513 LJ=IJSF(L,J)
MJ=IJSF(M,J)
514 TE=A(LJ)
A(LJ)=A(LJ)*C-A(MJ)*S
A(MJ)=A(MJ)*C+TE*S
IF(IR(J)-L) 515,525,515
515 IF(IR(J)-M) 517,525,517
517 TEM=ABS(A(LJ))
IF(TEM-AM(J)) 520,518,518
518 AM(J)=TEM
IR(J)=L
520 TEM=ABS(A(MJ))
IF(TEM-AM(J))540,521,521
521 AM(J)=TEM
IR(J)=M
GO TO 540
525 AM(J)=0.
JMI=J-1
DO 530 IT=1,JMI
IF(MF)601,526,527
526 ITJ=LT+IT
GO TO 528
527 ITJ=IJSF(IT,J)
528 TEM=ABS(A(ITJ))
IF(TEM-AM(J)) 530,529,529
529 AM(J)=TEM
IR(J)=IT
530 CONTINUE
540 CONTINUE
580 TE=A(LL)
A(LL)=A(LL)*CC-P+A(MM)*SS
A(MM)=A(MM)*CC+P+TE*SS
581 DO 585 I=1,N
IL=NB*(L-1)+I
IM=NB*(M-1)+I
TE=B(IL)
B(IL)=B(IL)*C-B(IM)*S
  B(IM)=B(IM)*C+TE*S
585 CONTINUE
GO TO 100
590 IF(MF)601,601,595
595 DO 600 I=2,N
II=IJSF(I,I)
600 A(I)=A(II)
601 CONTINUE
RETURN
END
C ***** TRANSP *****
C * SUBROUTINE TRANSP(A,B,M,N), IS USED TO FIND THE*
C * TRANSPOSE B(N,M) OF A MATRIX A(M,N). *
```

```

C * DIMENSION N,M MUST BOTH BE LESS THAN 25 *
C *****
C
SUBROUTINE TRANSP(A,B,M,N)
DIMENSION A(25,25),B(25,25)
DO 1 I=1,M
DO 1 J=1,N
B(J,I)=A(I,J)
1CONTINUE
RETURN
END

C ***** PRODMA *****
C * SUBROUTINE PRODMA(A,B,C,M,N,L), EXECUTES THE *
C * PRODUCT OF THE MATRIX A(M BY N) BY B(N BY L) *
C * AND RETURNS THE MATRIX C(M BY L) *
C * N,M,L MUST ALL BE LESS THAN 25. *
C *****
C
SUBROUTINE PRODMA(A,B,C,M,N,L)
DIMENSION A(25,25),B(25,25),C(25,25)
DO 1 I=1,M
DO 1 J=1,L
C(I,J)=0
DO 1 K=1,N
C(I,J)=C(I,J)+A(I,K)*B(K,J)
1 CONTINUE
RETURN
END

C *****SUBROUTINE ORD(ETA,U,M)*****
C
SUBROUTINE ORD(ETA,U,H,M)
DIMENSION ETA(25),U(25,1),X(25),Y(25)
DIMENSION H(25,25),A(25,25)
M1=1
L=M
K=M-1
DO 10 J=1,K
CALL MAX(ETA,X,U,Y,H,A,L,M1,J,M)
CALL RELAB(ETA,U,H,M1,L,M)
L=L-1
10CONTINUE
X(M)=ETA(1)
Y(M)=U(1,1)
DO 15 I1=1,M
A(I1,M)=H(I1,1)
15CONTINUE
DO 20 I=1,M
ETA(I)=X(I)
U(I,1)=Y(I)
DO 17 I1=1,M
H(I1,I)=A(I1,I)

```

```

17CONTINUE
20CONTINUE
RETURN
END
SUBROUTINE RELAB(ETA,U,H,M,K,N)
DIMENSION ETA(25),U(25,1)
DIMENSION H(25,25)
DO 1 I=M,K
ETA(I)=ETA(I+1)
U(I,1)=U(I+1,1)
DO 1 J=1,N
H(J,I)=H(J,I+1)
1CONTINUE
RETURN
END
C
C          **SUBROUTINE ROOT**
C
SUBROUTINE ROOT(A1,A2,V,S,X,K,ALP)
DIMENSION V(25,1),S(25)
XINT=A2-A1
K1=1
IF(XINT)50,90,50
50X=A1
DO 90 J=1,30
XINT=XINT/2
X=X+XINT*K1
XFU=0
DO 80 L=1,K
XFU=XFU+(ALP*(V(L,1)**2))/(X+S(L))
80CONTINUE
IF(XFU-X) 85,86,87
85K1=-1
GO TO 88
86K1=0
GO TO 88
87K1=1
88K1=K1
90CONTINUE
RETURN
END
SUBROUTINE GRAPH(N,M,F,VMIN,DEL,SCA)
DIMENSION F(20,1),JOUT(45)
50FORMAT(16X,"ESTIMATED DISTRIBUTION")
55FORMAT(" ")
60FORMAT(1X,"VEL'S",48X,"DIST.")
65FORMAT(7X,"-20  -15  -10  -5   0   5   10   15   20")
70FORMAT(1X,"-----I---I---I---I---I---I---I---I---I---I---I---I---I---I---I---I")
&-----")
75FORMAT(1X,F6.2,3X,41A1,1X,E9.3)
76FORMAT(1X,"-20 CORR. TO ",E10.4,2X,"20 CORR. TO ",E10.4)

```

```

PRINT 55,
PRINT 50,
PRINT 55,
PRINT 60,
PRINT 65,
PRINT 70,
NOTH=" "
KI="*"
XMAX=0
DO 79 I=M,N
IF(XMAX-ABS(F(I,1))) 78,79,79
78XMAX=ABS(F(I,1))
79CONTINUE
SA=20/XMAX
A1=-XMAX
A2=XMAX
DO 90 I=M,N
J=F(I,1)*SA+20
DO 85 L=1,41
JOUT(L)=NOTH
85CONTINUE
DO 86 K=1,J
JOUT(K)=KI
86CONTINUE
XV=SCA*EXP(VMIN+(I-1)*DEL)
PRINT 75,XV,(JOUT(J1),J1=1,41),F(I,1)
90CONTINUE
PRINT 70,
PRINT 65,
PRINT 55,
RETURN
END
SUBROUTINE MAX(ETA,ETA1,U,U1,H,A,K,M,J,N)
DIMENSION ETA(25),ETA1(25),U(25,1),U1(25)
DIMENSION H(25,25),A(25,25)
XMAX=ETA(1)
M=1
DO 3 I=1,K
IF(ETA(I)-XMAX) 3,3,2
2XMAX=ETA(I)
M=I
3CONTINUE
ETA1(J)=ETA(M)
U1(J)=U(M,1)
DO 4 L=1,N
A(L,J)=H(L,M)
4CONTINUE
RETURN
END

```

PROGRAM NAME : ARTIF

PURPOSE: It is designed to estimate the artefact parameters and remove it from the data.

SEQUENCE:

1 - Relevant data parameters and the data are read in; they are:

START AND STOP - are the discrete time indices corresponding to the times t_0 and t_f defined in (A2.6).

TOTAL LENGTH - is the total number of data points.

ALPHA \emptyset - is the initial guess for alpha.

DATA - is the actual data sequence.

MEAN - is the best initial guess for the mean.

2 - ITERATIONS - Equations (A2.10) and (A2.9) are solved iteratively as indicated in (A2.28) and (A2.29).


```

C *****
C *                               ARTIF                               *
C *                               *                                   *
C * GIVEN :                       *                                   *
C *                               *                                   *
C *   Y(T)=S(T)+A(T)+N(T)   0<T<N   *                                   *
C *   S(T)=DESIRED SIGNAL   *                                   *
C *   A(T)=(1-B*T)EXP(-B*T) = ARTIFACT *                                   *
C *   N(T)=NOISE           *                                   *
C *                               *                                   *
C * THIS PROGRAM WILL ESTIMATE (LEAST SQRS) *
C * THE PARAMETER B USING DATA IN A INTER- *
C * WHERE S(T) IS KNOWN TO BE ZERO. THEN *
C * WILL SUBTRACT IT FROM Y(T) AND RETURN *
C * ESSENTIALLY Y(T)=S(T)+N(T) *
C *****
C
DIMENSION Y(300)
DIMENSION MY(300)
PRINT,"START AND STOP ART="
READ,L,N
PRINT,"TOTAL LENGHT="
READ,NA
PRINT,"ALPHA 0="
READ, ALPHA
XN=1.*N
B=XN/ALPHA
PRINT,"DATA="
READ,Y
PRINT,"MEAN="
READ,XME
DO 10 I=1,NA
Y(I)=(Y(I)-XME)
10CONTINUE
DEL=1./N
XN=N
XL=L
EP=XL/XN
C
C ***** ITERATIONS *****
C
20M=M+1
XINT=0
XPR=0
XEN=0
DO 30 I=L,N
XED=DEL*I
XINT =XINT+Y(I)*XED*DEL*(2-B*XED)*EXP(-B*XED)
XPR=XPR+Y(I)*(1-B*XED)*DEL*EXP(-B*XED)
XEN=XEN+((1-B*XED)**2)*DEL*EXP(-2*B*XED)
30CONTINUE

```

```

BA=XPR/XEN
XINT=ABS(XINT/BA)
CALL PSITRI(XINT,C,EP)
ER=ABS((C-B)/C)
40 IF(M-30)50,60,60
50 B=C
GOTO 20
60 PRINT 70,C,BA
70 FORMAT("ALPHA=",E10.4,2X,"AMPLITUDE=",E10.4)
PRINT," "
DO 80 I=1,NA
XED=DEL*I
MY(I)=Y(I)-BA*(1-B*XED)*EXP(-B*XED)
80 CONTINUE
M=NA/9+1
DO 100 I=1,M
L1=9*(I-1)+1
L2=9*I
PRINT 120,(MY(J),J=L1,L2)
100 CONTINUE
120 FORMAT(1X,9(I6,""))
END

```

```

C *****PSITRI*****
SUBROUTINE PSITRI(X,B,EP)
M=1
B=1
Y=2*B
1XAL1=(1-(1+2*B-6*B*B+4*B*B*B)*EXP(-2*B))/(8*B*B)
D=EP*B
XAL2=(1-(1+2*D-6*D*D+4*D*D*D)*EXP(-2*D))/(8*B*B)
XAL=XAL1-XAL2
IF(X-XAL)2,30,3
2B=2*B
Y=2*B
GOTO 1
3M=M+1
Y=Y/2
IF(M-20)4,30,30
4XAL1=(1-(1+2*B-6*B*B+4*B*B*B)*EXP(-2*B))/(8*B*B)
D=EP*B
XAL2=(1-(1+2*D-6*D*D+4*D*D*D)*EXP(-2*D))/(8*B*B)
XAL=XAL1-XAL2
IF(X-XAL)5,30,6
5B=B+Y/2
GOTO 3
6B=B-Y/2
GOTO 3
30B=B
RETU RN
END

```

REFERENCES

- B1 - Buchthal F., Rosenfalck A., "Evoked Action Potentials and Conduction Velocity in Human Sensory Nerves", Brain Research vol-3, 1966.
- B2 - Buchthal F., Trojaborg, W., "Electrophysiological findings in Entrapment of the Median Nerve", Journal of Neurol., Neurosurg. and Psychiatry, vol 37, pp. 340-360, 1974.
- B3 - Buchthal F., "Sensory Potentials in Polyneuropathy", Brain vol 94, pp. 241-262, 1971.
- B4 - Brown M, Martin J.R., Asbury A.K., "Painfull Diabetic Neuro-pathy", Archives of Neurology, vol 33, pp. 164-171, 1976.
- B5 - Boyd, I.D., "The relation Between Conduction Velocity and Diameter for the Three Groups of Efferent Fibers in the Nerves of Mammalian Muscles", J.Physiology, London, vol 175, pp. 33-35, 1964.
- B6 - Boyd, I.D., Davey M.R., "Composition of Peripheral Nerves", E.S.Livingstone Ltd., Eddinburgh and London, 1968.
- B7 - Brinley F.J., "Excitation and Conduction in Nerve Fibers", Chapter Two in Medical Physiology, V.Mountcastle ed., C.V. Mosby, 1974.
- B8 - Bruyn G.W., Garland H., "Neuropathies of Endocrine Origin", Chapter Two in the Handbook of Medical Neurophysiology,

vol 8, North Holland Publ. Co., Amsterdam, 1975.

- B9 - Burke D., Skuse N.F., Lethlean A.K., "Sensory Conduction of Sural Nerve in polyneuropathy", Jour. Neurophys., Neurosurg. and Psychiat., vol 37, pp. 647-652, 1974.
- B10 - Bradley W.G., "Disorders of Peripheral Nerves", Blackwell Scientific Publishing Co., London, 1974.
- B11 - Blair J., Erlanger J., American Journal of Physiology, vol 106, 1933.
- C1 - Casby J.U., Simminoff R., Houseknecht T., "An analogue cross-correlator to study naturally induced activity in intact nerve trunks", Jour. Neurophysiology, vol 26, pp. 432-448, 1963.
- C2 - Chopra J.S., Hurwitz L.J., "Femoral nerve conduction in diabetes and chronic vascular disease", Jour. Neurol., Neurosurg. and Psych., vol 31, pp. 28-33, 1968.
- C3 - Chopra J.S., Hurwitz L.J., "Sural Nerve Myelinated fiber density and size in diabetes", Jour. of Neurol, Neurosurg. and Psych., vol 32, pp. 149-154, 1969.
- C4 - Chopra J.S., Hurwitz L.J., Montgomery D.A.D., "The pathogenesis of sural nerve changes in diabetes mellitus", Brain, vol 92, pp. 391-418, 1969.
- C5 - Cragg B.G., Thomas P.K., "Conduction velocities of regene-

rating peripheral nerve fibers", Jour. Neurol., Neurosurg. and Psych., vol 27, 1964.

- D1 - Douglas W.W., Ritchie J.M., "A technique for recording functional activity in specific groups of nerve fibers", Journal of Physiology, vol 138, pp.19-30, 1957.
- D2 - Dawson G.D., Scott J.W., "Recording of Nerve action potentials through skin in man", Jour. Neurol., Neurosurg., and Psych., vol 12, pp.259-367, 1949.
- D3 - Dawson G.D., "The relative excitability and conduction velocity of sensory and motor nerve fibers in man", Journal of Physiology, vol 131, pp.431-451, 1956.
- E1 - Erlanger J., Gasser H.S., "Electrical Sign of Nervous Activity", University of Pennsylvania Press, Philadelphia, 1937.
- E2 - Erlanger J., Gasser H.S., Bishop G.H., "The compound nature of the action current of a nerve as disclosed by the CR oscillograph", Amer. Jour. of Physiol., vol 70, 1924.
- E3 - Eccles J. and Sherrington W., Proc. of the Royal Soc., vol 106, pp. 326-357, 1930.
- E4 - Eichler W., "Uber die ableitung der aktionspotentialle von menshirchen neven in situ", Z.Biol., vol 98, 1938.

- F1 - Fullerton P., Gilliatt R.W., Lascelles R.G., "The relation between fiber diameter and internodal length in chronic neuropathy", J. Physiology, vol 178, pp. 26P-28P, 1965.
- F2 - Fitzhugh R., "Computation of the impulse initiation and saltatory conduction in a nerve fiber", Biophysics J., vol 2, 1962.
- G1 - Gasser H.S., Erlanger J., "A study of the action currents of nerve with the cathode ray oscillograph", American Jour. of Physiol., vol 62, 1922.
- G2 - Gasser H.S., Erlanger J., "The role played by the size of the constituent fibers of a nerve trunk in the form of its action potential", American Jour. of Physiol., vol 80, 1927.
- G3 - Gilliatt R.W., "Recent advances in the pathophysiology of nerve conduction", in New Developments in EMG and Clinical Neurophysiology, ed. J.Desmedt, vol 2, pp 2-18, Krager, Baeel, 1973.
- G4 - Gilliatt R.W., "The recording of the action potential in man", Electroenceph. Clinic. Neurophys., vol 22, 1962.
- G5 - Gutman R., Sanders F.K., "Recovery of the fiber number and diameter in the regeneration of peripheral nerves", J. Physiology., vol 101, 1943.

- G6 - Gilliatt R.W., Sears T., "Sensory nerve action potentials in patients with peripheral nerve lesions", Jour. Neuroph. Neurosurg. and Psych., vol 21, 1958.
- G7 - Gasser H.S., Grundfest H, "American. Journal of Physiol.", vol 127, pp. 393-402, 1939.
- G8 - Gilliatt R.W., Goodman H.V., Willison R.G., "The recording of lateral poplietal fossa nerve action potentials in man", Jour. of Neurol., Neursurg. and Psych., vol 24, 1961.
- G9 - Cesselowitz D. "On bioelectric potentials in a inhomogeneous Volume conductor", Biophysics Jour., vol 7., 1967.
- H1 - Hursh J.B., "Con unction velocity and diameter in nerve fibers", Amer. Jour. of Physiol., vol 127, 1939.
- H2 - Huxley A.F., Stampfli R., "Evidence for saltatory conduction in peripheral myelinated nerve fibers", J. Physiology, vol 108, pp. 315-339, 1949.
- H3 - Hodgkin A.L., Huxley A.F., "A quantitative description of membrane currents and its applications to conduction and excitation in nerve", J. Physiology, vol 117, 1952.
- K1 - - Kaeser H.E., "Nerve conduction velocity measurements", Chap. 5 in Handbook of Clinical Neurology, vol 7, ed. Vinken and

- Bruyn, North Holland Publishing Co., Amsterdam, 1975.
- K2 - Katz B., "Nerve, Muscle and Synapse", McGraw Hill, 1966.
- L1 - Lamontagne A., Buchthal F., "Electrophysiological studies in diabetic neuropathy", Jour. Neurol., Neurosurg. and Psych., vol 33, 442-452, 1970.
- L2 - Lascelles R.G., Thomas P.K., "Changes due to age in internodal length in the sural nerve", Jour. of Neurol. Neurosurg. and Psych., vol 29, 1966.
- L3 - Lehman H.J., "Segmental Demyelination and changes in experimental circumscribed neuropathy", in New Developments in EMG and Clinical Neurophysiology, ed. J.Desmedt, vol 2, Krager, Basel, 1973.
- L4 - Lovelace R.E., Myers S.J., Zablow L., "Sensory conduction in peroneal and posterior tibial nerves using averaging techniques", Jour. Neurol. Neurosurg. and Psych., vol 36, 1973.
- L5 - Luenberger D.G., "Optimization by vector space methods", John Wiley and sons, 1969.
- L6 - Landau W.M., Clarke M.H., Bishpp G., "Reconstruction of the Myelinated tract action potentials", Expriment. Neurology, vol 22, 1968.
- L7 - Lillie R.S., Jour. of Gen. Physiol., vol 7, pp. 473, 1925.

- L8 - Lorente de N6 R., "Analysis of the distribution of the action currents of nerve in volume conductors", chapter 16, Rockefeller Institute Series, vol 132, 1947.
- M1 - McDonald I.W., "The effects of experimental demyelination on conduction in peripheral nerve: a histological and electrophysiological study", Brain, vol 86, 1963.
- M2 - McLoed J.G., Wray S.H., "Conduction velocity and fiber diameter of the median and ulnar nerves of the baboon", Jour. of Neurol., Neurosurg. and Psych., vol 30, 1970.
- N1 - - Nicholson C., "Field Potentials in Anisotropic Ensemble of neuronal elements", IEEE Trans. on Biomed. Eng., vol BME-20, number 4, 1973.
- O1 - Offner K.F., Weinberg A., Young G., Bulletin of Mathematical Biophysics, vol 2, 1940.
- P1 - Plonsey R., "Bioelectric Phenomena", McGraw Hill, 1969.
- P2 - Plonsey R., "Active Fiber in Volume Conductor", IEEE Trans. on Biomed. Eng., vol BME-21, 1974.
- P3 - Paintal A.S., "Conduction in Mamalian Nerve Fibers", in New Developments in EMG and Clinical Neurology, ed. J.Desmedt,

vol 2, Krager, Basel, 1973.

- P4 - Poussard D.J.M., "Measurement of the latency distribution in peripheral nerve fibers", M.S. Thesis, Dept. of Elect. Eng., M.I.T., Cambridge, Massachusetts, 1965.
- R1 - Rao C.R., "Linear Statistical Inference and Its Applications" 2nd. edition, John Wiley and Sons, 1973.
- R2 - Rothchild R.D., "Decoding electrical artifact from large nerve bundles in vivo", ScD Thesis, M.I.T., Dept. of Mechanical Eng., Cambridge, Mass., 1973.
- R3 - Rothchild R.D., "Isolating peripheral nerve activity with respect to propagation velocity", IEEE Trans. on Biomed. Eng., vol BME-21, 1974.
- R4 - Rushton W.A.H., "A theory of the effects of fiber size in medullated nerve", J. Physiology, vol 115, pp.101-122, 1951.
- R5 - Rasminsky M., Sears T.A., "Saltatory conduction in Demyelinated Nerve Fibers", in New Development in EMG and Clinical Neurophysiology, ed. J.Desmedt, vol 2, Krager, Basel, 1973.
- R6 - Ross, Sheldon, "Applied Probability Models with optimization applications", Holden Day, 1971.
- R7 - Rosenblueth R. and Dempsey M., "A study of Wallerian degeneration ", American Jour. of Physiol., vol 128, 1939.

- S1 - Sayers McA. B., "Inferring Significance from Biological Signals", in
- S2 - Sanders F.K., Whitteridge D., "Conduction velocity and myelin thickness in degenerating nerve fibers", J.Physiology, vol 105, 1946.
- S3 - Smith R.S., Koles Z.J., "Myelinated fibers: computed effect of myelin thickness on conduction velocity", Amer. Jour. of Physiology, vol 219, number 5, 1970.
- S4 - Sherrington S., Journal of Physiology, vol 17, pp. 211-258, 1894.
- T1 - Thomas P.K., Lascelles R.G., "Schwann cell abnormalities in diabetic neuropathy," The Lancet, june 26, 1965,=
- T2 - Thomas P.K., "Pathology of diabetic neuropathy", Quart. Jour. of Medicine, vol 35, 1966.
- T3 - Tasaki I., "Nervous transmission", Charles Thompson Publisher, Springfield, Illinois, 1953.
- T4 - Tasaki I., Pflug. Arch. ges. Physiol., vol 246, pp. 32, 1942.
- V1 - Von Helmholtz , "Messungen über fortpflanzungsgeschwindigkeit der reizung in der nerven ", John Muller's Arch. Anat. Physiol.

1850.

- V2 - Verveen A.A., Derksen H.E., "Fluctuation Phenomena in Nerve Membranes", Proc. IEEE, vol 56, number 6, 1968.

BIOGRAPHICAL NOTE

Zsolt Laszlo Kovacs was born on March 22, 1946 in a war refugee camp in Germany, from hungarian parents. In 1949 his family went to Sao Paulo, Brazil, where he was raised. In 1967, entered the Polytechnic School of the University of Sao Paulo. For two years worked in the evenings as a high school teacher of physics and mathematics. In 1969 he received from the Fundacao de Amparo a Pesquisa do Estado de Sao Paulo an undergraduate research assistantship to study digital communication systems. He carried this assistantship until 1971 when he graduated as an electrical engineer. In 1971 got married to Elizabeth MacNevin. In 1972, entered the graduate school at the University of Sao Paulo where he was also employed as a teaching assistant. Finished his master thesis in the field of algebraic coding theory in 1973. In the fall of 1973, he entered the graduate school at M.I.T. to work toward the PhD degree. He has two children, Eliane, born in 1974 and Robert, born in 1976.